6-1988

Structural Geology and Finite Strain Analysis of the Precambrian Thunderhead Sandstone Along the Greenbrier Fault and the Roundtop Klippe: Great Smoky Mountains, Tennessee

Jonathan C. Lewis
University of Tennessee - Knoxville

To the Graduate Council:

I am submitting herewith a thesis written by Jonathan C. Lewis entitled "Structural Geology and Finite Strain Analysis of the Precambrian Thunderhead Sandstone Along the Greenbrier Fault and the Roundtop Klippe: Great Smoky Mountains, Tennessee." I have examined the final electronic copy of this thesis for form and content and recommend that it be accepted in partial fulfillment of the requirements for the degree of Master of Science, with a major in Geology.

<div align="right">Nicholas B. Woodward, Major Professor</div>

We have read this thesis and recommend its acceptance:

Theodore Labotka & Steven Driese

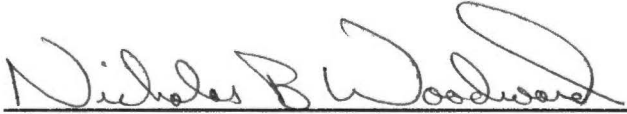<div align="right">Accepted for the Council:
Dixie L. Thompson</div>

<div align="right">Vice Provost and Dean of the Graduate School</div>
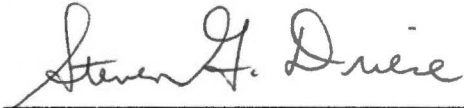
(Original signatures are on file with official student records.)

To the Graduate Council:

I am submitting herewith a thesis written by Jonathan C. Lewis entitled "Structural Geology and Finite Strain Analysis of the Precambrian Thunderhead Sandstone Along the Greenbrier Fault and the Roundtop Klippe: Great Smoky Mountains, Tennessee." I have examined the final copy of this thesis for form and content and recommend that it be accepted in partial fulfillment of the requirements for the degree of Master of Science, with a major in Geology.

_____
Nicholas B. Woodward, Major Professor
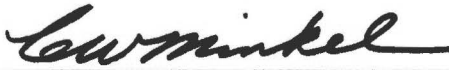
We have read this thesis
and recommend its acceptance:

_____

_____

Accepted for the Council:

_____
Vice Provost and Dean
of The Graduate School

STRUCTURAL GEOLOGY AND FINITE STRAIN ANALYSIS OF THE

PRECAMBRIAN THUNDERHEAD SANDSTONE ALONG THE

GREENBRIER FAULT AND THE ROUNDTOP KLIPPE:

GREAT SMOKY MOUNTAINS, TENNESSEE

A Thesis

Presented for the

Master of Science

Degree

The University of Tennessee, Knoxville

Jonathan C. Lewis

June 1988

AKNOWLEDGEMENTS

the latter stages of this research.

The list of additional individuals that I am indebted to for assistance during the course of this research is too lengthy to include here. Without the help of all of the above sources this work would not have been possible.

Abstract

The Precambrian Thunderhead Sandstone, along the Greenbrier Fault and the Roundtop Klippe, records strain from two distinct episodes of deformation. The first strains are generally related to the emplacement of the Greenbrier Fault. These strains are probably due to simple shear along the base of the fault, and appear similar to the strain fabrics within in the Cades Sandstone to the southwest. This strain fabric is characterized by principal strain axes which lie subparallel to the orientation of the Greenbrier Fault. These strains were later effected by strains related to the emplacement of the Sinks Fault, a high angle thrust which displaced the Greenbrier Thrust Sheet. This fabric is probably also the result of simple shear on the Sinks and is similarly characterized by the subparallelism of the principal extension axes and the Sinks Fault plane.

Finite strains were calculated for 17 samples of Thunderhead Sandstone, using the R_f/ϕ and Fry methods. Twelve samples show that uniaxial extension is dominant over flattening within the Thunderhead. In five samples flattening is dominant over uniaxial extension. The Greenbrier main sheet shows less strain in the same

iv

orientations than that seen in the Roundtop Klippe. King (1964, 1968) shows two interpretations of the area, one with the Sinks as a folded part of the Greenbrier and one with the Sinks as a later fault. Superposed strain patterns suggest that both are correct.

TABLE OF CONTENTS

LIST OF PLATES

PLATE

CHAPTER I

INTRODUCTION

Purpose Of Study

The purpose of this study is to establish the geometry and significance of finite strain data within the Precambrian Thunderhead Sandstone along the northwestern edge of the Greenbrier Fault and the Roundtop klippe to the northwest, in the Wear Cove quadrangle (Figure 1). The Thunderhead Sandstone here shows a variably developed tectonic fabric generally in the form of elongate quartz and feldspar grains showing a strong preferred orientation. This fabric is not penetrative and where present is not always equally developed. The strain data from the Thunderhead provide a better understanding of how these rocks responded to the deformation which affected this area. The strain magnitudes and how the strains relate geometrically to the various regional structural elements are of principal interest. It is expected that this work will further our understanding of the mechanical responses of the rocks adjacent to the Greenbrier and Sinks Faults. The

Figure 1. Location of study area showing localities
discussed in the text. The Wear Cove vicinity is
indicated on the map of Tennessee and enlarged to show
the area of study. Localities referred to in the text
are indicated by number. GF=Greenbrier Fault, SF=Sinks
Fault, LSF=Line Springs Fault, GSF=Great Smoky Fault,
OF=Oconaluftee Fault, RCF=Rabbit Creek Fault, DCF=Dunn
Creek Fault, WC=Wear Cove Window, TC=Tuckaleechee Cove
Window, CC=Cades Cove Window, TN=Tennessee, NC=North
Carolina.
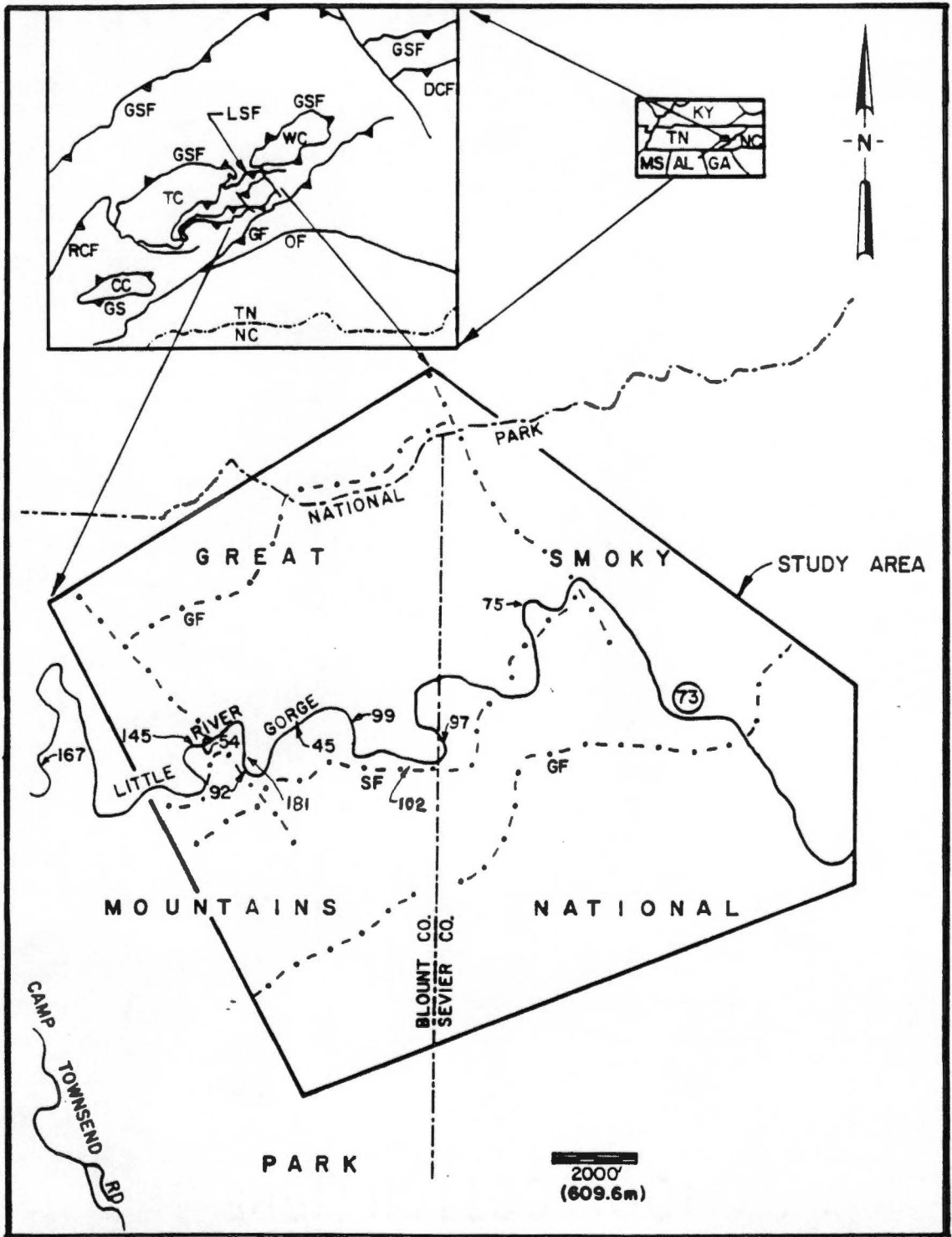
importance of such analyses has been demonstrated by a variety of recent studies (e.g., Coward, 1976; Coward, 1984; Coward and Kim, 1981; Coward and Potts, 1983; Hossack, 1968). The present study will establish a strain survey in one part of the western Great Smoky Mountains. It is expected that this data base will be expanded by future workers.

Stratigraphy

King's (1968) stratigraphic interpretation (Figure 2) of the central Great Smoky Mountains region is similar to that of Keith (1904). The Precambrian Thunderhead Sandstone is the unit of most concern here. It is part of the Great Smoky Group, the middle group of the three which comprise the Ocoee Series (King, 1964). The Snowbird Group lies beneath the Great Smoky Group, whereas the Walden Creek Group lies above it (King, 1964). The Great Smoky Group is made up of the Elkmont Sandstone, the Thunderhead Sandstone, and the Anakeesta Formation.

Metcalf Phyllite

The Metcalf Phyllite is the uppermost unit of the

4

Age	North of and below Greenbrier fault					South of and above Greenbrier fault	
Cambrian(?) and Cambrian	Chilhowee Group	Cochran Formation and higher units				Rocks of Murphy marble belt	Nantahala Slate and higher units (Early Paleozoic(?))
		─── Disconformity? ───					─── Lithologic break, but probably conformable ───
Later	Ocoee Series — Walden Creek Group	Sandsuck Formation Wilhite Formation Shields Formation Licklog Formation			Correlation between these sequences uncertain	Ocoee Series — Great Smoky Group	Unnamed sandstone Anakeesta Formation Thunderhead Sandstone Elkmont Sandstone
		─── Fault contact, sequence uncertain ───					
		Western part of area	Eastern part of area				
Precambrian	Ocoee Series — Unclassified formations	Cades Sandstone	Rocks of Webb Mountain and Big Ridge	Rich Butt Sandstone			
	Snowbird Group	Metcalf Phyllite	Pigeon Siltstone Roaring Fork Sandstone Longarm Quartzite Wading Branch Formation			Snowbird Group	Roaring Fork Sandstone Longarm Quartzite Wading Branch Formation
		─── Base not exposed ───	─── Unconformity ───				─── Unconformity ───
Earlier Precambrian		Basement complex					Basement complex

Figure 2.   Stratigraphic units found in the central Great Smoky Mountains.   From King et al., (1968).

Snowbird Group (?), which lies statigraphically below the Great Smoky Group. In the report area it structurally overlies the Thunderhead Sandstone beneath the Greenbrier Fault (King, 1964). Here the Metcalf is dominated by argillaceous rocks, with bedding largely obliterated by varying degrees of cleavage development. Siltstone beds occur within the Metcalf here as well, but also contain foliations which generally obliterate bedding. Both the siltstone and the argillite strata contain high proportions of metamorphic muscovite and sericite, with lesser chlorite (King, 1964). The argillite units are fine- grained, lustrous, and usually pale green, gray-green, or light gray (King, 1964). The siltstone lithologies are for the most part similar in appearance, except for their more granular texture.

Cades Sandstone

The Cades Sandstone is one of the unclassified formations of the Ocoee Series, and its exposures in the area lie west-southwest of the Roundtop Klippe, in a thin belt that extends to Whiteoak Sink in the Wear Cove Quadrangle. Although the relation with the Thunderhead was not understood, King (1964) separated the two by a proposed fault just southwest of the study area. Cades

Sandstone of this narrow belt is generally finer grained and thinner bedded than the Thunderhead of the klippe, and its argillaceous layers are generally thicker than those within the Thunderhead (King, 1964). In this area the Cades also contains fewer conglomeratic layers and less blue quartz than the Thunderhead (King, 1964).

Elkmont Sandstone

The Elkmont Sandstone, lowest unit of the Great Smoky Group, occurs outside of the area of study. It is described here because recent work by Walters (1988) suggests that the Elkmont may be a facies equivalent of the Cades Sandstone, which in turn may be equivalent to the Thunderhead, as suggested by the present study.

Although the Elkmont's base is always truncated by faults and thus the surface upon which it was deposited is unknown, the unit is clearly stratigraphically overlain by the Thunderhead Sandstone (King, 1964). In the area of the present study, King (1964) described the top of the Elkmont as ascending stratigraphically toward the southwest and its upper part changing facies, toward the northeast, to the Thunderhead Sandstone. The Elkmont Sandstone which occurs to the south and west of the Roundtop Klippe is generally finer grained and thinner

7

bedded than the Thunderhead Sandstone, and only rarely contains blue quartz.

Thunderhead Sandstone

The Thunderhead Sandstone consists of a variety of lithologies ranging from dark gray argillite to coarse grained conglomerate. Along the Little River, within the area of study, the Thunderhead Sandstone consists of thick, graded beds of fine to coarse sandstone with thin, dark gray argillite partings. The sandstone contains white potassium feldspar and glassy quartz with lesser smoky quartz. Thin sections cut for this study reveal white plagioclase in many of the sandstone samples. The coarse conglomerate strata of the Thunderhead also contain white potassium feldspar, white plagioclase and, glassy quartz pebbles. Although King (1964) rarely found blue quartz in the foothills exposures of Thunderhead, it does occur quite commonly within the conglomerate exposed along the Little River. Smoky quartz also occurs regularly in these conglomerate units. Many of the quartz pebbles, feldspar pebbles, and quartzofeldspathic lithic fragments within the conglomerate lithologies are from 1-3 cm in diameter (Figure 3). These are likely to be granitic fragments and are referred to by King (1964)

8
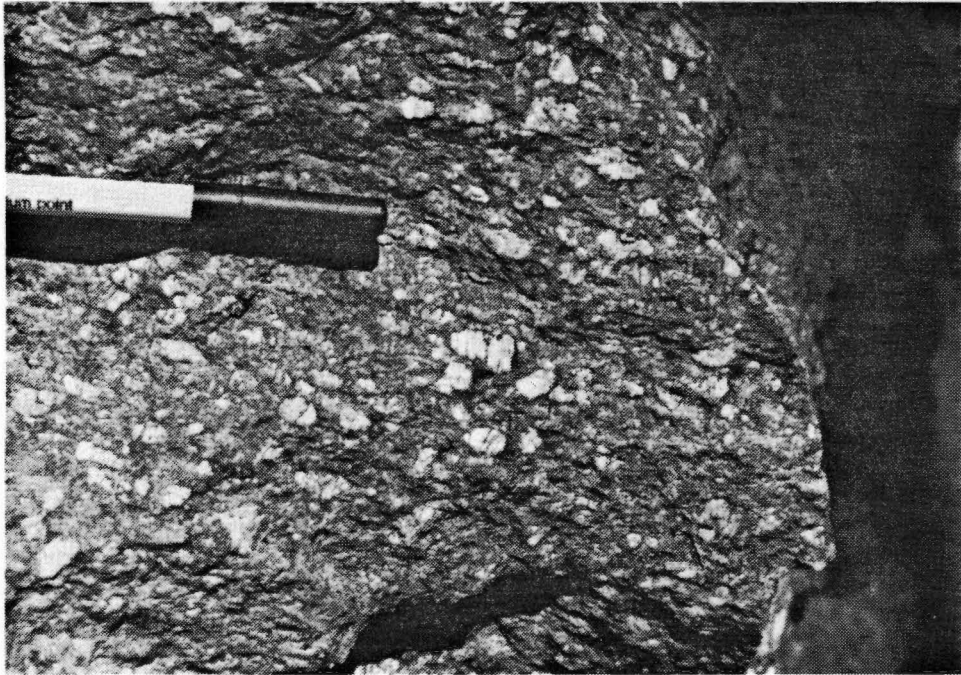
Figure 3. Photograph of Thunderhead Sandstone showing clasts of feldspar up to 1.2 cm in length. Photo taken at locality 45 (Figure 1, page 2). The length of the pen cap is 4 cm.

as leucogranite pebbles. Such pebbles are found
throughout the Thunderhead of the Roundtop Klippe, but
are rarely found in the Thunderhead of the main thrust
sheet (King, 1964). Mudrock clasts appear more rarely
within these conglomerate units, but in places are as
long as 70 cm (Figure 4). Well-exposed conglomerate
sequences are found at localities 45, 54, and 102
(Figure 1). Along the Little River near the Roundtop
Klippe's southwestern corner (Locality 92, Figure 1) the
Thunderhead is dominated by argillite. Here the
argillite is dark gray, slaty, and commonly shows one or
two generations of cleavage (see Chapter II for a
discussion of the cleavages). King (1964) described this
lithology as dominating the Thunderhead of the klippe
southwest of Meigs Creek and in the main sheet along the
Middle Prong near Walker Flats. This is confirmed by the
present study, although in the vicinity of the quarry at
the klippe's southwestern border (Locality 54, Figure 1),
fine- to medium-grained sandstone is predominant. At
this locality there are several beds of coarse
congomerate which contain mudrock chips as long as 10 cm.
Some of these chips are bent indicating that they were
probably not well indurated during deposition. They are
likely rip-up clasts from a muddy horizon upon which the
conglomerate was deposited.
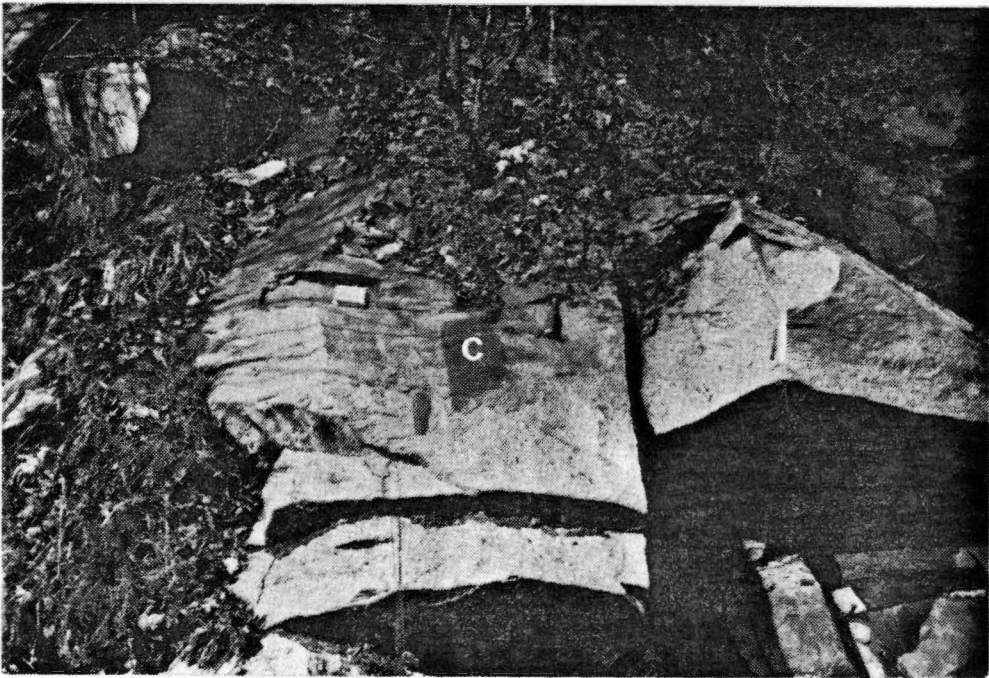
Figure 4. Photograph of Thunderhead Sandstone showing a mudrock clast (C) 70 cm in length. Photo taken at locality 54 (Figure 1, page 2). Fieldbook at upper left is approximately 20 cm in length.

The Thunderhead of the main thrust sheet consistently occurs as massive graded beds, generally of coarse grained sandstone (King, 1964). Eastward, it tends to contain more pebbly horizons with larger pebbles (King, 1964). It is this consistency which distinguishes the Thunderhead of this area from that of the foothills area to the west. The foothills area including the Roundtop Klippe contains Thunderhead of more variable lithologies as discussed above.

Previous Work

The most recent geologic research in this region is contained in three United States Geological Survey Professional Papers (Hadley and Goldsmith, 1963; King, 1964; Neuman and Nelson, 1965). These papers are based on fieldwork done during the 1950's. Prior to these studies, relatively little work had been done on the geology of this area. Gerard Troost, the first State Geologist of Tennessee, made brief mention of the area in 1841, but it was James M. Safford, the second State Geologist of Tennessee, who published the early significant works (1856 and 1869). Another significant contribution was Arthur Keith's Knoxville folio (1895) which he later realized contained many

12

misinterpretations. Keith (1892) also divided Safford's "Ocoee conglomerate and slate" and "Chilhowie sandstone" into a number of better defined formations. During an 1898 field conference attended by Keith, and C. R. Van Hise, Cooper Curtice, and G. W. Stose, it was recognized that the Ocoee rocks did not lie unconformably on Ordovician rocks, but rather had been thrust over them (Keith, 1899). This was also noted by Stose and Stose in (1944). Keith (1904) revised his interpretation of the stratigraphic section and later briefly discussed the structural geology of this area in his report on the "Great Smoky Overthrust" (Keith, 1927). During continued studies of the Great Smoky Mountains Keith greatly refined his understanding of the geology and made a great contribution to the geology of this region.

The area under study here was examined by King (1964). His report contains detailed geologic maps of the Walden Creek, Pigeon Forge, Wear Cove, Gatlinburg, Thunderhead, and Silers Bald Tennessee quadrangles, all at a scale of 1:24,000. The present study is in the southeastern quarter of the Wear Cove quadrangle.

CHAPTER II

STRUCTURAL GEOLOGY

Regional Structure

The structural setting of the study area is complex (King, 1964). The area lies within the Great Smoky Thrust sheet in the western part of the Blue Ridge Province (Figure 1). This sheet contains several windows of considerable size, notably those at Cades, Tuckaleechee, and Wear Coves (King, 1964; Neuman and Nelson, 1965). The Great Smoky Thrust surface shows a folded geometry which trends northeast-southwest (King, 1964). Structural highs in this folded surface are coincident with these three windows. The thrust sheet includes several generations of faults (King, 1964; Neuman and Nelson, 1965). The Greenbrier Fault is a low-angle thrust which places "younger" Great Smoky Group rocks onto "older" Snowbird Group rocks. It is a relatively early feature because it is cut by later generations of faults and Ordovician metamorphic isograds (King, 1964). The Greenbrier Fault is cut by the Sinks, Gatlinburg, and Norton Creek Faults. Still later

14

high-angle faults cut the faults of the Greenbrier family and the Sinks-Gatlinburg-Norton Creek family (King, 1964).

From King's (1964) map it appears that the Sinks fault uplifted the southeastern part of the Greenbrier thrust sheet and isolated a body of Thunderhead and Cades Sandstone northwest of the Little River. This narrow body of sandstone stretches from Roundtop Mountain southwest to Whiteoak Sink and includes the Roundtop Klippe. The Roundtop Mountain area lies southeast of the area between Wear and Tuckaleechee Coves, and is in an area of structural depression. Roundtop Mountain is held up by Thunderhead Sandstone of the Roundtop Klippe.

Local Structure

Geologic mapping at a scale of 1:12,000 has produced a map which is more detailed, but in almost complete agreement with the 1:24,000 scale map of the Wear Cove, Tennessee quardrangle of King (1964) (see Plate 1 in pocket). The Roundtop Klippe, west of the Greenbrier thrust sheet, as mapped by King (1964) is bounded to the northwest by the Greenbrier Fault, to the southeast by the Sinks Fault, and to the northeast and southwest by high angle faults.

15

Mapping during the present study could find no structural evidence to support a fault separating "Cades lithologies" from "Thunderhead lithologies" as King (1964) indicates is possible just southwest of the Roundtop Klippe. His mapping of the Thunderhead sandstone intersected the Cades Sandstone as Neuman and Nelson (1965) mapped it eastward. Lack of definitive field evidence for either a stratigraphic or structural contact between the two resulted in the dashed fault contact on King's (1964) map (Neuman, pers. comm.).

Greenbrier Fault

The Greenbrier Fault along the klippe's northwestern edge could only be constrained to within three meters because good exposures are limited. The Thunderhead there is upright, as shown by scour-and-fill structures. Metcalf Phyllite underlies the Thunderhead and is characterized by what appear to be slivers of Thunderhead Sandstone within the fault zone.

The two windows through the klippe as mapped by King (1964) were remapped with a slight change in shape of the larger of the two. A third, apparently very small window is found about 150 meters west-northwest of the 1420 foot bench mark along highway 73, where the Sinks Fault is cut

16

by the high angle fault which borders the klippe. This window is only exposed along its northeastern side as a 15-20 m long overhanging outcrop. The overlying Thunderhead is highly broken and entrained in the fault zone as meter-scale slivers completely surrounded by Metcalf Phyllite (Figure 5). The larger window of the two mapped by King (1964) displays the same features and is better exposed (Figure 6).

These three windows through the Greenbrier Fault allow the construction of a structure contour map of the Greenbrier Fault underlying the klippe (Figure 7). The fault surface dips south and shows some warping and complex folding in the vicinity of the two windows near Metcalf Bottoms.

The main trace of the Greenbrier Fault as mapped by King (1964) was not modified, although additional orientation data were collected. The Greenbrier Fault is imbricated above the cliffs which flank the northwestern part of Curry He Mountain east of the Sinks. This imbrication is seen as repetition of the fault contact, with Thunderhead Sandstone overlying Metcalf Phyllite. Several small exposures in this area show well exposed Thunderhead cropping out above less well exposed but well-cleaved Metcalf. This Metcalf shows a penetrative first generation cleavage. Due to the extremely steep

Figure 5. Photograph of the Greenbrier Fault at the window through the Greenbrier Fault at the klippe's southwestern corner. Above is massive Thunderhead Sandstone, whereas below is the Metcalf Phyllite. At the middle of the photograph the fault zone is characterized by meter-scale slivers of Thunderhead (T) enveloped by Metcalf (M). Photo taken at locality 181 (Figure 1, page 2). The horizontal field of view is approximately 13 m.
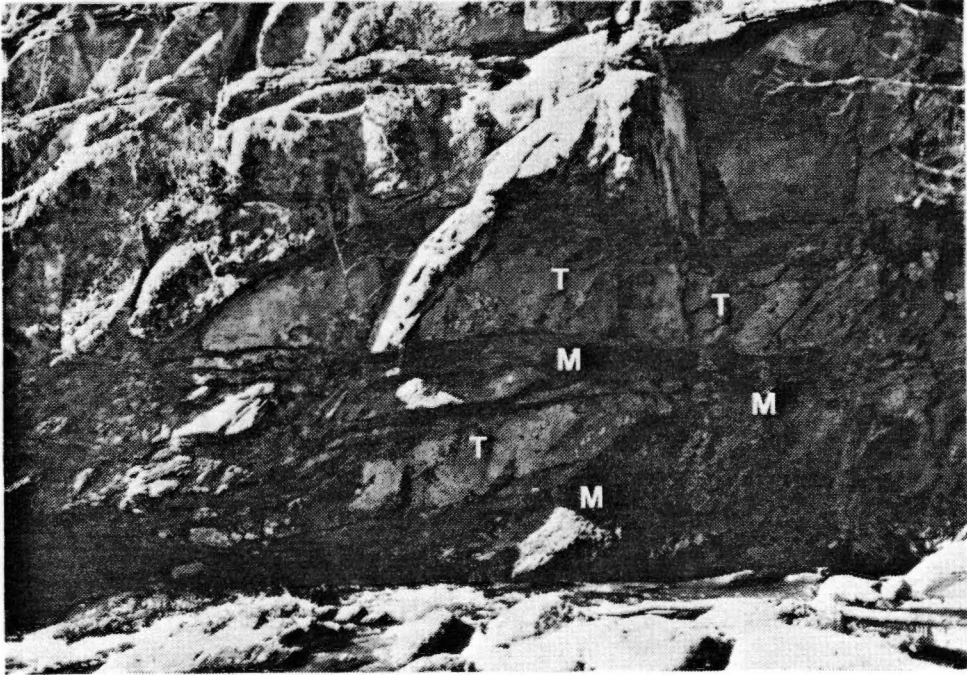
Figure 6. Photograph of the Greenbrier Fault at the large window through the Greenbrier Fault along the Klippe's southeastern margin described by King (1964). The fault zone is characterized by meter-scale slivers of Thunderhead (T) enveloped by Metcalf (M). Photo taken at locality 75 (Figure 1, page 2). The horizontal field of view is approximately 15 m.
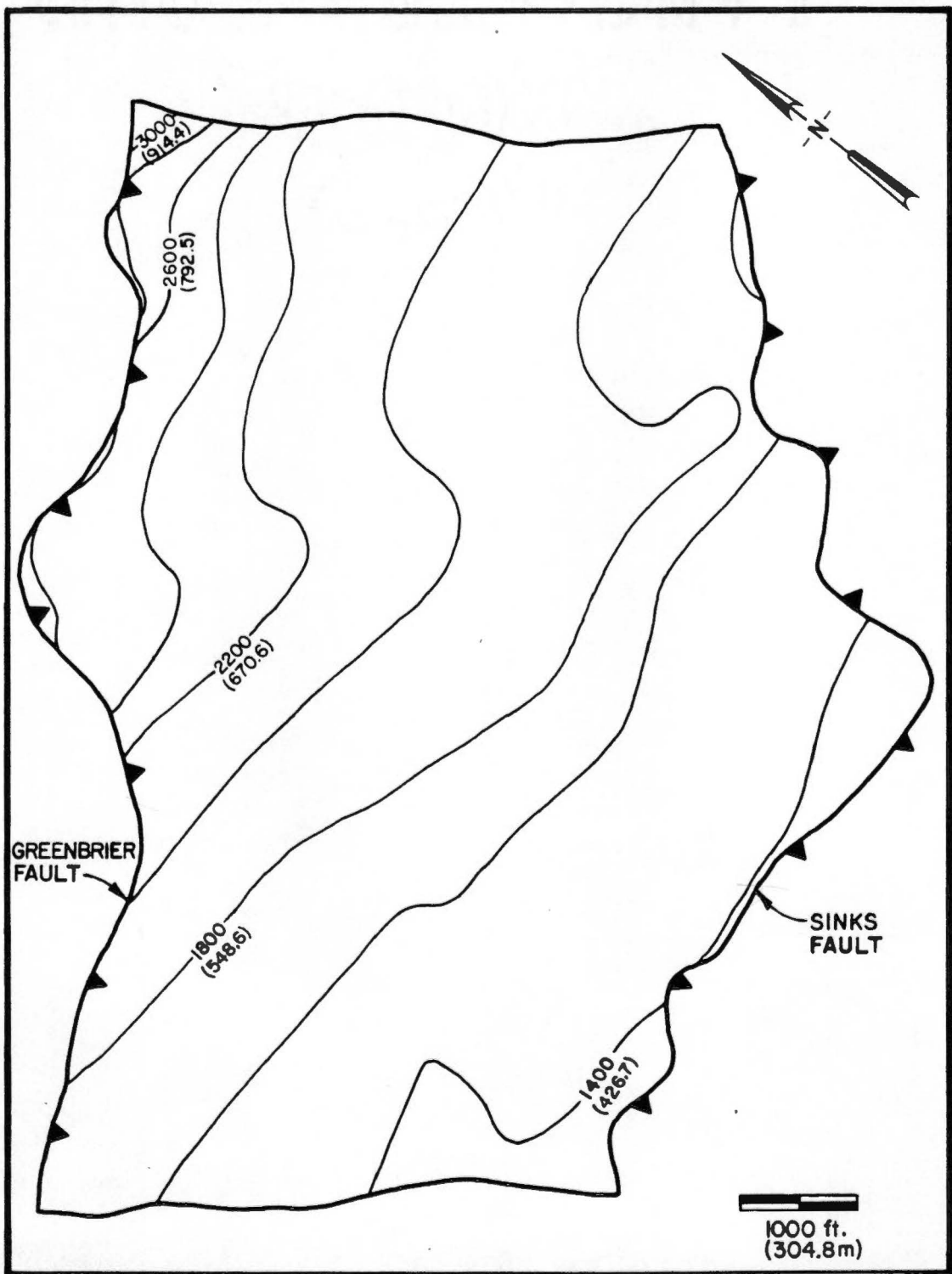
Figure 7. Structure contour map of the Greenbrier Fault underlying the Roundtop Klippe. Contour lines are relative to mean sea level. The metric equivalents of the elevations are given in the parenthesis.

20

topography along the cliffs below this area, the location of the lowest and thus northwesternmost occurrence of the main body of the Greenbrier Thrust sheet was not mapped any differently from the report of King (1964). The geometry of the Greenbrier Fault of the main sheet is variable, as indicated by examining the map pattern of the fault.

Sinks Fault

The Sinks Fault was mapped by King (1964) as a thrust fault that propagated from the southeast to the northwest and thereby isolated the rocks of the Roundtop Klippe. West of the Sinks along the Little River Gorge, King (1964) mapped the Sinks Fault with a dashed contact, indicating a lack of control on its position. During this study the position of the Sinks Fault along this part of the Little River was mapped closely for approximately 360 m.

A variety of styles are displayed along the Sinks Fault in several locations. Along Meigs Creek and above Meigs Falls, the fault zone is approximately 30 m wide and is characterized by meter-scale and centimeter-scale layers of Thunderhead surrounded by Metcalf. The Metcalf shows two generations of cleavage at moderate angles to

one another (discussion in later section). The first is a phyllitic foliation and the second a poorly developed crenulation cleavage. The layers of Thunderhead surrounded by Metcalf appear to be fault slivers.

The Thunderhead north of the Sinks contains several minor fault zones which dip less steeply than the bedding, which is overturned. These minor faults are similar in orientation to the adjacent Sinks Fault and appear to be contractional, as indicated by a repeated quartz vein offset by one of them (Figure 8). Offset of this vein and of bedding is minimal. These faults are inferred to be minor imbricates of the Sinks Fault. They cut up stratigraphic section from southeast to northwest, in beds which had likely been already overturned.

At locality 45 (Figure 1) along highway 73 near Meigs Falls, minor fault zones are found within the Thunderhead Sandstone. Two sets of fault zones are found in the upright beds which dip 45° to 50° northeast, one oriented at $N68^OE$, 52^OSE and the other generally at $N70^OW$, 43^OSW. These faults show slickensides and mineral growth lineations on their surfaces. The latter gives the better exposed fault surfaces a stepped appearance (Figure 9). The mineral growth lineations on the fault surface are oriented $N68^OE$, 52^OSE, with trend and plunge $S49^OE$, 45°. The steps created by the mineral growths
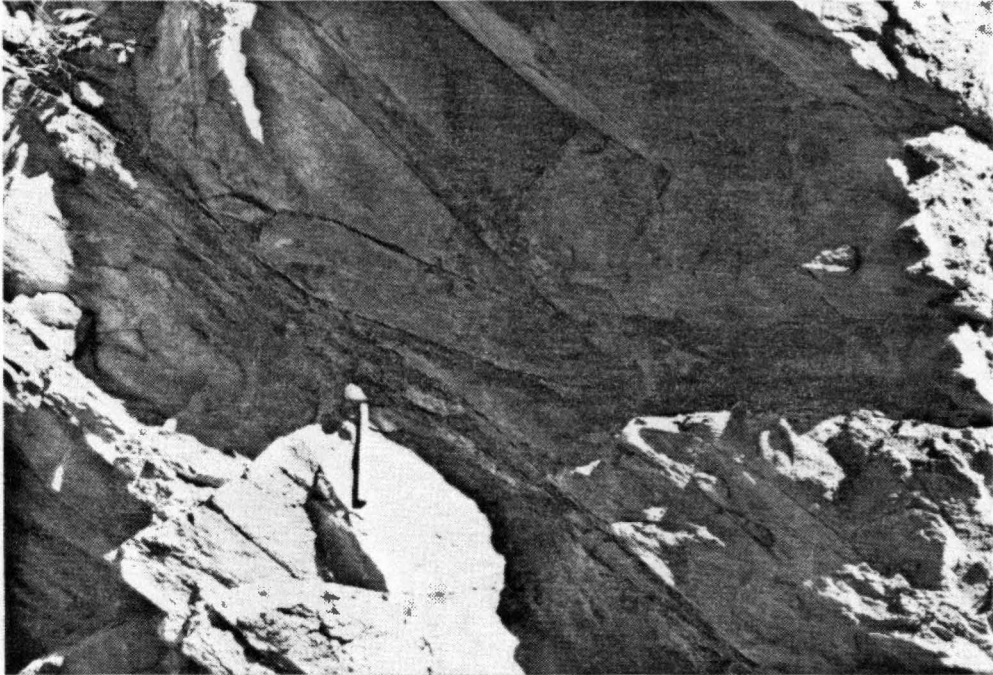
Figure 8. Photograph of a minor fault cutting beds of Thunderhead Sandstone at a lower angle than bedding. Bedding is seen dipping from upper left to lower right (southeast) and the fault is seen cutting bedding with a dip more shallow than that of the Thunderhead. The quartz vein to the right of the hammer is repeated by the fault, indicating that the fault is contractional. Bedding here is overturned, as indicated by graded bedding and cross-stratification (King, 1964). Photo taken at locality 97 (Figure 1, page 2). The hammer at left-center is for scale.
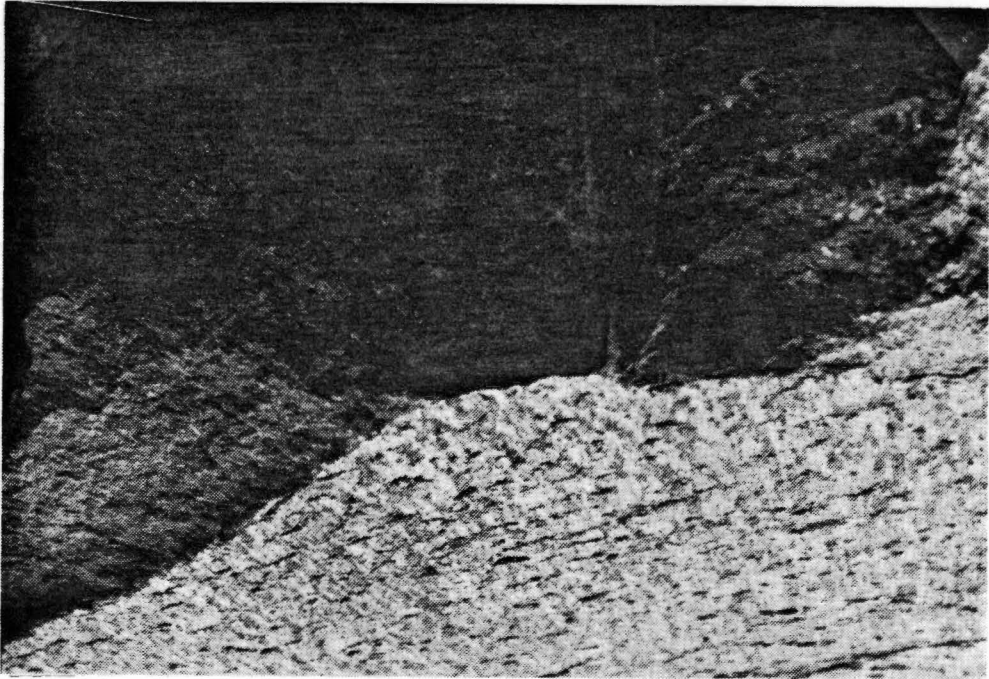
Figure 9. Fault surface within the Thunderhead Sandstone
which displays stepped appearance due to fibrous mineral
growth. Photo taken at locality 45 (Figure 1, page 2).
The horizontal field of view is approximately 45 cm.

step downward toward the southeast and thus indicate movement along this fault in this direction (Durney and Ramsay, 1973). The fault displaying these mineral growths is almost parallel to the Sinks Fault to the south, yet it shows movement sense opposite that of the Sinks Fault.

High-Angle Faults

The two high-angle faults which border the Roundtop Klippe on the northeast and southwest as mapped by King (1964) were not significantly modified in this study. Exposure of these faults is very limited and they were mapped largely by float. The fault along the northeastern border of the klippe was located within several meters using outcrops along the trail from the Wear Cove Gap, and outcrops topographically below the trail.

King (1964) indicated that the fault along the klippe's southwestern border shows oblique movement, with left lateral strike-slip motion. This could not be confirmed in the field, yet it is consistent with the structure contour map of the Greenbrier Fault (Figure 7) which shows the fault dipping south. This high angle

25

fault also cuts the Greenbrier Fault, and offsets it near the klippe's southern corner.

Other Structural Features

As King (1964) indicated, the beds of Thunderhead sandstone in the southeastern part of the klippe, near the Sinks, are overturned and dip southeast 40°-45°. This is clearly indicated by truncated cross-beds exposed in the cliffs overlooking the Sinks, just south of the parking area. Overturned graded beds are also seen here as well as just north of the Sinks in the cliffs along Highway 73. These beds make up the overturned limb of the recumbent synform, which trends east-northeast along this southeasternmost edge of the klippe. The overturned limb is only preserved in this area. The fold geometry of this synform is not parellel to the adjacent antiform on the northwest, whose axis plunges shallowly almost due east.

Bedding within the Thunderhead Sandstone of the main body of the Greenbrier Thrust sheet is upright and generally dips about 45° southeast. Outcrop-scale folds within the sheet are not observed away from Highway 73 probably due to poor exposure. Along Highway 73 at the

eastern edge of the Wear Cove quadrangle, a synform in the Thunderhead occurs in the vicinity of Watertank Branch.

Structural Fabrics

Structural fabrics within the study area are described below. Included here is a description of the cleavages found in the Metcalf and the tectonic lineations found in the Thunderhead.

Deformed Thunderhead Sandstone

Throughout the study area the Thunderhead Sandstone is deformed to varying degrees. This most commonly occurs as a tectonic lineation of quartz and feldspar grains in sandstone, or as tight, centimeter-scale folds in the argillite. These argillite strata also display variably developed first-and second-generation cleavages. The first-generation cleavage gives the rock a slaty appearance whereas the second, where present, crenulates the first.

Undeformed or weakly deformed argillite lithologies are found as partings between beds of sandstone. Deformation in these partings, where present, is

displayed as a first generation cleavage characterized by phyllosilicate mineral grains showing strong preferred orientation parallel to bedding. This fabric can be described as a bedding fissility.

Deformed argillite lithologies are found in the bed of the Little River along the Roundtop Klippe's southwestern border near the quarry (Figure 1). These strongly deformed argillite strata are characterized by two generations of cleavage, and in some locations, folds and minor faults. The first- generation cleavage appears to obliterate bedding, and is made up of mica grains showing strong preferred orientation. The second-generation cleavage crenulates the first generation cleavage about planes which cut the latter at moderate to high angles. Tight, centimeter-scale folds occur in these argillite units at locality 94 (Figure 1). These fold layers which appear to be bedding are defined by fine grained pyrite trains. The core of one of these folds shows a small scale wedge fault.

Sandstone and conglomerate beds of the Thunderhead show a variably developed tectonic lineation, characterized by quartz and feldspar grains with strong preferred orientation. The feldspar grains show brittle fractures along mineralogic cleavage planes oriented perpendicular to the direction of the lineation. It

appears that the feldspar grains adjusted during whole rock strain by rotation and behaved brittly as strains continued. Quartz grains also show elongation in the direction of the tectonic lineation, although they do not show brittle features associated with this.

Deformed Metcalf Phyllite

Deformation features in the Metcalf Phyllite in the vicinity of the study area include two generations of cleavage, small-scale fault zones, and type II S-C mylonites (Lister and Snoke, 1984).

Two generations of cleavage are common, but are not always present. The first is always a dominant phyllitic foliation and is characterized by a strong preferred orientation of phyllosilicate mineral grains. This cleavage and subsequent cleavages generally obliterate bedding in the Metcalf in the vicinity of the Roundtop Klippe. In contrast, the Metcalf along the Cades Cove Road east of Cades Cove is, in places, silty to sandy, and consequently bedding is preserved. The first generation cleavage imparts the phyllitic "sheen" on the rock, which is mostly the result of high concentrations of metamorphic minerals (i.e., muscovite and sericite).

The second-generation cleavage either crenulates the

first, or it is well-developed enough to create C-bands (Figure 10) and thus form type II S-C mylonites (Lister and Snoke, 1984). The crenulation cleavage generally cuts the first-generation cleavage at moderate to high angles and is defined by aligned phyllosilicate grains.

The second generation cleavage which results in type II S-C mylonites generally cuts the first generation cleavage at moderate to low angles along closely spaced planes (e.g., 1-2 cm spaces). These crenulation planes are referred to as C-bands, and are defined by phyllosilicate grains showing strong preferred orientation (Lister and Snoke, 1984). King (1964) referred to this mylonitic fabric as "shear cleavage". Mapping reveals that the Metcalf contains these mylonites in zones that vary in thickness from several cm to more than 10 m, both southwest and northwest of the Roundtop Klippe (e.g., locality 167, Figure 1). Mylonites of this sort are less well-developed in the Metcalf directly northeast and southeast of the klippe, although they are present, contrary to Witherspoon's (1981) report.

The S-C mylonitic fabric or shear band cleavage is very common, both beneath the Roundtop Klippe and within the fault slice of Cades Sandstone southwest of it. Thus both the Cades and Thunderhead seem to have been transported together above the largest S-C mylonite zone.

30
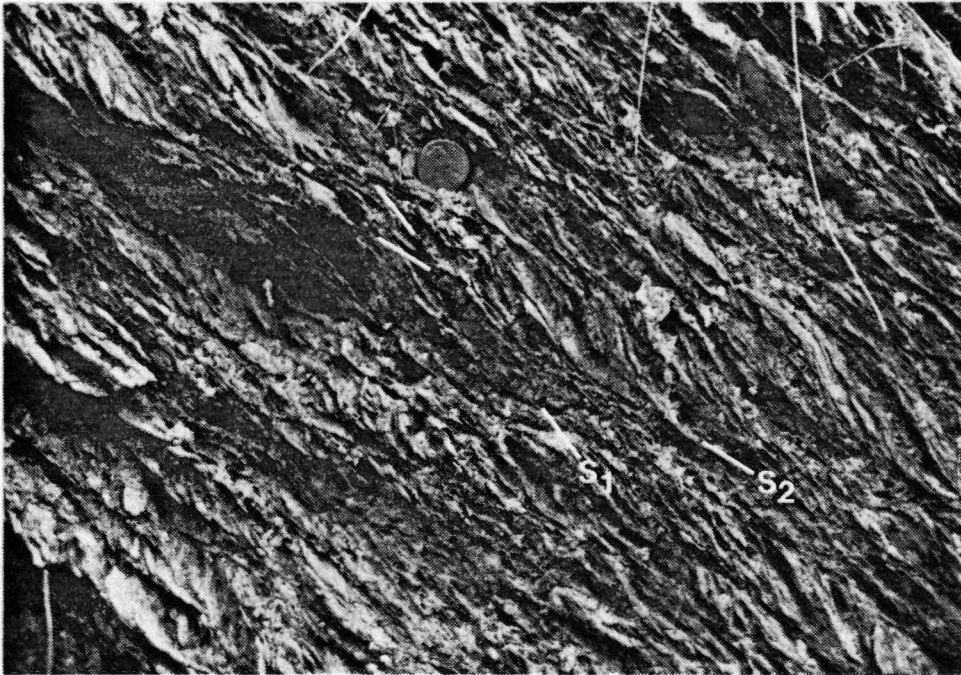
Figure 10. Photograph of well-developed Type II S-C mylonite within the Metcalf phyllite at locality 145 (Figure 1, page 2). The second generation cleavage (S_2) cuts the first generation cleavage (S_1) into C-bands. The figure displays the highly deformed nature of the Metcalf in the study area. Penny at upper-middle for scale.

Minor fault zones within the Metcalf are found in the study area, but are difficult to trace for any significant distances. A small-scale fault zone is found at locality 52 (Figure 1) just southwest of the klippe (Figure 11). This fault can be traced across the outcrop for about 8 m in a highly deformed zone. This fault zone displays an undulating geometry and shows several surfaces of movement. These surfaces show slickensides and fibrous mineral growth lineations in many orientations in an overlapping array. Due to the highly cleaved nature of the Metcalf in the study area these fault zones are extremely difficult to locate and/or trace.
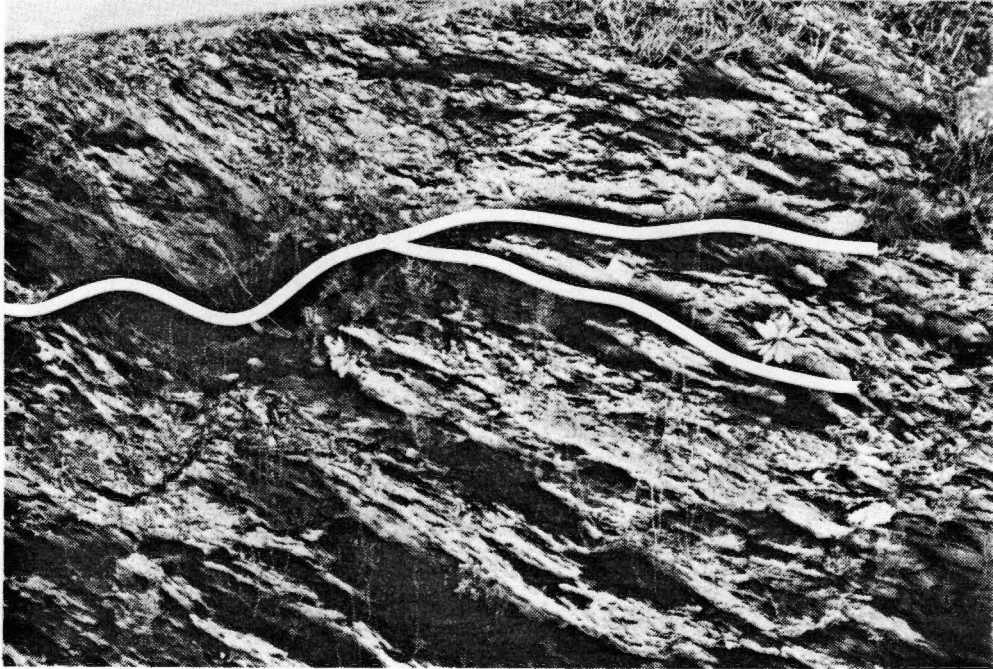
Figure 11. Photograph of minor fault in the Metcalf Phyllite showing the complexity of the various movement surfaces. The fault surfaces are indicated by the white lines. Photo taken at locality 52 (Figure 1, page 2). The horizontal field of view is approximately 10 m.

CHAPTER III

STRAIN ANALYSIS RESULTS

Discussion Of Geologic Strain

Strain can be described as the change in shape that results from stress. In rocks the evaluation of strain is very important. A deformed geologic material generally has a complex strain path in which the material has passed from its initial state, through various stages of deformation to arrive at its final state (Ramsay, 1967). This is known as progressive deformation and can be described theoretically as the modification of a particular state of strain by small, incremental distortions called infinitesimal strains (Ramsay, 1967). The final product of progressive deformation by geologic processes is called the finite state of strain or simply the finite strain.

Through studying the deformation of objects of known original shape embedded in rocks, geologists can describe the finite strains within mappable rock bodies. This quantitatative data can be helpful in describing the structural geometry, as well as the deformation history

34

of an area. As mentioned above, the final state of strain in a rock body is not enough to allow the description of the states of stress that were responsible for the deformation. However, in conjunction with detailed mapping it gives an idea of the significant structural features to consider in describing possible strain "events" and thus insight about the deformation history.

For the present study, finite strain was calculated for samples of Thunderhead sandstone using both the Fry method (Fry, 1979) and the R_f/ϕ method (Ramsay, 1967; Dunnet, 1969; and Lisle, 1977). The details of both methods are included in Appendix B. The remainder of this chapter is devoted to describing the results of the finite strain analyses and how these relate to the structural geometry of the study area.

Large samples are designated by the letter T, followed by a one, or two digit number. Small samples were cut from these bulk samples, on three mutually perpendicular sides, designated xy, xz, and yz. The small samples were used for the the strain analyses and throughout the remainder of the text are referred to with their appropriate suffixes (e.g., xz).

Fry Method

The Fry method creates a graphical estimate of strain based on the distribution of grain centers in two dimensions. This distribution is controlled by how close grain centers are to one another. During deformation this distribution changes as the grains change shape. As grains become elongate the grain centers move farther apart in the direction of elongation. As grains flatten the grain centers become closer to one another in the direction of flattening. The strain fabric of a rock in two dimensions can therefore be estimated by the distribution of grain centers.

In samples where the grains are spaced in a nearly homogeneously deformed matrix the Fry method yields an estimate of the matrix strain, whereas in samples where the grains themselves have deformed the method yields an estimate of grain strain (Fry, 1979). Measurements of matrix strain are essentially estimates of bulk strain because components of grain strain are incorporated in the data set in this method. For this reason, estimates of matrix strain generated by the Fry method tend to be higher than estimates of grain strain (e.g., using the R_f/ϕ method).

The Fry method proved quick and easy to use, and it

yielded data generally in agreement with the two-dimensional data from the R_f/ϕ method.

In spite of easy application and conceptual simplicity, the Fry method has several shortcomings. The most fundamental for this study is that the two-dimensional results which it yields cannot be easily transformed to give the three dimensional strain ellipsoid. This makes comparison with the easily generated three dimensional data from the R_f/ϕ and PASE5 computer programs difficult.

Another problem with the Fry method deals with the operator's choice of grain sizes used in the analyses. It became apparent, when using the Fry method program of Kligfield et al. (1982), that in order to generate a void ellipse of uniform shape, a fairly consistent grain size must be used. This rule cannot always be adhered to, and consequently, the form of the void ellipses may be unclear due to several points scattered within the area of the void ellipse (Figure 12). This can lead to problems in determining the orientation and magnitude of the void ellipse.

A problem that appears in some instances to relate to the grain size problem discussed above is that low-strain samples tend to yield ambiguous results. For a low strain sample the orientation of the strain ellipse

37
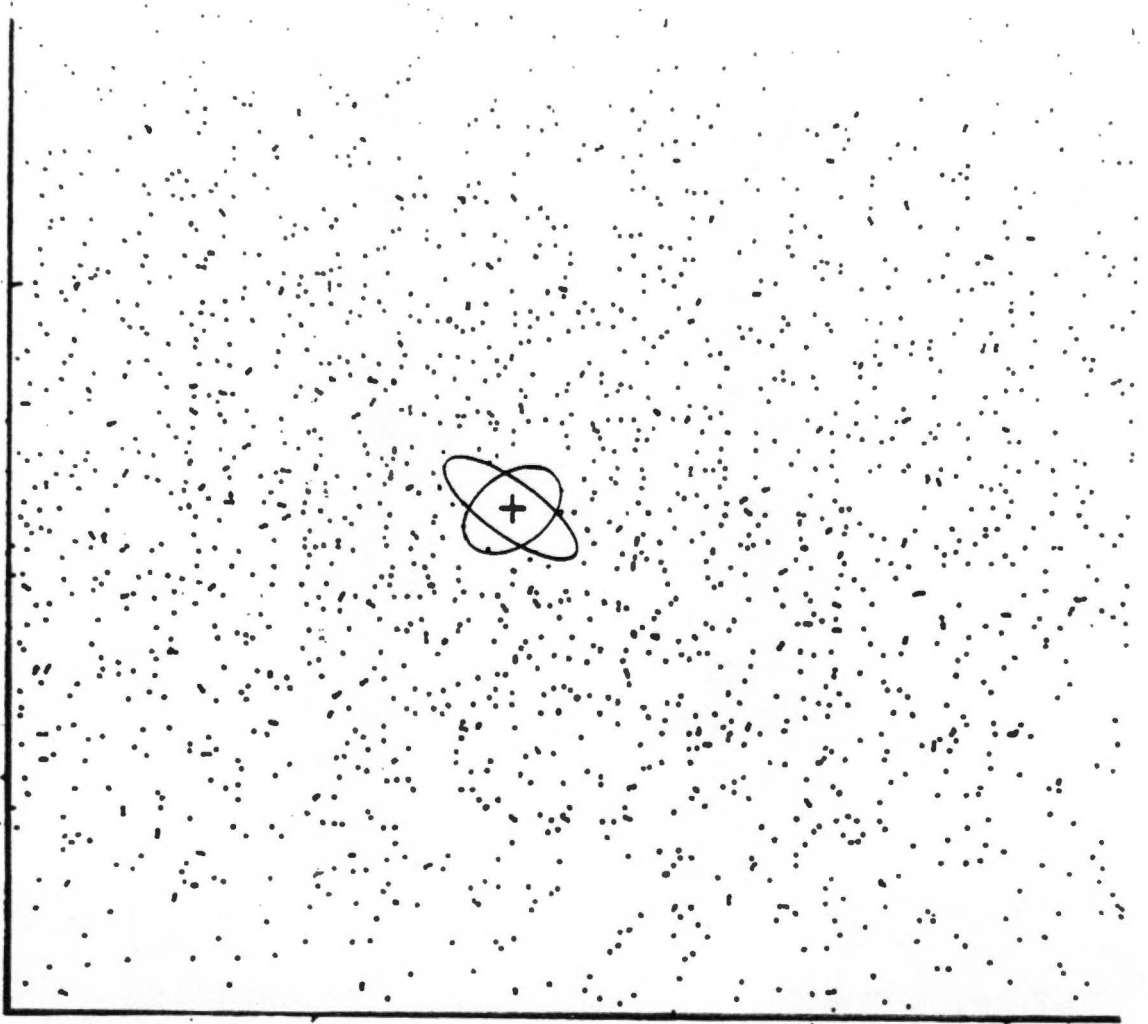
Figure 12. Plot generated by the Fry method for sample
T29xz. This plot is an example of the ambiguous nature
of some of the void ellipses generated with this method.
It is difficult to establish the form of the ellipse due
to "scattered" points at the plot's center. Two
interpretations are included to demonstrate this problem.

long axis is difficult to determine, because the ellipse has a low aspect ratio and the method creates a spread of points that often contain "strays". As discussed above, when grains of varying sizes are used in a Fry analysis the void ellipse becomes cluttered with points. These "stray" points within the void ellipse are the result of using closely spaced grains that are smaller than those used for the bulk of the analysis.

The T49xz sample demonstrates the ambiguity encountered in determining the ellipse long axis using the Fry method, due to an unclear point distribution. Without knowledge of the sample's appearance two possible long axes could be "seen". After examining the xz surface the proper choice was easily made.

As these problems indicate, the Fry method's usefulness is limited in low-strain samples, and in samples with poor grain-size sorting. The method is also limited for this study because comparison between the three-dimensional results of the R_f/ϕ method and the Fry method is difficult, because the latter are not easily calculated. It is, however, important that the Fry method quickly yielded two dimensional results that can be compared to the two dimensional results of the R_f/ϕ method.

R_f/ϕ Method

The R_f/ϕ method describes strain by comparing the axial ratios and orientations of individual grains in two dimensions. The finite strain can be estimated by plotting the orientation data on a linear scale against the axial ratio data on a logarithmic scale. The resulting point distibution is then used to measure and describe the strain in two dimensions. The quality of the data can then be checked by the theta-curve computer program, which sequentially "removes" the strain from the sample data until the most uniform point distribution is attained. The amount of strain "removed" corresponds to the reciprocal strain ellipse and should be in close agreement to the amount of strain calculated by the R_f/o method. R_f/ϕ data from three mutually perpendicular sides of a rock sample can be further evaluated using the PASE5 computer program to yield an estimate of the three dimensional strain ellipsoid.

The R_f/ϕ method was used to analyze strain in the 17 samples collected for this study. The theta-curve method was implemented to check the results of the R_f/ϕ method. The magnitudes and orientations of the ellipses generated by the theta-curve method are in close agreement with those obtained with R_f/ϕ. These theta-curve ellipses

were run in the PASE5 program to give the strain
ellipsoids. The ellipsoids calculated in this fashion
are also in agreement with those calculated with the R_f/ϕ
method. The theta-curve method thus proved to be a
useful check of the R_f/ϕ data. Because the R_f/ϕ
technique yields accurate data which match those of the
theta-curve method, the results of the R_f/ϕ method are
used as the basis of this study.

Fry Method Versus R_f/ϕ Method

For surfaces showing high strain the ellipse long
axes of the Fry method tend to be parallel to those of
the R_f/ϕ method. For these high strains the magnitudes
of strain determined by the Fry technique tend to be
slightly greater than those by R_f/ϕ. For example, side
xy of T56 has R_s equal to 2.08 as calculated by R_f/ϕ
versus 2.21 by the Fry method. In some instances the Fry
value is significantly greater than the R_f/ϕ value. The
xz side of T49, for example, has an R_s value of 1.90 via
the R_f/ϕ method and an R_s of 4.11 by the Fry method. A
similar result was found for T34xz. The fact that the
Fry results tend to be higher than the R_f/ϕ results for
high strain samples is reasonable since the former yields
an estimate of whole-rock strain including a component of

41

matrix strain (Fry, 1979). Matrix strain is generally higher than grain strain because the matrix minerals are smaller, and tend to rotate and/or recrystallize more readily.

An important point to consider in light of the comparison of these two methods is that the R_f/ϕ method may systematically underestimate the strains by not considering matrix strain. As indicated above the Fry method indicates that the Thunderhead Sandstone probably shows a ductility contrast between its grains and matrix. Many recent workers have nonetheless used this method with apparent success on graywacke lithologies and it is therefore concluded that the R_f/ϕ data presented below are representative of the strain in the Thunderhead Sandstone.

Trends In The R_f/ϕ Data

Seventeen strain measurements were made at 14 localities across the area of study (Figure 13). Ten were made along the klippe's southeastern margin, in the well exposed Thunderhead along Highway 73, and seven were made in the Thunderhead along the northwestern edge of the Greenbrier thrust sheet. Each calculated strain ellipsoid was considered relative to other structural

Figure 13. Results of 17 strain calculations by the R_f/ϕ method. The data are presented as plots of principal strain axes lambda$_1$, lambda$_2$, and lambda$_3$, on lower hemisphere equal-area projections. Bedding is indicated by a great circle. Sample collection localities are indicated by the curved lines. GF=Greenbrier Fault, SF=Sinks Fault, LSF=Line Springs Fault, GSF=Great Smoky Fault, MBF=Mannis Branch Fault, OF=Oconaluftee Fault.

LEGEND

	p€wc & Ok
	p€c
	p€t
	p€e
	p€m

N

0   ½   1

MILE

GREENBRIER FAULT

44
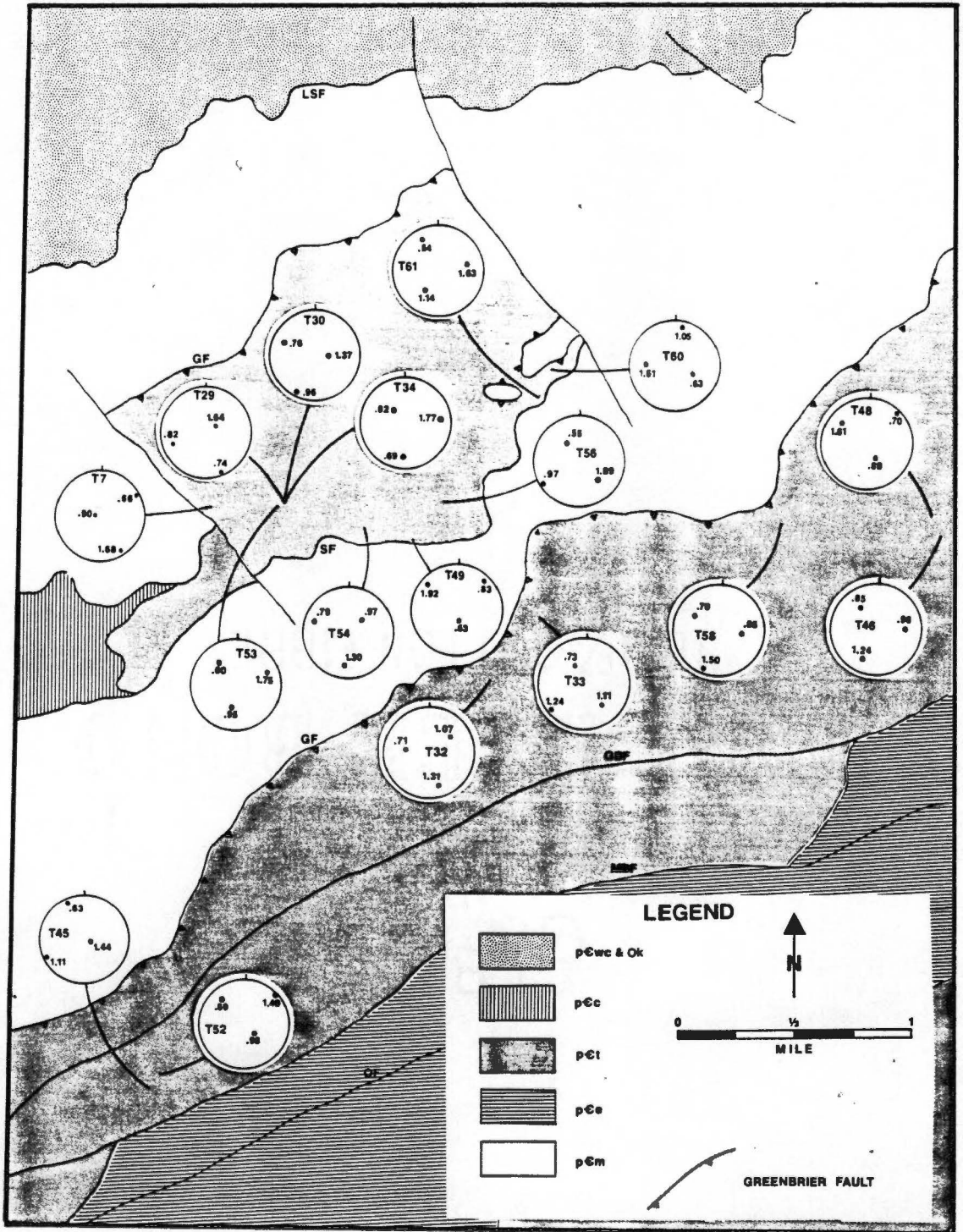
features to determine the geometric relations between the strain field and the major structures.

Strain magnitudes varied with lambda$_1$ (maximum extension) having a low value of 1.24 and a high value of 1.92. Lambda$_2$ (intermediate extension) varied from 0.82 to 1.14 whereas lambda$_3$ (minimum extension or maximum shortening) varied from 0.54 to 0.85. Maximum strain ratios (i.e., the lambda$_1$/lambda$_3$ ratios) thus varied from a low of 1.46 (sample T46) to a high of 3.44 (sample T56).

Strain Relative to Bedding

Although few consistent geometric relations between strain and structural elements are apparent, eight samples show the lambda$_1$-lambda$_2$ plane of the strain ellipsoid nearly lying within bedding. These are samples T32, T33, T34, T49, T52, T56, T58, and T61.

Four of these are from the main Greenbrier sheet. These four, T32, T33, T52, and T58, are distributed along the front of the thrust sheet. Of these four the two samples taken from nearest the outlier (T32 and T33) show more flattening relative to stretching than the other two. The lambda$_1$-lambda$_2$ plane is 25° from bedding in T32 and 17° from bedding in T33. The latter shows 27.03%

45

flattening to 23.85% stretching, whereas the former shows 28.93% flattening to 30.89% stretching. Based on three point solutions for fault orientation, T32 was collected an estimated 127 m above the Greenbrier Fault and T33 an estimated 216 m. The other two samples showing $lambda_1$-$lambda_2$ near bedding (T52 and T58) were collected geographically farther from the Greenbrier Fault trace than T32 and T33, although T58 was taken an estimated 542 feet above the fault. These two samples show stretching percentages significantly greater than flattening percentages. Sample T52, taken an estimated 331 m above the Greenbrier Fault, shows 31.21% flattening versus 49.08% stretching, whereas T58 shows 30.36% flattening versus 50.40% stretching. The $lambda_1$-$lambda_2$ plane of T52 is 38° from bedding versus 29° for T58.

These four samples from the Greenbrier thrust sheet show a weak correlation between proximity to the Greenbrier thrust and the angle between bedding and the $lambda_1$-$lambda_2$ plane (Figure 14). This angle, decreases from 38° in sample T52 (331 m) to 25° in sample T32 (127 m). Sample T33 is anomalous because it lies 216 m from the fault yet has a 17° angular relationship between these two features. This may be due to its relatively low strain and relatively high matrix percentage (15%). That is, the higher matrix percentage might be

Figure 14. Strain analysis results and the geometric relationships displayed by each sample. Column headings are indicated by the following abbreviations: K/S=Klippe sample/Greenbrier Thrust sheet sample, Q=quartz, F=feldspar, M=matrix, S_O=bedding orientation, GF=Greenbrier Fault orientation, SF=Sinks Fault orientation, =the angle between.

SAMPLE			LITHOLOGY			PRINCIPAL STRAINS			GEOMETRIC RELATIONSHIPS					
SAMPLE NUMBER	LOCATION	K/S	%Q	%F	%M	λ_1	λ_2	λ_3	So∠$\lambda_1\lambda_2$	So∠$\lambda_1\lambda_3$	GF∠$\lambda_1\lambda_2$	GF∠$\lambda_1\lambda_3$	SF∠$\lambda_1\lambda_2$	SF∠$\lambda_1\lambda_3$
T7	54	K	65	20	15	1.68	.90	.66	54°	38°		15°		40°
T29	45	K	50	30	20	1.64	.82	.74	89°	34°			43°	
T30	45	K	50	30	20	1.37	.96	.76	58°	39°			35°	
T32	139	S	75	15	10	1.31	1.07	.71	25°		33°			
T33	141	S	60	25	15	1.24	1.11	.73	17°		21°			
T34	45	K	60	25	15	1.77	.82	.69	38°			28°		25°
T45	148	S	72	17	11	1.43	1.11	.63	68°	68°	35°			
T46	141	S	45	37	18	1.24	.96	.85	62°	49°				
T48	152	S	40	40	20	1.61	.89	.70		49°	29°			
T49	102	K	55	30	15	1.92	.83	.63	42°		31°		40°	
T52	154	S	52	38	10	1.49	.98	.69	38°		12°			
T53	45	K	55	35	10	1.75	.95	.60	73°	33°			13°	
T54	155	K	75	15	10	1.30	.97	.79				32°		26°
T56	156	K	55	40	5	1.89	.97	.55	13°		34°		20°	
T58	159	S	50	31	19	1.50	.95	.70	29°		34°			
T60	18	K	60	35	5	1.51	1.05	.63						38°
T61	160	K	50	35	15	1.63	1.14	.54	15°	74°			18°	

48

responsible for the relatively low angle between the λ_1-λ_2 plane and bedding, in much the same way that cleavage tends to refract from low angles to bedding in shaly rocks, to higher angles in sandy rocks (Ramsay, 1967). Cleavage occurs along the λ_1-λ_2 plane of strain (Ramsay, 1967), and therefore the latter should be expected to reflect orientation changes much the way cleavage does.

Samples T34, T49, T56, and T61 are from the Roundtop Klippe and as mentioned also show the λ_1-λ_2 plane nearly parallel to bedding. In samples T56 and T61 the λ_1-λ_2 plane is closer to bedding than in the four samples from the main sheet already discussed, 13° in T56 and 15° in T61. Samples T34 and T49 contain λ_1-λ_2 38° and 42° from bedding respectively. All four of these samples from the outlier show stretching percentages significantly higher than shortening, and all are estimated to be less than 61 m above the Greenbrier Fault, with T34 only 6 m above the fault. These estimates are based on map pattern and the structure contour map constructed for the Greenbrier Fault as it underlies the outlier (Figure 7)

When plotted on a Flinn diagram (Flinn, 1962) three of the eight samples showing bedding parallel or subparallel to λ_1-λ_2, have K values less than

49

unity and thus fall in the apparent flattening field (Figure 15a). These three, T32, T33, and T61, thus show oblate spheroid strain ellipsoids. Only two other samples in the study have K values less than one. These are T45, taken from the main sheet, and T60, taken from the outlier. Flattening in these two shows no apparent geometric relationship with respect to bedding.

Twelve of the seventeen samples of this study thus fall in the apparent stretching field of Flinn (1962)(Figure 15b). This indicates that stretching is dominant over flattening in the Thunderhead Sandstone and that variably developed extension dominated within the hangingwall of the Greenbrier Thrust and hanging wall of the Sinks Fault. This is typical of hanging wall rocks in thrust belts due to the complex distribution of simple shear strains during thrust propagation. Flattening is more typical of deformation due to burial and/or structural thickening, in which pure shear strains dominate.

Strain Relative to the Sinks Fault

All of the ten klippe samples also show either the lambda$_1$-lambda$_2$ or the lambda$_1$-lambda$_3$ plane at low angles to the orientation of the nearby Sinks Fault.
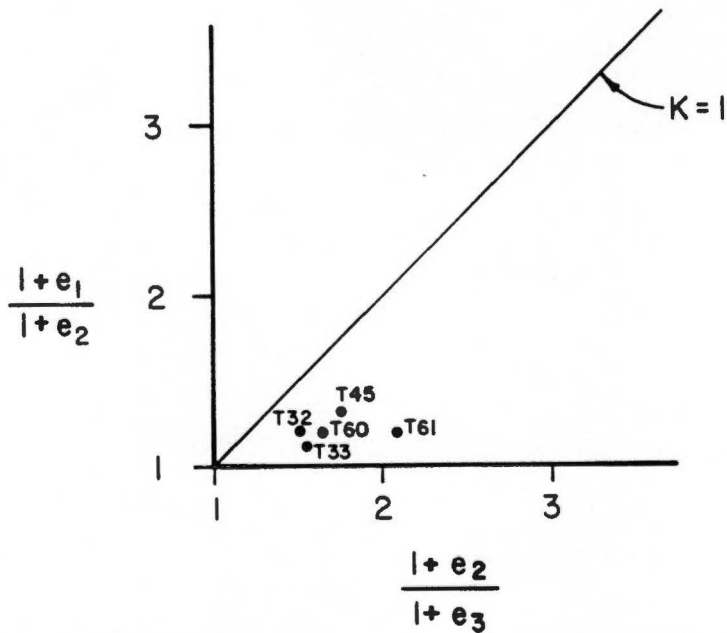
A. Flinn diagram of the five strain ellipsoids which show apparent flattening. Sample numbers are indicated on the figure.
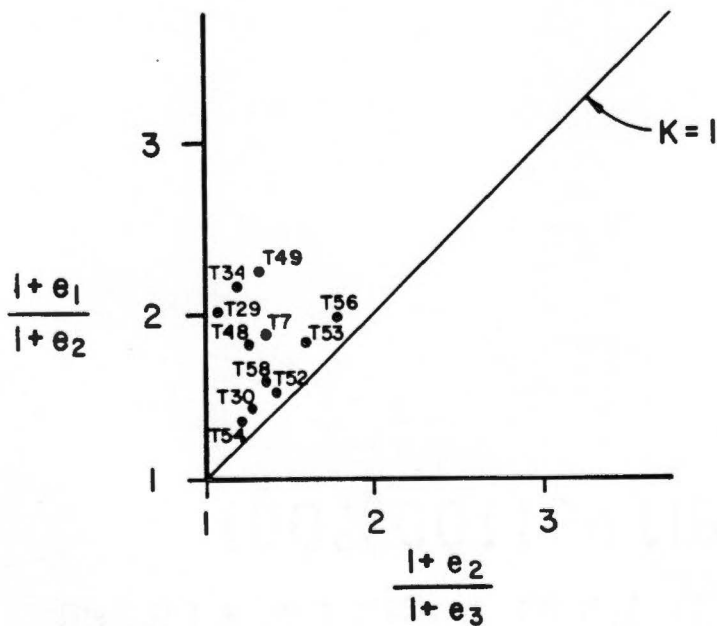
B. Flinn diagram of the twelve strain ellipsoids which show apparent stretching. Sample numbers are indicated on the figure.

Figure 15. Flinn Diagrams.

Samples T29, T30, T49, T53, T56, and T61 contain lambda_1-lambda_2 at angles from 13° to 43° to the Sinks Fault, whereas samples T7, T34, T54, and T60 contain lambda_1-lambda_3 between 25° and 40° from the Sinks Fault. Lambda_2 and lambda_3 appear to switch with one another where lambda_2 and lambda_3 are similar in magnitude. Samples from the main sheet were not compared to the orientation of the Sinks Fault.

Strain Relative to the Greenbrier Fault

Of the seven samples collected from the main Greenbrier thrust sheet, only three are from near the edge of the thrust sheet. These are T32, T33, and T58. Each of these contains the lambda_1-lambda_2 plane of the strain ellipsoid subparallel to the orientation of the Greenbrier Fault, as calculated from map relations via three point solutions. T32 shows lambda_1-lambda_2 33° from the fault, whereas T33 is at 30° and T58 at 34°.

The strain ellipsoids for all but one of the outlier samples were compared to the orientation of the Greenbrier Fault at each sample locality. The fault's orientation was estimated from the structure contour map of its surface (Figure 7). T61 was not examined because of the lack of control on the fault's orientation at this

locality. It occurs at a point where the fault surface is folded in a fashion that is hard to determine. Samples T49 and T56 contain the $lambda_1$-$lambda_2$ plane 31° and 34° from the fault plane respectively. Samples T7, T34, and T54 contain the $lambda_1$-$lambda_3$ plane 15°, 28°, and 32° from the fault respectively. Five of the outlier samples thus show either $lambda_1$-$lambda_2$ or $lambda_1$-$lambda_3$ subparallel to the Greenbrier Fault.

All four samples from locality 45 were collected from within 10 m of one another and in all four, $lambda_1$ plunges east to northeast (Figure 1). Of these four, T29 and T30 show $lambda_2$-$lambda_3$ subparallel to the fault, and sample T34 shows $lambda_1$-$lambda_3$ 28° to the fault. In contrast, sample T53 shows no apparent geometric relation with the Greenbrier Fault. In spite of the consistent orientation of $lambda_1$ in these four samples, together they show how much strain patterns can vary on the meter-scale (i.e., the principal planes vary greatly in orientation).

Summary of Geometric Relationships

The most obvious geometric relationship in the strain data is that in most cases the $lambda_1$ direction is at high angles to the thrust transport direction. The

dominance of prolate spheroids indicates variably developed extension within the thrust sheet at high angles to thrust transport and relatively low angles to bedding. Eight samples show $lambda_1-lambda_2$ from 14° to 42° from bedding. These are samples T32, T33, T34, T49, T52, T56, T58, and T61. The remainder show $lambda_1-lambda_3$ from 33° to 49° from bedding. These are samples T7, T29, T30, T46, and T53. Although the $lambda_1-lambda_3$ plane is not the geometric plane of flattening it is significant because it contains the $lambda_1$ axis or maximum extension direction. Because it also contains $lambda_3$, the direction of maximum shortening, the $lambda_1-lambda_3$ plane displays the strain ellipse with the greatest axial ratio possible for the particular strain ellipsoid.

Projection of four of the calculated strain ellipsoids into the cross sections of King (1964) shows the ellipses to be elongate and dipping toward the southeast (Figure 16). This strain geometry is typical of the leading edge of a thrust sheet in areas not adjacent to the thrust tips or lateral ramps (Coward and Potts, 1983).

Although less obvious, the geometric relationships between strain and the orientations of the Sinks and Greenbrier Faults appear to be significant. These

54
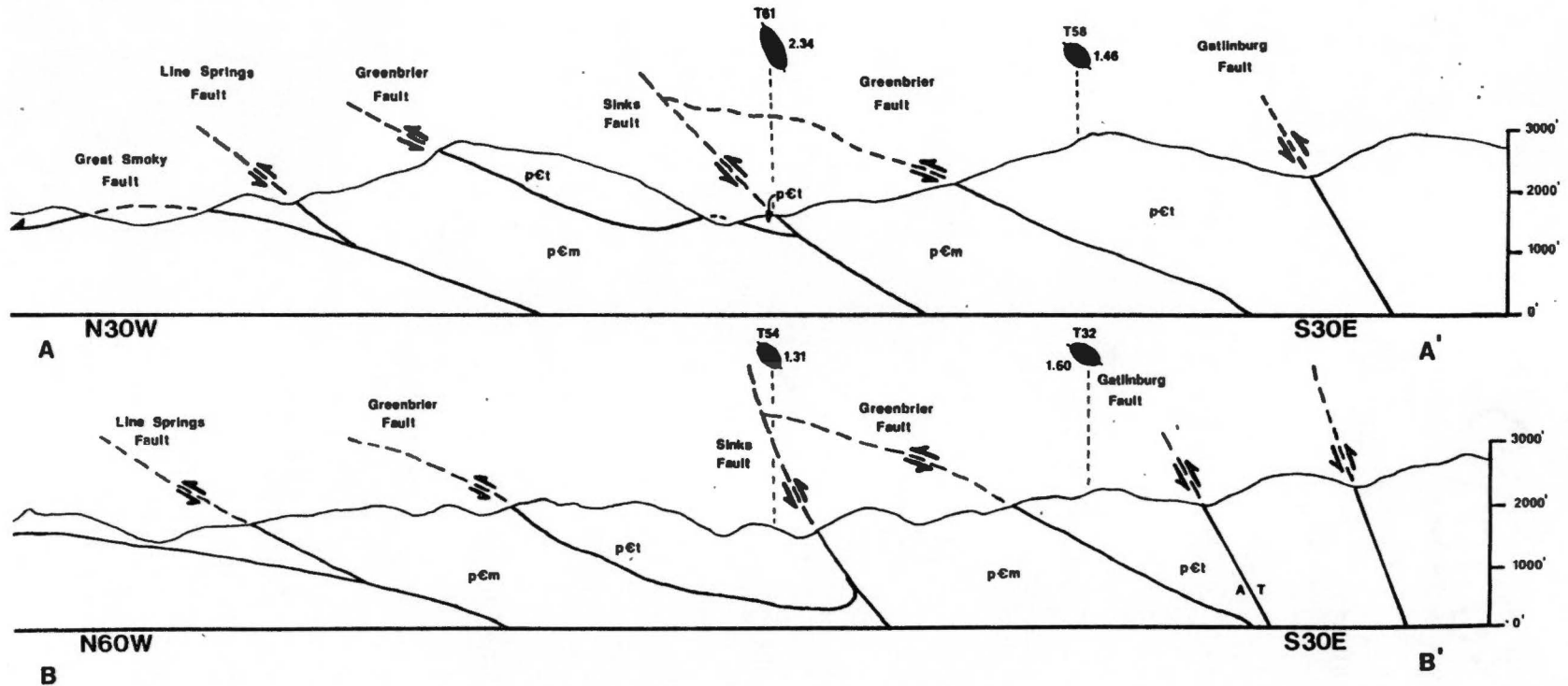
Figure 16. Projection of strain ellipsoids into the cross sections of King (1964) which pass through the study area. The resulting ellipses are elongate and dipping to the southeast. The cross section lines are indicated on Plate 1 (In pocket). The cross sections are approximately 9.5 km (6 mi) in length.

relationships appear to reflect the states of strain in the hanging wall rocks as these faults were emplaced.

The proposed sequence of strain events which effected the rocks of the study area are shown in figure 17. This model, based on the theory discussed by Mitra and Elliott (1980), Ramsay and Graham (1970), and Sanderson (1982), describes how the Greenbrier thrust and the Sinks fault each imparted a component of strain on the Thunderhead Sandstone as follows: During emplacement of the Greenbrier Thrust (T1), simple shear strains developed in the hanging wall rocks, with $lambda_1$ axes generally dipping toward the hinterland. These strains increased in magnitude and tended to become asymptotic to the thrust at deeper levels in the hanging wall. The orientations of the strain ellipses varied in accordance with the orientation of the thrust surface (e.g., as the fault cut up stratigraphic section). Strains that developed in the hanging wall of the Sinks Fault (T2) were similarly oriented with respect to the fault surface during its propagation. These strains were superimposed on the T1 strains. Several superposed strain ellipses are indicated in Figure 17, with the resulting strain ellipses indicated by the letter R. The ellipses that resulted from these strain events varied in orientation and magnitude. This is highlighted by the

Figure 17. Model showing the ideal strain geometries resulting from the emplacement of the Greenbrier Thrust followed by the Sinks Fault. This model is based on the theory discussed by Mitra and Elliott (1980), Ramsay and Graham (1970), and Sanderson (1982). The variable results of the superposition of these strains is shown schematically. These resultant ellipses are labelled R.

PRESENT TOPOGRAPHIC SURFACE

GREENBRIER FAULT

p-€m

p-€t

p-€m

GREENBRIER FAULT

SINKS FAULT

p-€sh

p-€t

p-€m

GREENBRIER FAULT

SINKS FAULT

p-€m

PRESENT TOPOGRAPHIC SURFACE

p-€t

GREENBRIER FAULT

p-€m

58
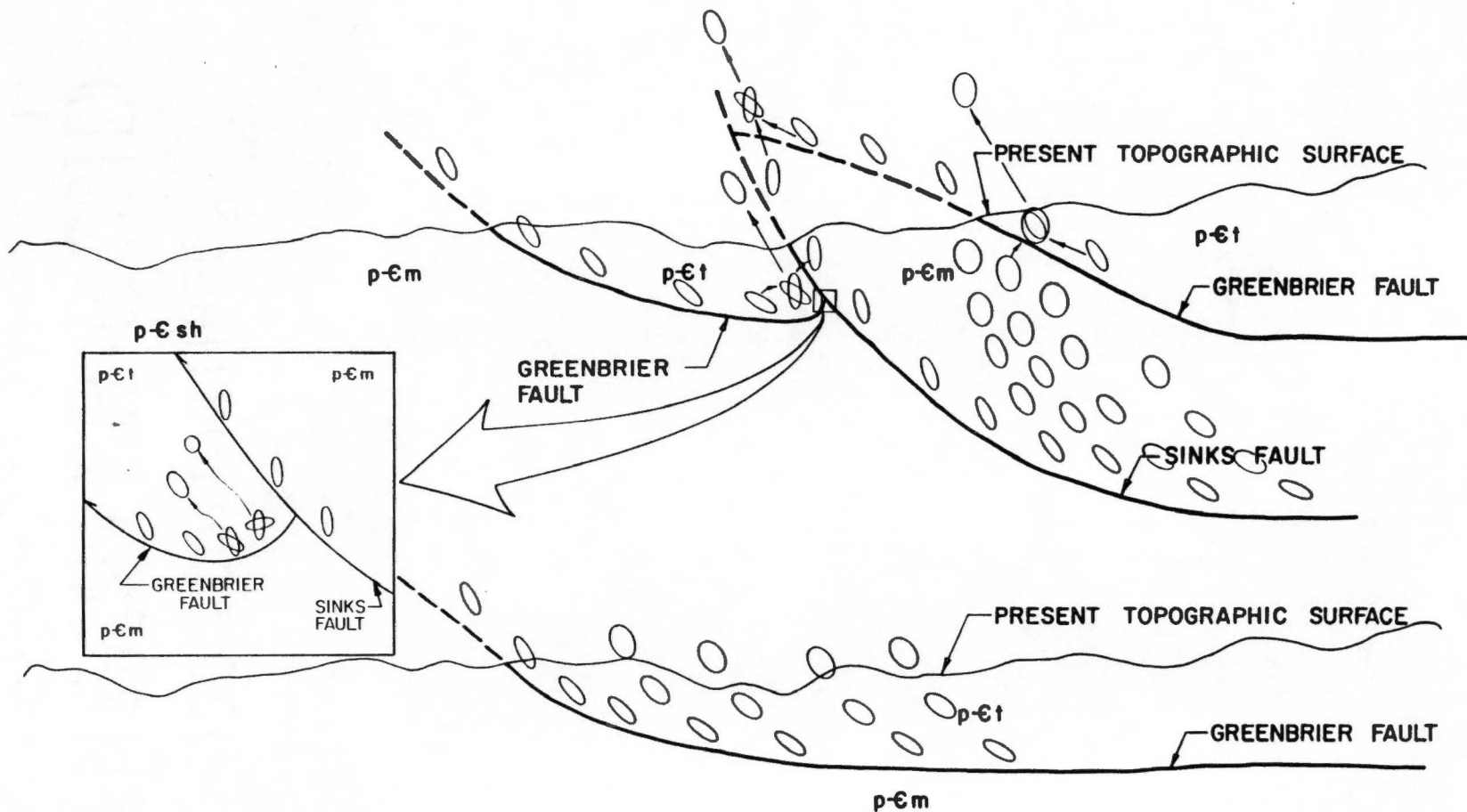
enlarged section of Figure 15, which shows the rotation of the footwall rocks of the Sinks Fault. This caused the T1 strains to rotate counterclockwise (in this example). The λ_1 axes of the subsequent T2 strain were therefore perpendicular to the λ_1 axes of the T1 strain. These superposed strains thus "cancelled" one another resulting in circular strain ellipses.

As illustrtated by this model the strain geometries which resulted from the Greenbrier Thrust and Sinks Fault appear in part to have been dependent on structural position.

CHAPTER IV

DISCUSSION AND CONCLUSIONS

Discussion

The strain analyses prove useful in examining the deformation history of this area and the mapping brings out the significant structural elements to consider in light of this strain data.

Strain Geometries

The study reveals some interesting geometric ties between strains and structural features. The geometric relationships between strain and bedding, strain and the Greenbrier Fault, and strain and the Sinks Fault appear to be significant.

The fact that five of 17 samples show the λ_1-λ_2 plane of strain less than $30°$ from the bedding plane is interesting. Also interesting is the observation that 11 of 17 samples show the λ_1 axis less than $40°$ from the bedding plane. This indicates that flattening subparallel to bedding is an important

strain geometry in the Thunderhead Sandstone, and that the maximum extension axis ($lambda_1$) usually lies at a low angle to bedding.

Such a pattern might be accounted for by invoking a pure shear flattening mechanism. This might involve depositional overburden and/or overburden due to structural thickening (i.e., stacked thrust sheets or fault duplication).

Conversely, this strain pattern might indicate that major simple shear strains have been impressed on the whole Thunderhead Sandstone within the Greenbrier Thrust sheet. This strain pattern is typical of major thrust sheets and probably accounts for the subparallelism between the $lambda_1$-$lambda_2$ plane and bedding within the Thunderhead Sandstone.

Figure 18 shows schematically how these two mechanisms might be invoked to explain the flattening subparallel to bedding. As indicated by ellipses c and g the flattening created by pure shear can be equalled by invoking simple shear plus a rotation. Although not truly parallel to bedding, ellipse g clearly displays a similar relationship to bedding as ellipse c.

Nine of the ten samples from the klippe contain either $lambda_1$-$lambda_2$ or $lambda_1$-$lambda_3$ $15°$ to $34°$ from the orientation of the Greenbrier Fault. Similarly, the

PURE SHEAR

SIMPLE SHEAR
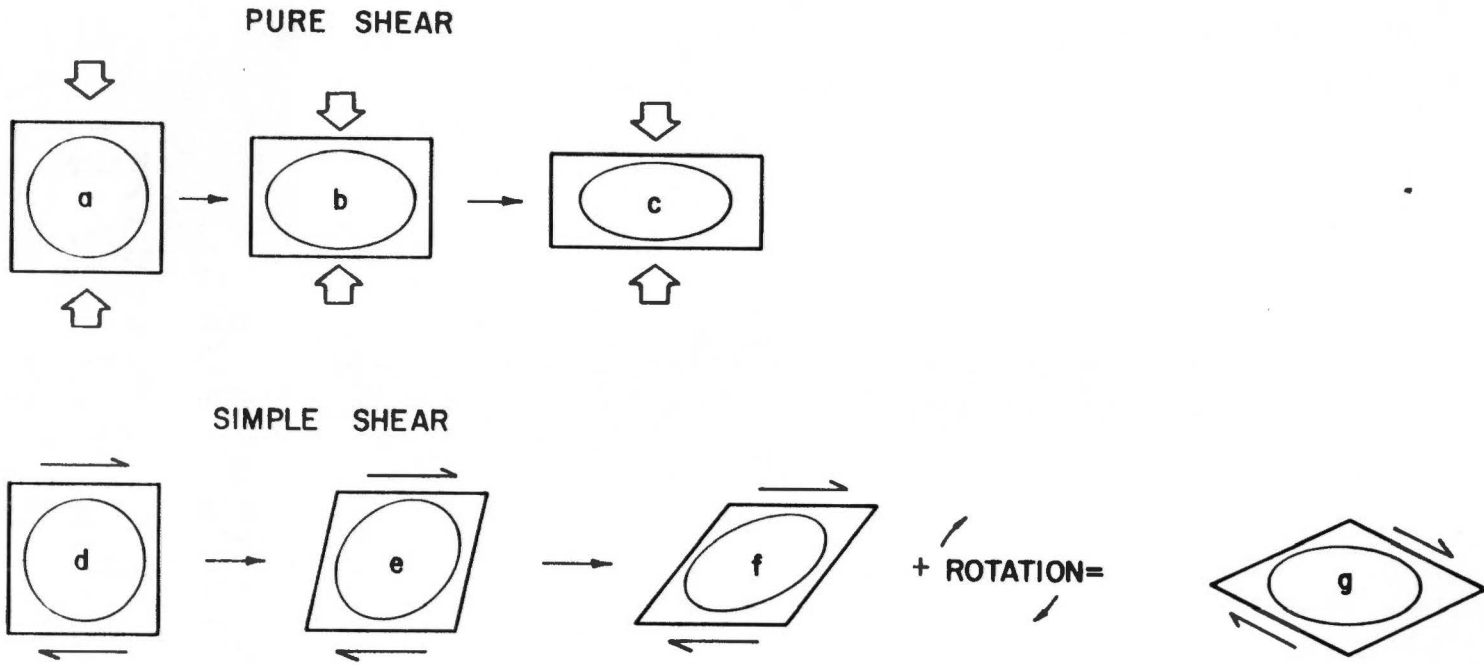
+ ROTATION=

Figure 18. Schematic diagram showing how simple shear plus a component of rotation can result in the same strain ellipse as pure shear.

three main sheet samples taken from near the sheet's edge show the λ_1-λ_2 plane 21° to 34° from the Greenbrier Fault. This can be explained by invoking a heterogeneous simple shearing in the hanging wall rocks of the Greenbrier Fault. As shown in Figure 19a, principal strains in hanging wall rocks are thought to become near parallel to the underlying thrust fault at the deeper levels in moving thrust sheets (Mitra and Elliot, 1979; Ramsay and Graham, 1970). At higher levels in thrust sheets, the principal strains are thought to be oblique to the fault, dipping toward the hinterland (Ramsay and Graham, 1970). This rotation of strain within thrust sheets is much like the fanning of cleavage in fine grained hanging wall rocks (Mitra and Elliot, 1979).

All ten samples from the klippe either show the λ_1-λ_2 plane or the λ_1-λ_3 plane subparallel to the Sinks Fault. This relationship might be the result of movement of the Sinks Fault, causing finite strains in the footwall to realign roughly parallel to the fault, as displayed by ellipse R_1 in Figure 17. The fabric in the footwall rocks can be described like the strain fabrics that develop in ductile deformation zones (Simpson, 1983). Simpson (1983) showed that during ductile deformation-zone formation, grains

63
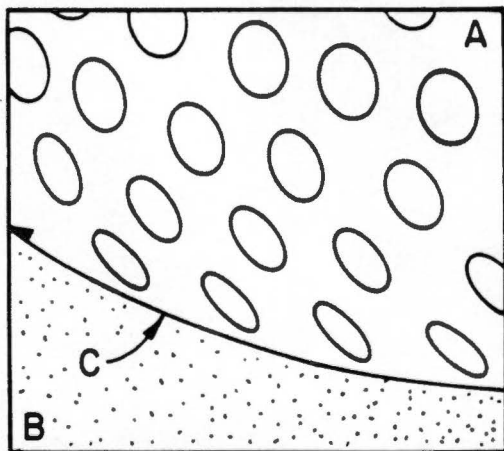
A. Diagram schematically illustrating the rotation of principal strain trajectories into parallelism with the fault plane (c) in the hanging wall rocks (a) as they are emplaced onto the footwall (b). This is based on the theory discussed by Mitra and Elliott (1980), Ramsay and Graham (1970), and Sanderson (1982).
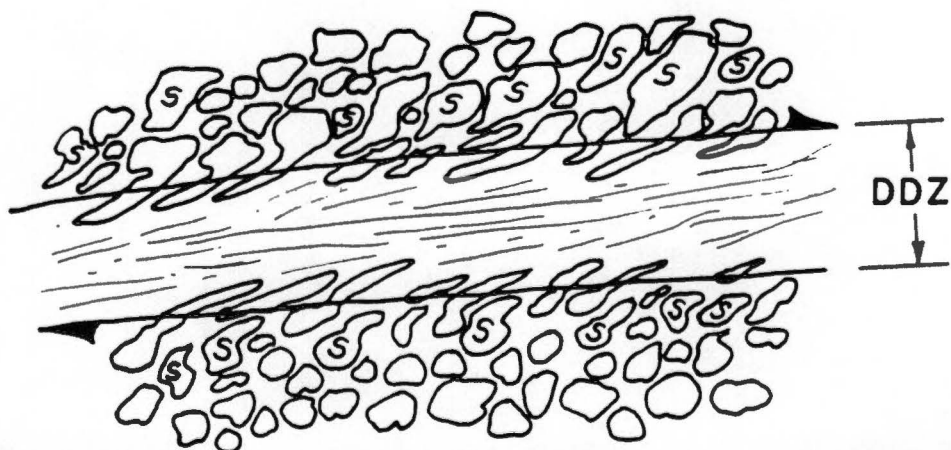
B. Diagram showing the development of a ductile deformation zone (DDZ) and the elongation of and rotation of grains into parallelism with the incipient DDZ (After Simpson, 1983). This is analogous to the development of strain patterns in fault zones. The grains labeled with the letter S display strain geometries analogous to those described in the samples of the present study.

Figure 19. Diagrams illustrating strain development.

become elongate at low angles to the incipient deformation zone (Figure 19b). If the strains cannot keep pace with the stresses, the ductile deformation zone fails, leaving the elongate grains along its borders to record the early development of the fault. This is analogous to the development of strain fabrics along mappable faults.

The fold within the Thunderhead Sandstone of the Roundtop Klippe at the Sinks, is not thought to have imparted a significant strain fabric on the Thunderhead. This is due to the lack of apparent geometric relationship between the principal strains and the east-west oriented fold axial plane. For example, sample T56 shows the $lambda_1$-$lambda_2$ plane dipping shallowly south-southeast whereas the fold axial plane dips steeply in this direction. The fold axial surface and the principal plane of strain would be expected to be subparallel if the strains were developed in conjunction with an axial plane cleavage (Ramsay, 1967). In addition, within the overturned limb of the fold, the principal plane of strain would be expected to have a steeper dip than the axial plane of the fold (i.e., where T56 was collected).

Map Relations

It is clear from the remapping done for this project that the maps and cross sections of King (1964) are reasonable explanations of the structure in this area, as discussed in this and the following sections.

The rocks of the klippe make up a synform whose axis is oriented east-northeast. The southeastern limb of this synform, in the vicinity of the Sinks, is overturned. Rocks of the main sheet in the study area are upright and mostly dip southeast.

Imbrication is present in both the Greenbrier and Sinks Fault zones, indicating that both are contractional features (i.e., thrust faults). Another important feature which the mapping revealed is that of variably oriented small fault zones within the Thunderhead Sandstone. Centimeter-scale shear zones of varied orientation occur close to these faults. These features indicate that the Thunderhead was deformed both by mesoscopic structural features as well as by bulk strain.

The occurrence of type II S-C mylonites show that the Metcalf has taken up a significant amount of strain as well (Lister and Snoke, 1984). It is probable that these mylonite zones are major movement horizons and are related to the emplacement of the Greenbrier fault,

66

although the fault places "younger" Thunderhead sandstone on top of "older" Metcalf phyllite and thus is close to to being a bedding plane fault.

Strain Data Relative to King's (1964) Interpretations

The deformation history of the study area can be postulated as follows (Figure 20). T1: The Greenbrier thrust carried "younger" Thunderhead Sandstone over "older" Metcalf Phyllite. This fault was probably nearly parallel to the statigraphic contact between these units and close to the contact. T2: The Sinks fault cut through the Greenbrier Fault near the sheet's edge, and thus moved a block of Thunderhead and Metcalf over the Thunderhead that was later to become the Roundtop Klippe. T3: The Line Springs Fault later splayed off the Sinks Fault in a forward progression, thus moving Metcalf and Thunderhead together over rocks of the "younger" Walden Creek Group. T4: The Great Smoky Fault moved the Precambrian rocks of the study area onto sedimentary rocks of Ordovician age.

Strains near the base of the hanging wall of the Greenbrier Fault might be expected to be asymptotic to the thrust, that is, subparallel to the fault near its surface, and oblique to it at higher levels within the
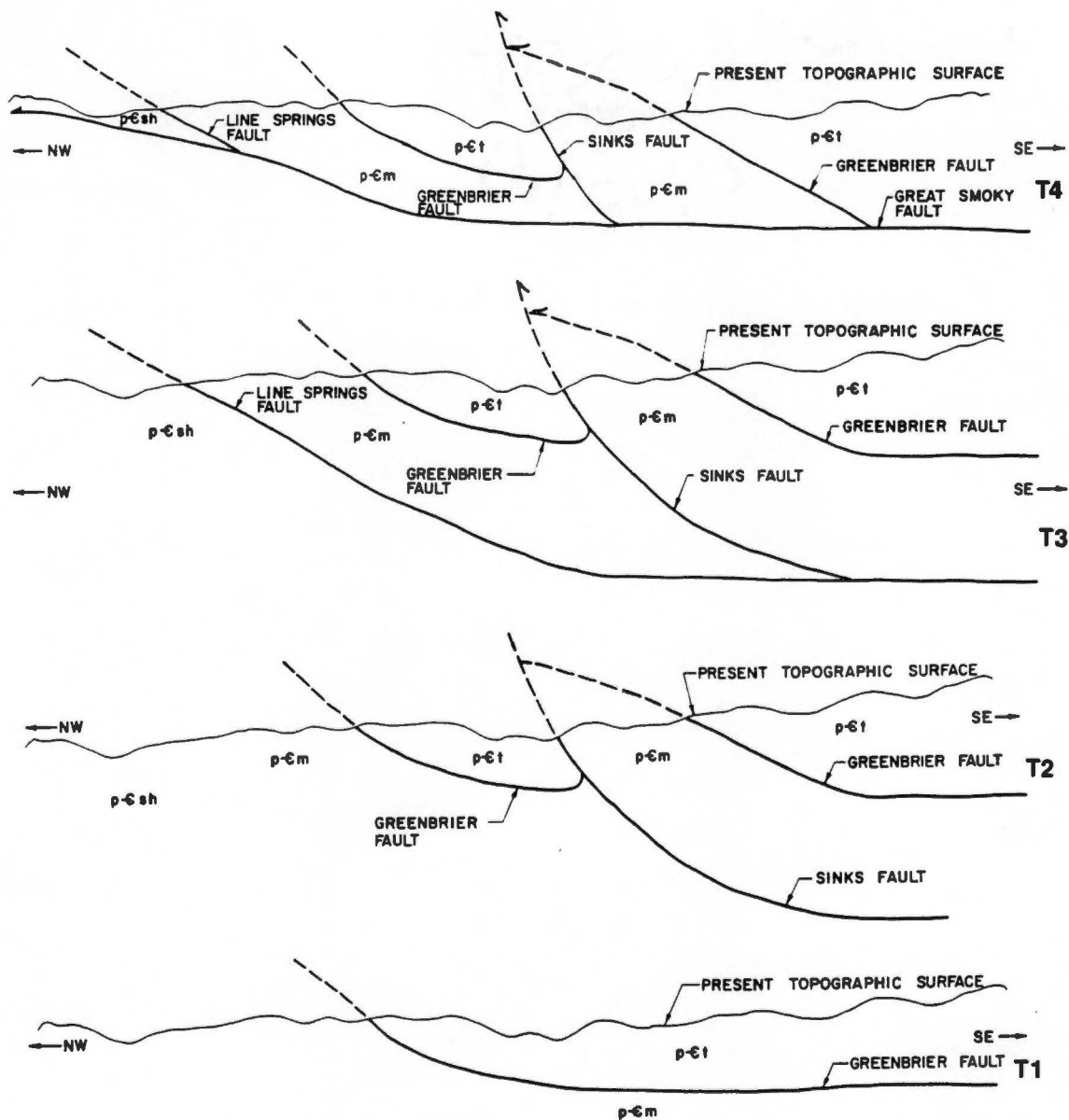
Figure 20. Cross section sketches showing the relative
timing of the emplacement of the Greenbrier, Line
Springs, Sinks, and Great Smoky Faults. This
interpretation displays the Line Springs Fault as a
forward progressing splay off of the Sinks Fault. T1
shows the emplacement of the Greenbrier Thrust, T2 shows
the emplacement of the Sinks fault, T3 shows the
emplacement of the Line Springs Fault as a splay off of
the Sinks Fault, and T4 shows the emplacement of the
Great Smoky Fault.

sheet. The strain data collected are consistent with such a model. This is also in accord with the occurrence of type II S-C mylonites within the Metcalf Phyllite, which probably was the major movement horizon for the Greenbrier Fault.

Movement of the Sinks Fault would have probably resulted in a superimposed strain fabric in its footwall rocks. This may be indicated by the complex strain geometries of the samples taken from the klippe.

King (1964) indicated that evidence for the timing of the emplacement of the Line Springs Fault is inconclusive, but that it appeared to be prior to Great Smoky faulting. Based on map relations and common S-C mylonite textures in both fault zones it is hypothesized that the Line Springs Fault and the Sinks Fault are part of the same "fault family" although it is not possible to determine which was emplaced first. Therefore, in the above chronology the Sinks Fault and Line Springs Fault might exchange places, if the Sinks is considered to be an out-of-sequence splay off the Line Springs (Figure 21). This chronology is as follows: T1: As in the chronology above, the Greenbrier Thrust carried "younger" Thunderhead Sandstone over "older" Metcalf phyllite. T2: The Line Springs Fault moved at a deeper level than the Greenbrier, and therefore moved Metcalf Phyllite over the
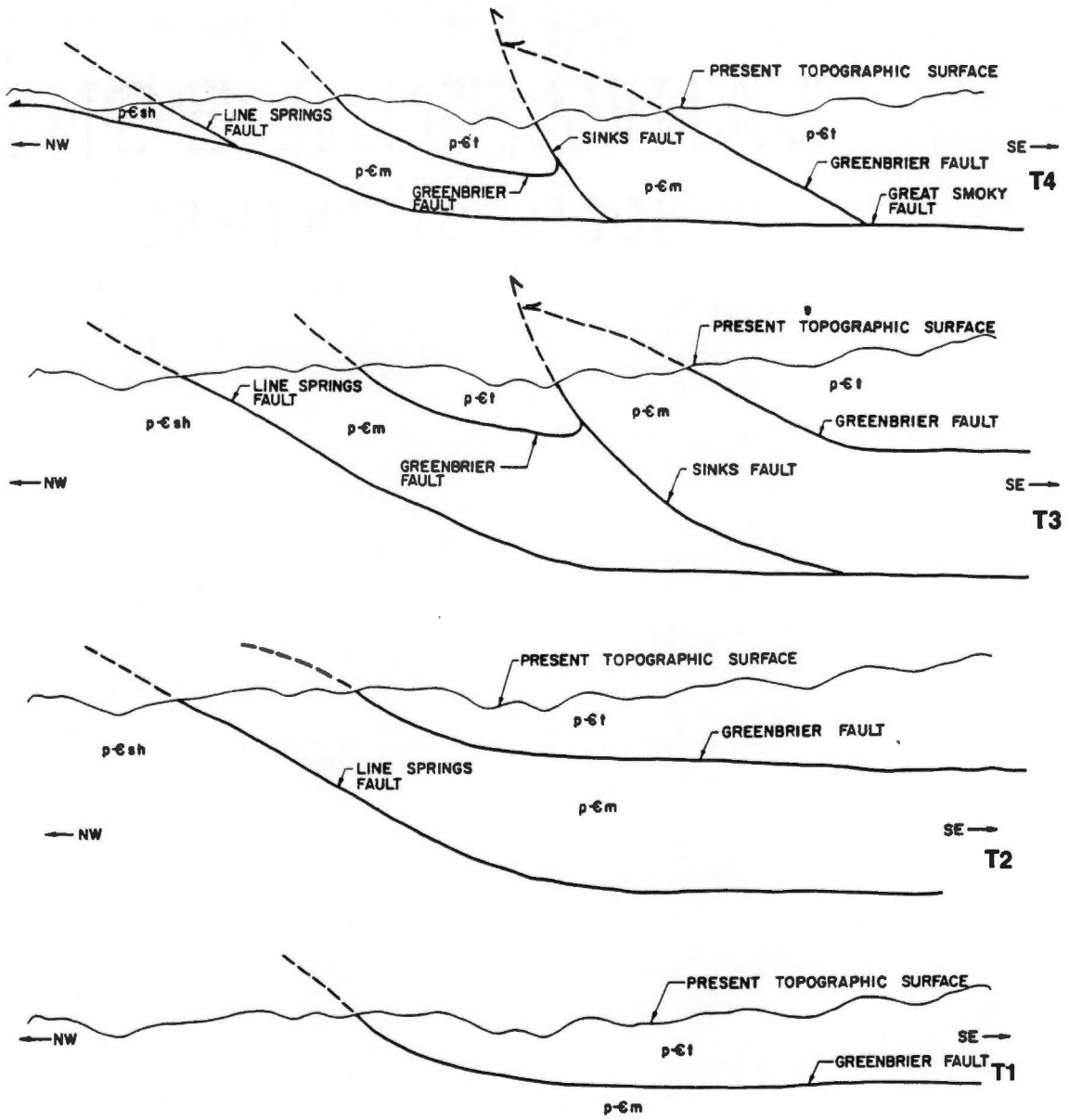
Figure 21. Cross section sketches showing an alternative interpretation of the relative timing of the emplacement of the Greenbrier, Line Springs, Sinks, and Great Smoky Faults. This interpretation displays the Sinks Fault as an out of sequence splay off of the Line Springs Fault. T1 shows the emplacement of the Greenbrier Thrust, T2 shows the emplacement of the Line Springs Fault, T3 Shows the emplacement of the Sinks Fault as an out-of-sequence splay off of the Line Springs Fault, and T4 shows the emplacement of the Great Smoky Fault.

Precambrian Shields Formation. T3: The Sinks Fault
formed as an out of sequence splay off the Line Springs
Fault and cut the Greenbrier Thrust sheet. The Sinks
Fault, therefore moved Metcalf phyllite and Thunderhead
Sandstone together over a smaller body of Thunderhead.
This body of Thunderhead was later to become the Roundtop
Klippe. T4: The Great Smoky Fault moved the Precambrian
rocks of the study area over sedimentary rocks of
Ordovician age. In either chronological model, the
emplacement of the Line Springs Fault is not thought to
have been a significant strain "episode" in the study
area.

The strains described in this study are the result
of at least two deformation events, and it is therefore
not possible to attribute any single strain ellipsoid to
a single deformation event. The strain ellipsoids are
thus representative of the incremental strains recorded
over a series of deformation events.

Conclusions

The following is a list of conclusions drawn from
the remapping and strain analyses of the present study.
1). The R_f/ϕ method and PASE5 method of strain analysis
yielded useable three dimensional results for samples of

Thunderhead Sandstone from the Roundtop Klippe.

2). The Fry method yielded useable two-dimensional results for samples of Thunderhead Sandstone showing high strain. This method suggests that matrix strains not measured by the R_f/ϕ method may account for as much as 40-50% of the total finite strains in these samples.

3). Field mapping showed that the 1:24,000 scale map of King (1964) is largely correct. A small window through the Greenbrier Fault was located at the southwestern corner of the klippe. Both the Greenbrier and Sinks Faults were verified as to their being contractional faults. This is evident in the high degree of imbrication observed along their traces. There is no evidence for a fault between Cades and Thunderhead strata southwest of the Roundtop Klippe, as King's (1964) map suggests. This implies that the Cades and Thunderhead are the same stratigraphic unit, with differing sedimentology as one goes from northeast to southwest. As suggested by Walters (1988), the Elkmont may be a facies equivalent of the Cades, and therefore may be related stratigraphically to the Thunderhead.

4). Inhomogeneous strain is observed throughout the Thunderhead Sandstone, most noteably in the Roundtop Klippe.

5). Lambda$_1$ often lies close to parallel to bedding and

could be the result of pure shear flattening due to sedimentary and/or structural overburden.

6). The $lambda_1$-$lambda_2$ plane or the $lambda_1$-$lambda_3$ plane of strain lies subparallel to the orientation of the Greenbrier Fault in ten samples. This is thought to be the result of simple shear along the base of the thrust sheet during emplacement of the Greenbrier Fault. This is likely an early strain feature in the Thunderhead just as the Greenbrier is also an early feature, as indicated by crosscutting relations.

7). The $lambda_1$-$lambda_2$ plane or the $lambda_1$-$lambda_3$ plane of strain for samples T7, T30, T49, T54, T56, T60, and T61 near the Sinks Fault lie subparallel to the orientation of that fault in the Thunderhead Sandtone of the Roundtop Klippe. This is thought to result from simple shear within the Sinks footwall during its emplacement. Erosion has removed the hanging wall Thunderhead rocks that were originally proximal to the fault. This is thought to be a later strain event than the strains resulting from Greenbrier faulting.

8). The relationships, at depth, between the Greenbrier, Sinks, and Line Springs Faults cannot be determined absolutely although it is clear that the Greenbrier occurred first.

9). It is possible that the Sinks and Line Springs

73

Faults connect at depth beneath the Metcalf Phyllite, but it is not possible in this model to prove which moved first. This is consistent with King's (1964) maps and cross sections through the area.

10). The strains calculated in this study are representative of two and possibly three different episodes of deformation. The strain ellipsoids represent the end result of incremental strains accumulated over time, making correlation between a single ellipsoid and a single deformation event impossible.

BIBLIOGRAPHY

BIBLIOGRAPHY

Coward, M. P., 1984, The strain and textural history of thin-skinned zones: examples from the Assynt region of the Moine thrust zone, N. W. Scotland: Journal of Structural Geology, v. 6, no. 1/2, p. 89-99

Coward, M. P. and J. H. Kim, 1981, Strain within thrust sheets: Thrust and Nappe Tectonics, Geological Society of London, p. 275-292

Coward, M. P. and G. J. Potts, 1983, Complex strain patterns developed at the frontal and lateral tips to shear zones and thrust zones: Journal of Structural Geology, v. 5, no. 3/4, p. 383-389

Dunnet, D., 1969, A technique of finite strain analysis using elliptical particles: Tectonophysics, v. 7, no. 2, p. 117-136

Dunnet, D. and A. W. B. Siddans, 1971, Non-random sedimentary fabrics and their modification by strain: Tectonophysics, v. 12, p. 307-325

Durney, D. W. and J. G. Ramsay, 1973, Incremental strains measured by syntectonic crystal growths, In: K. A. DeJong and R. Scholten (Eds.), Gravity and Tectonics, John Wiley and Sons, New York, 502 p.

Fry, N., 1979, Random point distributions and strain measurement in rocks: Tectonophysics, v. 60, p. 89-105

Holst, T. B., 1982, The role of initial fabric on strain determination from deformed ellipsoidal objects: Tectonophysics, v. 82, p. 329-350

Hossack, J. R., 1968, Pebble deformation and thrusting in the Bygdin area (Southern Norway): Tectonophysics, v. 5, no. 4, p. 315-339

Keith, A., 1892, Geology of the Chilhowee Mountain in Tennessee, Philosophical Society of Washington Bulletin, v. 12, p. 71-88

Keith, A., 1895, Description of the the Knoxville sheet (Tennessee-North Carolina), U. S. Geological Survey Atlas, Folio 16, 6 p.

Keith, A., 1904, Description of the Asheville quadrangle (North Carolina-Tennessee), U. S. Geological Survey Atlas, Folio 116, 10 p.

Keith, A., 1927, Great Smoky overthrust, Geological Society of America Bulletin, v. 38, p. 154-155

King, P. B., 1964, Geology of the Central Great Smoky Mountains Tennessee, Geological Survey Professional Paper 349-C, U. S. Government Printing Office, Washington, D. C., 148 p.

King, P. B., R. B. Neuman, and J. B. Hadley, 1968, Geology of the Great Smoky Mountains National Park, Tennessee and North Carolina, Geological Survey Professional Paper 587, U. S. Government Printing Office, Washington, D. C., 23 p.

Kligfield, R. L., et al., 1985, Strain Analysis Programs, unpublished programs compiled at The University of Colorado, Boulder

Lisle, R. J., 1984, Strain discontinuities within the Seve-Koli Nappe complex, Scandinavian Caledonides, Journal of Structural Geology, v. 6, no. 1/2, p. 101-110

Lisle, R. J., 1977, Estimation of the tectonic stain ratio from the mean shape of deformed elliptical markers: Geologie En Mijnbouw, v. 56, no. 2, p. 140-144

Lister, G. S. and A. W. Snoke, 1984, S-C Mylonites: Journal of Structural Geology, v. 6, no. 6, p. 617-638

Mitra, G. and D. Elliott, 1980, Deformation of basement in the Blue Ridge and the development of the South Mountain cleavage, In: D. R. Wones (Ed.), The Caledonides in the USA, Va. Polytech. Inst., State Univ., Memoir 2

Ramsay, J. G. and R. H. Graham, 1970, Strain variation in shear belts: Canadian Journal of Earth Sciences, v. 7, p. 786-813

Ramsay, J. G. and R. Kligfield, 1983, Strain measurement: techniques and tectonic implications, notes from Geologic Society of America Division of Structural Geology and Tectonics short course, Bloomington, Indiana, November 3-5, 1983, 87 p.

Safford, J. M., 1856, A geologic reconnaissance of the State of Tennessee, Tennessee Geologic Survey, 1st Biennial Report, 164 p.

Safford, J. M., 1869, Geology of Tennessee, Nashville, Tennessee, 550 p.

Sanderson, D. J., 1982, Models of strain variation in nappes and thrust sheets: a review, Tectonophysics, v. 88, p. 201-233

Simpson, C., 1983, Strain and shape-fabric variations associated with ductile shear zones: Journal of Structural Geology, v. 5, no. 1, p. 61-72

Stose, G. W. and A. J. Stose, 1944, The Chilhowee Group and Ocoee Series of the southern Appalachians, American Journal of Science, v. 242, p. 367-390, 401-416

Walters, R. R., 1988, Structural geometries, fabrics and stratigraphic relationships in the Cades Cove region, Great Smoky Mountains National Park, Tennessee, unpublished M. S. Thesis, University of Tennessee, Knoxville, 145 p.

Witherspoon, D. W., 1975, Structure of Blue Ridge Front, Tennessee, Southern Appalachians, unpublished Ph. D. Thesis, University of Tennessee, Knoxville, 165 p.

APPENDICES

APPENDIX A

METHODS OF STUDY

The area was remapped at a scale of 1:12,000 during this study (Plate 1). The finite strain recorded by the Thunderhead Formation sandstone and conglomerate strata was measured using both the R_f/o method (Ramsay, 1967; Dunnet, 1969; with enhancements by Lisle, 1977) and the "All object-object separations" method of Fry (1979). Oriented samples of Thunderhead Sandstone were collected from the localities indicated in Figure 1. Many of the localities are in the Little River Gorge where the exposure is best and the rock generally fresh. Conglomerate samples were cut and polished on three mutually orthogonal surfaces, whose orientations were recorded. These surfaces were photographed and the prints used for the strain analyses. Samples T7, T29, T30, T33, T34, and T54 are slab samples of conglomeratic Thunderhead. Medium- and coarse-grained sandstone samples were similarly slabbed and two inch by three inch thin sections were cut for each surface. The thin sections were placed in a photographic enlarger between two oriented polarizing filters and photonegatives were printed (Figure 22). These prints were then used for the strain analyses. This was done for samples T32, T45, T46, T48, T49, T52, T53, T56, T58, T60, and T61.

Computer Analyses

Kligfield et al. (1982) have compiled a package of strain analysis programs written for Tektronix hardware. The R_f/ϕ and theta-curve methods were carried out with this software using data generated with the ellipse tracing program from this package. Data generated by the R_f/ϕ program was then run in the PASE5 program in order to determine the strain ellipsoid (three-dimensional). The PASE5 program, developed by Siddans (1971, 1980), determines three-dimensional strain, from two-dimensional
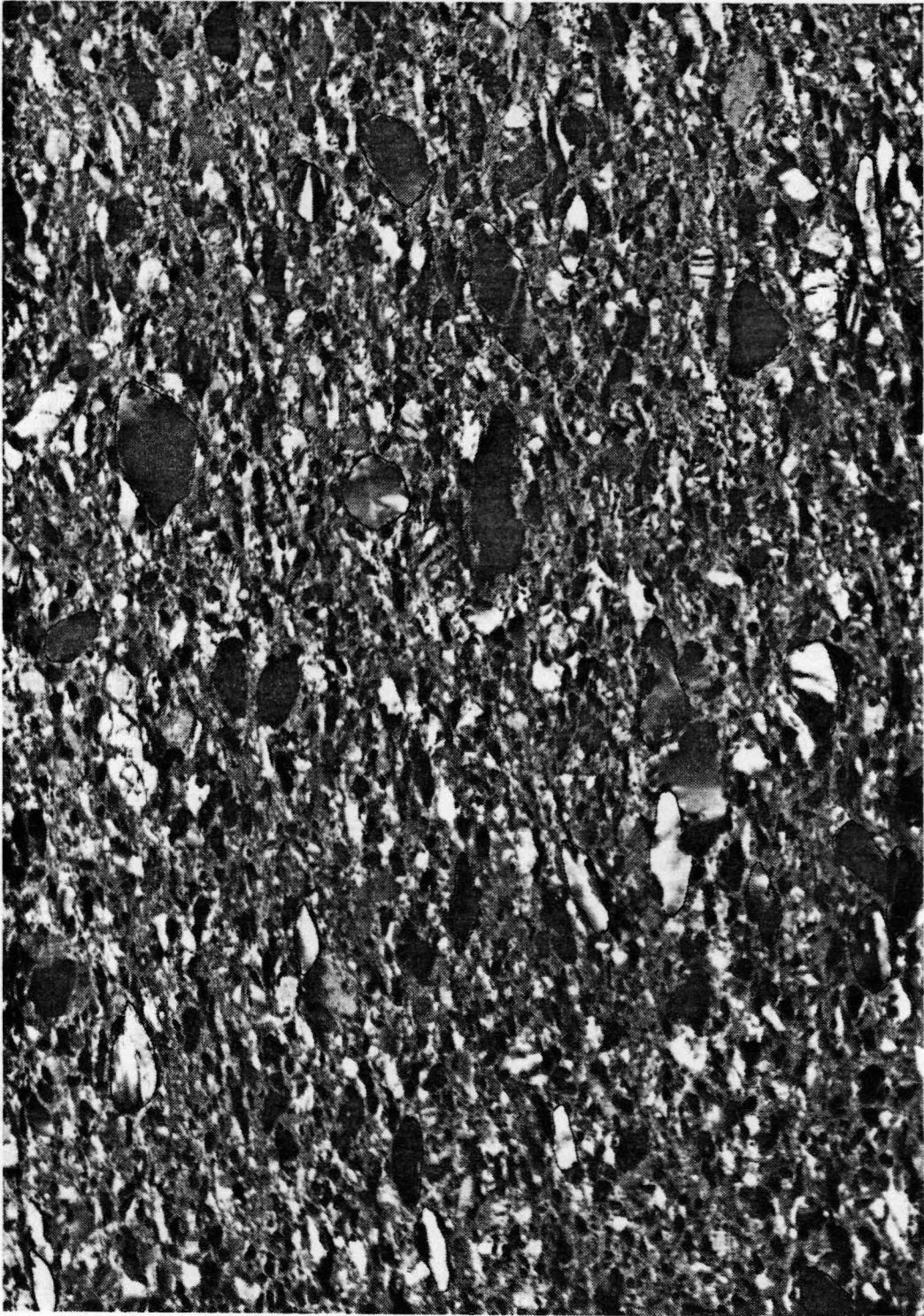
Figure 22. Example of thin section photonegative used for the strain analyses. This is the xz side of sample T61. The horizontal field of view is approximately 15 cm.

strain   data   on   three   mutually   perpendicular, non-principal planes.

The R_f/ϕ Method And Theta Method

The R_f/ϕ and theta-curve methods of strain analysis are based on the theory outlined below.   The former method yields an estimate of the strain ellipse magnitude and orientation based on the mean orientation and magnitude of the R_f/ϕ plot.   The R_f/ϕ plot symmetry is used to check the validity of this determination.   This is done using the harmonic mean of R_f and the vector mean of ϕ as prescribed by Lisle (1985).

The theta-curve method of Lisle (1977) is applied to further check the results of the R_f/ϕ analysis by destraining the data.   The long axis as determined by the R_f/ϕ method is used as the direction of step-wise destraining.   At each step the orientation of all of the strain markers are evaluated by a Chi-squared test for randomness.   This is performed until the cluster displays the most random orientation, at which point the amount of strain accumulated in the destraining process is noted. This value constitutes the reciprocal strain ellipse for the surface in question.   The fundamental assumption is that the sample initially showed a ramdom distribution of marker orientations. Step-wise destraining, along the strained array's long axis, is performed until the markers show a random distribution.   This randomly orientated array is thus assumed to be the starting point or pre-deformation array.

The following theoretical discussion is based on Lisle (1985).   The R_f/ϕ technique of strain analysis assumes homogeneous deformation of spherical objects which strain homogeneously with the matrix (see discussion of Fry method for differential strains with respect to the matrix).   An elliptical marker of shape R_i and orientation Θ subjected to a strain of magnitude R_s is transformed to an ellipse of shape R_f and orientation ϕ given by:

$$\tan 2\phi = \frac{2R_s(R_i^2-1)\sin 2\theta}{(R_i^2+1)(R_s^2-1)+(R_i^2-1)(R_s^2+1)\cos 2\theta}$$

$$R_f = \left[\frac{\tan^2\theta(1+R_i^2\tan^2\theta)-R_s^2(\tan^2\theta+R_i^2)}{R_s^2\tan^2\phi(\tan^2\theta+R_i^2)-(1+R_i^2\tan^2\theta)}\right]^{1/2}$$

Figure 2.1 from Lisle (1985) illustrates the relationships between R_i, Θ, R_s, R_f, and ϕ (Figure 23). A suite of particles of varying R_i and Θ, when strained, will yield a variety of R_f and ϕ values. When R_f is plotted on a logarithmic scale versus ϕ the result is a cluster of points about an axis (Figure 24). The shape of the data cluster indicates the nature of the strain. When the grain long axes show a preferred orientation, points cluster tightly about a certain ϕ value. This is best developed when the strains are large. Low strain samples tend to show a wider spread of ϕ values and less well-developed preferred orientation. The strain magnitude (R_s) is estimated by calculating the mean of R_f, and its orientation is determined by calculating the vector mean of ϕ. R_s in indicated on Figure 24, as well as the R_i curve which best encircles the data points. The R_i curves are generated as described in the following paragraph and are used to estimate the initial ellipticity of the grains being used in the analysis. Appendix E contains the R_f/ϕ plots for all of the samples used in this study. These plots were generated using the Kligfield et al. (1982) computer programs.

A suite of ellipses of identical R_i but variable Θ (initial orientation) deforms to yield ellipses of variable R_f and ϕ. This deformed suite plots on an R_f/ϕ diagram as a curve given by:

$$\cos 2\phi = \frac{(R_f + 1/R_f)(R_s + 1/R_s) - 2(R_i + 1/R_i)}{(R_f - 1/R_f)(R_s - 1/R_s)}$$

with R_s and R_i as constants. Repetition of this operation with several values of R_i results in plots showing a definite range of final shapes. The axial ratios of the extreme ellipses ($R_{f\ max}$, $R_{f\ min}$), that is the maximum final and minimum final ratios, are simple products or quotients of R_i and R_s as "they result from the parallel or perpendicular superimposition of these shape components." (Lisle, 1985). These values can be calculated with the following formulas:

$$R_{f_{max}} = R_s R_i$$

$$R_{f_{min}} = \text{the greater of } \frac{R_s}{R_i} \text{ or } \frac{R_i}{R_s}$$
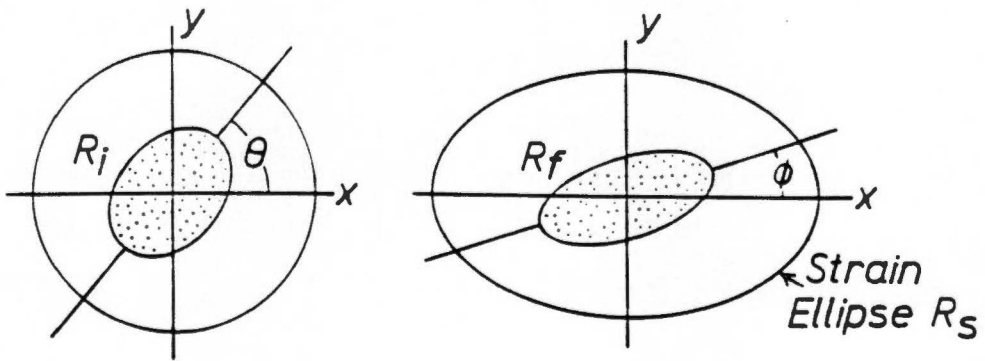
Figure 23. Diagram showing the relationship between R_i, Θ, R_s, R_f, and ϕ (From Lisle, 1985). Elliptical marker of shape R_i and orientation Θ (with reference to coordinate axis x) subjected to a strain of magnitude R_s is transformed to ellipse of shape R_f with orientation ϕ (with reference to coordinate axis x).

Figure 24. R_f/ϕ plot of sample T61xz. The original zero is the orientation of the reference line from which o was measured. When the grain long axes show a preferred orientation the points cluster tightly about a certain ϕ value. This occurs in high strain samples. Low strain samples tend to show less preferred grain orientation and thus a wider spread of ϕ values. R_s is indicated with a O symbol. The R_i line is chosen to encircle as many data points as possible and gives an estimate of the initial ellipticity of the strained grains.
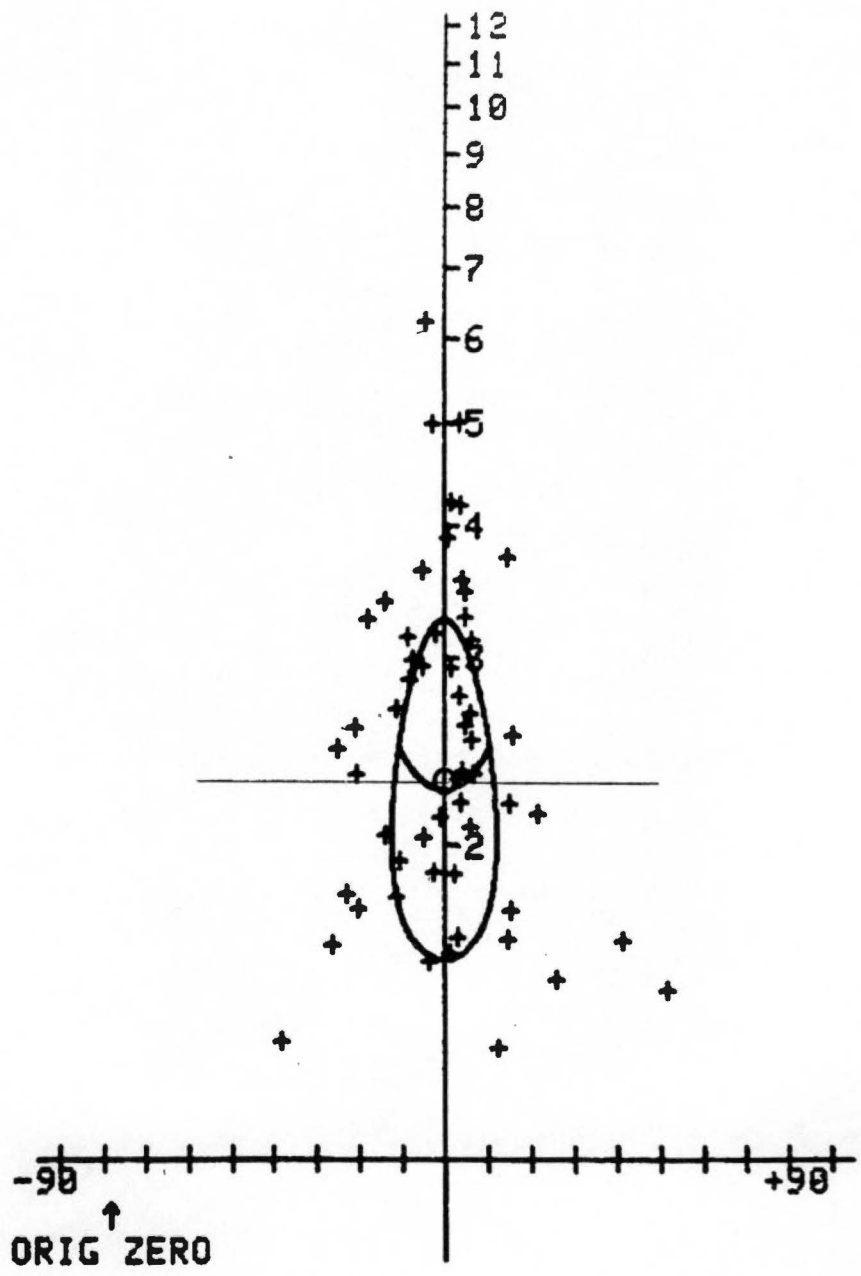
The curves generated in this way span a limited range of ϕ values. The fluctuation is defined as the limited spread of orientations which the deformed ellipses take. The magnitude of this angular spread is given by equation 2.7 of Lisle (1985) as follows:

$$\sin2\phi_{max} = \frac{R_i - 1/R_i}{R_s - 1/R_s}$$

In cases where $R_i > R_s$, the fluctuation is unrestricted or $2\phi_{max}$ is 180 degrees.

Markers sharing a constant initial orientation but of varying initial axial ratios deform to give a curve on an R_f/ϕ diagram termed a theta-curve (Lisle, 1977b). Varying the initial orientation of the suite results in a series of curves which radiate from the point ($\phi = 0$, $R_f = R_s$). These curves are drawn by substituting the appropriate values of R_s and Θ into equation 2.9 of Lisle (1985) which follows:

$$R_f = \left[\frac{\tan2\Theta(R_s^2 - \tan^2\Theta) - 2R_s\tan\phi}{\tan2\Theta(1 - R_s^2\tan^2\phi) - 2R_s\tan\phi}\right]^{1/2}$$

"To draw the $\Theta = 45^{\circ}$ curve, use is made of:

$$R_f = \left[\frac{\tan2\phi - R_s^2}{R_s^2\tan^2\phi - 1}\right]^{1/2}$$

When Θ is greater than 45°, the curves have a minimum at a ϕ value obtained by differentiating equation 2.9 and equating $dR_f/d\phi$ to zero. This yields

$$\tan\phi_{min\ R_f} = 1/2R_s\left[\tan2\Theta(R_s^2 + 1) \pm (\tan^2 2\Theta(R_s^2 + 1)^2 4R_s^2)\right]^{1/2}$$

The All Object-Object Separation Method Of Fry (1979)

The method of Fry (1979), henceforth referred to as the Fry method, is based on the distribution of grain centers on two dimensional sample surfaces. The

technique creates a graphical representation of strain on a flat surface, based simply on how close grain centers can get to one another. An originally isotropic (uniform) distribution of grains is assumed. In an initally random distribution, object positions are mutually independent and no strain can be measured (Fry, 1979). An isotropic distribution is reasonable for most geologic materials because of grain size sorting limits. Sediments, for example, are usually deposited with some degree of consistent sorting.

The graphical construction used in this technique follows. While maintaining a constant orientation on a rectangular coordinate system the center point of a clear overlay is placed over the first grain, and all other grain centers are marked on the overlay. The overlay center point is then moved to a second grain and again all grain centers, including that of the first grain, are marked on the overlay. This is continued for grains three, four, five, and so on until all of the chosen grains (50-100) have been treated. The result is an area void of points around the original center point. This void is representative of the orientation and magnitude of the strain ellipse for that two dimensional surface (figure 25).

The Fry method yields an estimate of the matrix strain in samples where objects are spaced in a nearly homogeneously deforming matrix. In cases where the objects in the sample have deformed Fry (1979) suggested that this method may be an alternative one to strain measurements based on object shapes. He stated that in rocks consisting of tightly packed objects (grains) that deform homogeneously there should be no difference in strain as determined by object shape and as determined with his method or any other center-to-center method.

Six of the 17 samples were evaluated using slab photographs for the strain measurements. For the Fry analyses only feldspar grains were chosen because of the ease with which their grain boundaries can be determined in slab samples as compared to the great difficulty encountered with quartz grain boundaries. Due to the abundant but dispersed nature of the feldspar grains, these slab analyses likely yield an estimate of the strain experienced by the whole rock, primarily by its matrix (Fry, 1979). In contrast, the remaining eleven samples were analyzed with two inch by three inch thin section photonegatives and the quartz grains were used in the Fry analyses as their boundaries are easily deciphered in thin section. These eleven analyses yielded results similar to those obtained by object shape techniques like the R_f/ϕ method (Fry, 1979).
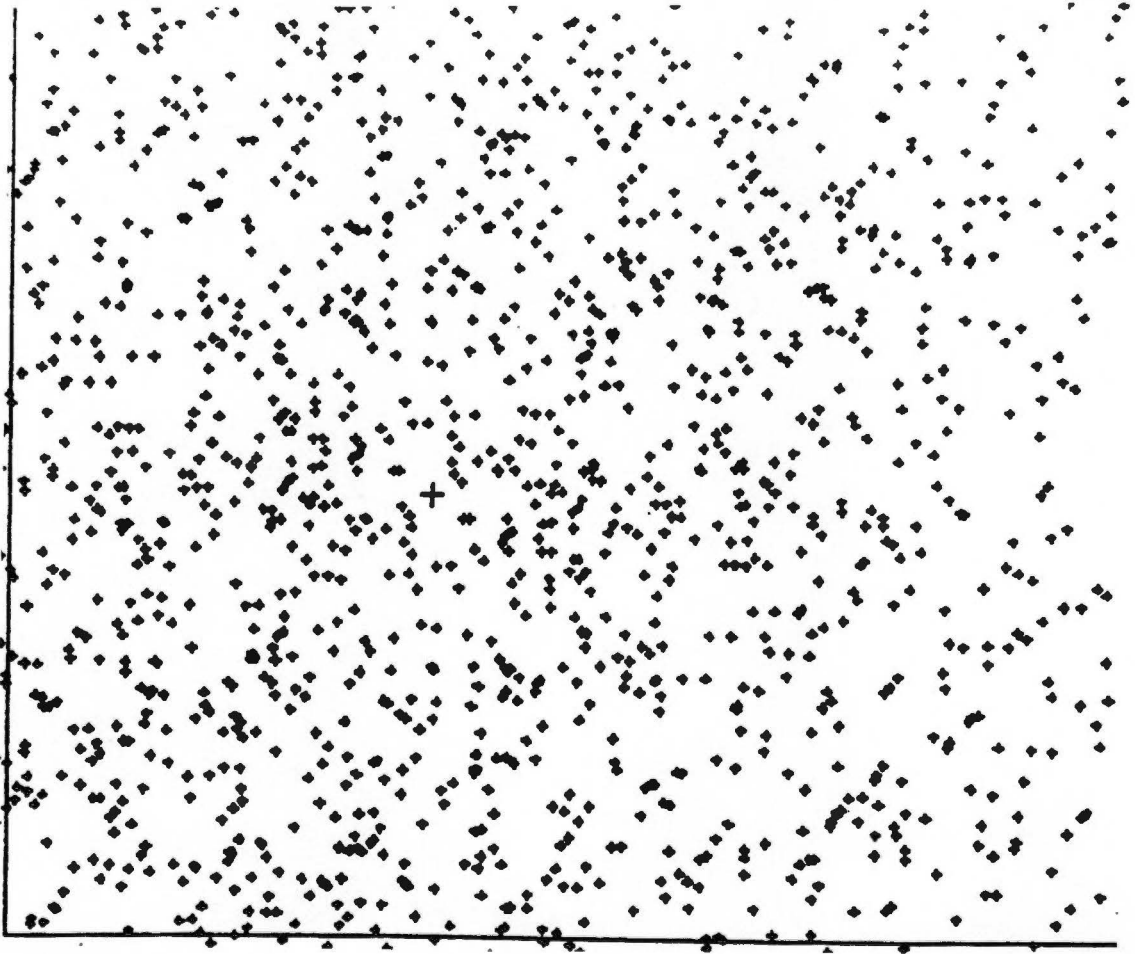
Figure 25. Void ellipse generated by the Fry method for sample T61xz. The void ellipse is found at the center of the plot indicated with the plus symbol.

The Fry method was used in this study for two reasons. First, in order to compare the results with those of the R_f/ϕ method, and second, because of the ease and relative speed of its application.

APPENDIX B

SAMPLE DESCRIPTIONS

The samples were all examined to describe their general mineralogy and texture. Estimated percentages of quartz, feldspar, and matrix are presented here and in Figure 14 with other significant characteristics. Estimated percentages of matrix include phyllosilicates, carbonates, heavy minerals and accessory minerals, but exclude very fine-grained quartz and feldspar. Quartzofeldspathic lithic fragments are broken down into percentages of each constituent so that the estimated percentages of quartz and feldspar are totals.

T7. This coarse conglomeratic slab sample contains 65% quartz, 20% feldspar, and 15% matrix. Quartz and feldspar clasts show a strong tectonic lineation with quartz ribbons up to 3 cm in length. Feldspar grains are seen broken along mineralogic cleavage planes due to extension. These grains are as long as 1.2 cm.

T29. This coarse conglomeratic slab sample contains 50% quartz, 30% feldspar, and 20% matrix. Quartzofeldspathic lithic fragments make up about 10% of the rock. A strong tectonic lineation is apparent with feldspars up to 1.7 cm long and lithic fragments up to 2.3 cm long. Feldspars are pulled apart along mineralogic cleavage.

T30. This conglomeratic slab contains 50% quartz, 30% feldspar, and 20% matrix. Approximately 10-15% of the sample is quartzofeldspathic lithic fragments. Tectonic fabric is moderate, with feldpars up to 1.5 cm long.

T32. These thin-section samples are highly quartzose with 75% quartz, 15% feldspar, and 10% matrix. Quartzofeldspathic lithic fragments make up 10-15% of the sample. The coarser fraction is mostly coarse to granule sized quartz. The tectonic shape fabric is weak. The matrix is composed dominantly of quartz.

T33. This conglomeratic slab sample contains 60% quartz, 25% feldspar, and 15% matrix. Tectonic fabric is weak with feldspar and quartz grains up to 1.2 cm in length.

T34. This coarse conglomerate similarly contains 60% quartz, 25% feldspar, and 15% matrix. Quartzofeldspathic lithic fragments make up about 10% of the rock. Tectonic lineation is strong, with feldspars up to 3 cm long and quartz ribbons up to 4 cm long.

T45. These thin-section samples are quartz-rich with 72% quartz, 17% feldspar, and 11% matrix. Quartzofeldspathic lithic fragments make up 15% of the rock. These samples are dominated by coarse-grained quartz sand, with disseminated granule-sized grains. A moderate tectonic fabric is present as elongate quartz grains.

T46. Thin section samples from sample T46 are relatively quartz-poor with 45% quartz, 37% feldspar, and 18% matrix. Quartzofeldspathic lithic fragments make up about 10% of each thin-section. The rock is mostly made up of grains from 0.5-2 mm in diameter, with dispersed granule-sized grains. Texturally and mineralogically T46 is immature. A weak tectonic lineation is evident with phyllosilicates of the matrix forming a weak, disseminated cleavage parallel to this grain elongation (lineation).

T48. Sample T48 thin-sections contain 40% quartz, 40% feldspar, and 20% matrix. Quartzofeldspathic lithic fragments make up only about 7% of the rock. Most of the grains are between 0.5-0.5 mm in diameter. Similar to sample T46, T48 has a weak cleavage, displayed by matrix phyllosilicates, which parallels the quartz and feldspar grain elongation (tectonic fabric).

T49. Sample T49 thin-sections contain 55% quartz, 30% feldspar, and 15% matrix. Quartzofeldspathic lithic fragments are rare. The dominant grain diameter is from 0.5-1 mm with 2 mm grains found more rarely, and grains as long as 4 mm even more rarely found. Phyllosilicates aligned parallel to the highly elongate quartz and feldspar grains create a cleavage.

T52. Thin-sections from sample T52 contain 52% quartz, 38% feldspar, and 10% matrix. Grain diameters are mostly between 0.5-1.5 mm, with the longest grain

being about 2 mm in length. A tectonic fabric is moderately well developed.

T53. Sample T53 thin-sections are 55% quartz, 35% feldspar, and 10% matrix. About 5-7% of the sample is composed of quartzofeldspathic lithic fragments. Strong tectonic lineation is displayed by quartz ribbons up to 5 mm long. The matrix minerals are carbonate, quartz, and feldspar and display a cleavage parallel to the tectonic lineation.

T54. This is the most quartzose of the slab samples containing 75% quartz, 15% feldspar, and 10% matrix. 10-15% of the rock is composed to quartzofeldspathic lithic fragments. A moderate strain fabric is evident with feldspars up to 1.5 cm long.

T56. These thin-sections contain 55% quartz, 40% feldspar, and 5% matrix. The average grain diameters are from 0.5-1.5 mm, but the high strain is recorded by quartz ribbons up to 4.1 mm in length. Feldspar clasts tend to be more angular than the quartz clasts. The sparse matrix is of carbonate and phyllosilicate minerals.

T58. Thin-sections of sample T58 contain 50% quartz, 31% feldspar, and 19% matrix. Quartzofeldspathic lithic fragments comprise less than 3% of the sample. The average grain diameter is from 0.5-1.5 mm, but some grains are as large as 3 mm across. The moderate strain fabric is parallel to the weak cleavage developed by the matrix phyllosilicates.

T60. These thin-sections are 60% quartz, 35% feldspar, and 5% matrix. Although some quartz ribbons are as long as 6 mm, the bulk of the grains are 0.5-1 mm in diameter. Feldspar grains show brittle deformation, in contrast to the quartz. The sparse matrix of phyllosilicate and carbonate minerals shows a weak cleavage parallel to the moderately strong grain elongation.

T61. Sample T61 thin-sections contain 50% quartz, 35% feldspar, and 15% matrix. Quartzofeldpathic lithic fragments make up about 5% of the sample and tend to occur in the coarser fraction (e.g., approximately 2 mm in diameter). Average grain diameters range from 0.25-1 mm, but quartz ribbons are as long as 6 mm. Feldspars appear brittley deformed. Matrix phyllosilicates show a weak cleavage parallel to the elongate quartz grains.

APPENDIX C

FIELD TRIP GUIDE

The following is a brief field trip guide to several key locations within the area of this study. As a starting point I have chosen the stop sign at the intersection of Tennessee Route 73 and the Cades Cove Road. This is located about one mile inside the National Park boundary and about 2 miles southeast of Townsend, Tennessee. This is the 0.0 mile mark for the trip. From this point turn left, heading to the northeast toward Gatlinburg, and begin keeping track of your odometer.

4.25 miles: Stop One (pull off to the right)

Just after crossing the last bridge you crossed into the area of the klippe. Across the road is well exposed Thunderhead Sandstone displaying interbedded fine sandstone and conglomerate. At the left end of the outcrop look up to see several large mudrock clasts within a very distinct layer of conglomerate.

4.85 miles: Stop Two (pull off to the right)

Park in the small pullout past the one which looks to Meig's Falls. Across the road note the well exposed Thunderhead Sandstone. Much of this exposure is made up of conglomeratic Thunderhead. Look at the flat surface dipping toward the road near the right end of the better exposures. The front edge of this flat surface is recognized by the remnant of a hole drilled through it. This is a slip surface displaying small steps. Carefully examine this area for large feldspar clasts which have been partially pulled apart. These clasts appear to have partially strained by shear along mineralogic cleavage planes.

5.88 miles: Stop Three (pull off to the right)

Park in the Sinks parking area. Here can be found evidence that the beds of Thunderhead Sandstone in this area are overturned. Walk down the pathway that leads

you past the trash cans. Soon thereafter turn to the right, working your way out to the top of the cliffs which overlook the water below the falls. Look for the spot which juts out significantly. Here you should look at the rocks underfoot. Careful inspection reveals crossbeds whose truncated tops are overturned.

Now walk back past where you parked and turn right on Route 73. Along the right side of the road is well exposed Thunderhead Sandstone. Careful inspection will reveal graded bedding, which supports the evidence for overturned bedding just examined. Bedding here dips to the right when looking from the road (i.e., bedding dips southeast). Note that there are several discrete planes which cut the beds at low angles. These surfaces lie at a lower angle than bedding. They appear to be minor fault surfaces which cut the Thunderhead at various angles and may be related to the nearby Sinks Fault.

7.25 miles: Stop Four (pull off to the right)

Park on the right side of the road just before a sharp right curve. Cross the road and follow the path down to the Little River. Across the river is a significant cliff. Notice that most of it is composed of Thunderhead Sandstone, but at the base of the cliff is a shaly looking unit. This is the Metcalf Phyllite. You are looking at the Greenbrier fault from within the larger of the two windows described by King (1964). Notice the large slivers or horses of Thunderhead which are completely surrounded by highly deformed Metcalf. Also note the shape of these slivers and the way several of them appear to be almost stacked upon one another. This is probably the best exposure of the Greenbrier fault in the are of study and nicely displays some of the features expected in fault zones.

APPENDIX D

R_f/ϕ AND PASE5 STRAIN ANALYSIS DATA

SPECIMEN REFERENCE.....
T 7XY

ELLIPSE NUMBER	AXIAL RATIO	LONG AXIS ORIENT.	CORREL.COEFF.
1	1.59	17.44	0.76
2	1.80	-45.83	0.84
3	1.55	-5.90	0.91
4	2.26	7.62	0.94
5	2.78	-4.83	0.91
6	1.52	11.77	0.49
7	1.26	26.36	0.40
8	1.35	1.81	0.49
9	2.14	1.89	0.91
10	5.02	-5.83	1.00
11	2.94	9.89	0.95
12	5.17	-2.62	0.99
13	2.29	-0.81	0.70
14	6.06	-0.93	0.92
15	1.66	-5.49	0.97
16	2.87	-5.37	0.98
17	2.84	-4.38	0.98
18	3.63	-8.44	0.99
19	2.50	-1.10	0.97
20	2.12	6.37	0.97
21	2.18	-2.71	0.97
22	3.32	1.03	0.99
23	2.81	-5.78	0.94
24	2.24	15.37	0.97
25	1.75	-7.24	0.86
26	2.44	27.01	0.98
27	3.81	-5.12	0.97
28	5.79	-15.01	0.99
29	3.77	17.28	0.99
30	2.90	-10.50	0.97
31	6.11	-8.35	0.98
32	1.65	7.14	0.94
33	1.18	21.23	0.56
34	3.46	-1.16	0.99
35	2.74	-7.37	0.72
36	2.32	3.48	0.98
37	3.39	-1.56	0.96
38	3.99	21.21	0.99
39	1.64	5.09	0.73
40	1.91	2.63	0.98
41	1.96	-1.71	0.85
42	3.37	11.00	0.93
43	6.21	-3.77	0.96
44	4.42	4.32	0.98
45	1.90	-11.50	1.00
46	3.25	7.26	0.96
47	3.25	-0.37	0.98
48	2.16	0.26	0.91
49	1.73	-18.58	0.91

Press <RETURN> when ready to continue

SPECIMEN PEFERENCE.....
T 7X2

ELLIPSE NUMBER	AXIAL RATIO	LONG AXIS ORIENT.	CORREL.COEFF.
1	3.92	78.85	0.97
2	7.51	95.57	0.99
3	5.24	-83.60	0.93
4	2.54	-87.53	0.96
5	3.53	-94.78	0.96
6	3.33	97.87	0.80
7	1.51	-96.35	0.94
8	3.45	66.85	0.87
9	1.86	84.27	0.91
10	3.21	89.07	0.96
11	2.06	78.31	0.98
12	1.56	81.93	0.85
13	3.66	72.11	0.89
14	2.27	88.33	0.97
15	4.01	79.95	0.97
16	4.67	61.30	0.95
17	1.33	-81.52	0.59
18	3.26	80.75	0.78
19	1.78	-86.99	0.81
20	1.99	88.93	0.94
21	3.66	-88.54	1.00
22	2.12	-89.38	0.96
23	4.59	-83.92	0.93
24	1.79	66.64	0.97
25	3.26	80.74	0.99
26	1.82	86.75	0.91
27	3.29	76.74	1.00
28	5.37	59.31	0.92
29	3.00	89.39	0.98
30	1.66	70.48	0.85
31	3.98	84.51	0.99
32	4.38	-98.33	0.93
33	1.85	79.17	0.92
34	1.71	-87.23	0.90
35	1.49	60.09	0.91
36	2.99	90.53	0.96
37	2.92	79.10	0.94
38	1.59	-72.50	0.91
39	1.34	82.26	0.79
40	2.20	79.74	0.98
41	2.22	-87.48	0.83
42	2.94	89.45	0.97
43	2.74	80.19	0.99
44	1.53	-76.13	0.87
45	1.38	61.49	0.89
46	2.46	85.35	0.95
47	2.76	71.56	0.99

Press <RETURN> when ready to continue

97

SPECIMEN REFERENCE.....
T 7YZ

ELLIPSE NUMBER	AXIAL RATIO	LONG AXIS ORIENT.	CORREL.COEFF.
1	2.36	-51.36	0.99
2	4.42	-41.32	0.79
3	2.53	-51.90	0.75
4	1.76	-38.94	0.87
5	1.61	-59.44	0.94
6	2.45	-46.29	0.99
7	1.34	-86.91	0.83
8	3.20	-62.41	0.95
9	1.62	-53.86	0.93
10	1.86	53.22	0.91
11	1.89	-37.11	0.95
12	2.10	-36.36	0.90
13	1.37	84.71	0.74
14	2.41	-28.67	0.96
15	2.52	-38.78	0.92
16	3.71	-57.93	0.91
17	3.83	-66.50	0.98
18	2.43	-39.21	0.98
19	3.15	-90.92	0.95
20	1.44	-39.31	0.93
21	4.06	-99.83	0.99
22	2.68	-37.11	0.90
23	3.03	-53.51	0.97
24	1.33	-50.58	0.79
25	5.14	-67.39	0.96
26	3.43	-64.10	0.98
27	2.29	-56.21	0.99
28	1.35	82.38	0.60
29	2.06	-49.45	0.95
30	1.69	-60.45	0.97
31	1.64	-55.58	0.89
32	2.20	14.20	0.91
33	2.75	-62.12	0.79
34	2.46	-76.30	0.88
35	1.33	79.09	0.45
36	1.62	-10.89	0.95
37	4.24	-46.89	0.93
38	1.61	-63.63	0.74
39	4.34	-69.29	1.00
40	2.84	67.70	0.90
41	2.09	-64.77	0.82
42	1.53	-81.20	0.86
43	1.82	-94.49	0.81
44	1.73	-32.11	0.95
45	1.57	-51.77	0.92
46	1.39	65.56	0.48

Press <RETURN> when ready to continue

98

T 7XY
49 DATA POINTS
FLUCTUATION = 73
LOGMEAN Rf =   2.597
ORIGINAL ZERO =   0.930

TRY AN Rs ESTIMATE.....
Rs Ri = 2.27,1.60

SYMMETRY.....

16   9

8   15
Hard copy now
Press <RETURN> when ready

WANT TO TRY ANOTHER? N
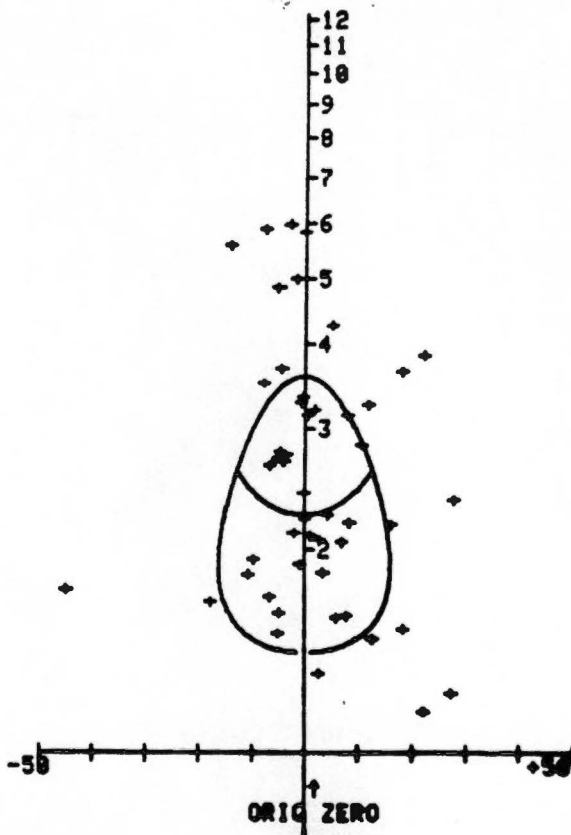
T 7XZ
47 DATA POINTS
FLUCTUATION = 48
LOGMEAN Rf =   2.599
ORIGINAL ZERO =   -84.512

TRY AN Rs ESTIMATE.....
Rs Ri = 2.33,1.60

SYMMETRY.....

12   12

11   11
Hard copy now
Press <RETURN> when ready

T 7YZ
46 DATA POINTS
FLUCTUATION = 141
LOGMEAN Rf =   2.227
URIGINAL ZERO =   60.458

TRY AH Rs ESTIMATE.....
Rs Ri = 1.63,1.60

SYMMETRY.....

12   18

11   12
Hard copy now
Press <RETURN> when ready

ORIG ZERO
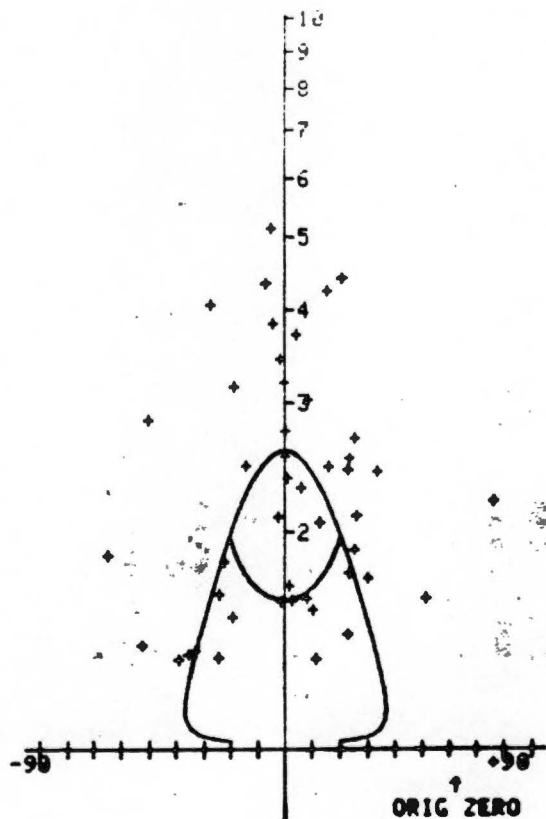
SPECIMEN REFERENCE.....
T 29 XY

ELLIPSE NUMBER	AXIAL RATIO	LONG AXIS ORIENT.	CORREL.COEFF.
1	1.86	86.99	0.81
2	1.55	77.53	0.71
3	2.27	84.85	0.97
4	2.58	88.92	0.92
5	2.06	87.97	0.82
6	2.40	-86.92	0.79
7	2.94	80.27	0.97
8	1.77	-82.77	0.94
9	1.68	-90.00	0.64
10	2.17	84.41	0.96
11	1.40	-43.25	0.77
12	1.72	-69.84	0.87
13	3.27	-88.31	0.93
14	3.26	82.91	0.97
15	2.19	-88.30	0.92
16	2.16	82.58	0.80
17	1.85	-61.20	0.73
18	3.16	-80.15	1.00
19	1.51	-53.32	0.97
20	3.14	-81.09	1.00
21	3.89	-77.35	0.93
22	1.93	-70.27	0.90
23	2.34	76.70	0.99
24	2.33	87.10	0.79
25	1.62	58.67	0.82
26	1.77	74.87	0.96
27	2.03	-84.42	0.94
28	1.27	42.10	0.87
29	2.31	34.01	0.71
30	1.67	-70.11	0.75
31	1.58	81.99	0.84
32	2.03	-87.51	0.99
33	3.14	85.83	0.88
34	2.29	85.13	0.98
35	1.27	-47.94	0.62
36	3.66	-88.98	0.93
37	3.86	88.17	0.84
38	2.40	80.37	0.95
39	5.46	88.98	0.81
40	2.21	-88.99	0.92
41	2.97	87.29	0.91
42	2.01	88.19	0.97

Press <RETURN> when ready to continue

SPECIMEN REFERENCE.....
T 29YZ

ELLIPSE NUMBER	AXIAL RATIO	LONG AXIS ORIENT.	CORREL.COEFF.
1	2.29	-4.56	0.83
2	1.18	-68.38	0.39
3	1.52	14.84	0.81
4	1.25	87.18	0.43
5	2.03	0.36	0.80
6	6.02	-3.77	0.98
7	1.83	4.29	0.95
8	4.80	6.20	0.99
9	4.00	-6.55	0.98
10	2.54	-30.60	0.85
11	2.98	20.97	0.77
12	2.76	-7.37	0.92
13	3.74	4.88	0.99
14	5.27	4.67	0.91
15	2.63	1.14	0.99
16	3.58	-2.52	0.84
17	1.58	5.72	0.87
18	4.05	10.22	0.99
19	1.61	-10.39	0.93
20	1.93	-16.07	0.97
21	1.86	-28.17	0.81
22	2.06	7.30	0.89
23	7.53	13.43	0.92
24	2.90	-6.67	0.98
25	1.82	-0.11	0.86
26	3.60	2.37	0.90
27	1.50	-7.43	0.74
28	2.52	-0.58	0.88
29	3.20	-5.02	0.98
30	2.82	4.17	0.97
31	2.92	-6.45	0.98
32	2.25	-20.70	0.81
33	2.74	0.08	0.98
34	4.26	1.30	0.91
35	4.44	9.25	0.86
36	4.19	-10.96	0.97
37	2.83	-12.87	0.96
38	2.71	-5.35	0.86
39	3.65	-18.52	0.91
40	2.23	17.47	0.98
41	1.70	-8.91	1.00
42	3.63	-1.70	0.98
43	2.41	-6.00	0.97
44	2.27	6.13	0.96
45	1.29	0.82	0.54
46	2.87	9.55	0.84
47	1.99	-3.96	0.75
48	1.71	12.03	0.85
49	1.71	-7.51	0.82
50	2.28	6.45	0.80
51	2.53	6.34	0.89
52	2.45	-15.65	0.96
53	3.53	2.87	0.93
54	2.48	-1.84	0.96
55	3.28	-9.49	0.86
56	2.31	-0.32	0.96
57	2.44	4.87	0.99
58	2.41	17.33	0.71
59	2.30	-31.25	0.95
60	1.28	2.48	0.63
61	2.95	11.76	0.97
62	1.88	9.88	0.84

Press <RETURN> when ready to continue

ELLIPSE NUMBER	AXIAL RATIO	LONG AXIS ORIENT.	CORREL.COEFF.
1	1.43	64.89	0.56
2	1.84	-20.12	0.93
3	3.44	0.46	0.82
4	1.60	72.55	0.73
5	1.84	-11.21	0.91
6	1.14	32.71	0.58
7	1.31	12.72	0.99
8	1.10	-70.55	0.36
9	1.58	-1.07	0.75
10	1.58	-14.77	0.88
11	1.05	-7.04	0.24
12	2.07	20.34	0.95
13	1.44	7.82	0.61
14	1.50	-12.22	0.69
15	1.25	-17.17	0.58
16	1.45	-11.14	0.55
17	1.56	13.14	0.98
18	2.45	-25.14	0.74
19	1.38	34.69	0.54
20	1.58	-44.78	0.92
21	1.24	87.67	0.47
22	1.25	-2.75	0.65
23	1.61	-41.01	0.95
24	3.04	-1.96	0.92
25	1.28	49.26	0.59
26	1.54	-89.12	0.91
27	1.15	-59.36	0.77
28	1.14	-6.57	0.42
29	2.31	-30.51	0.97
30	1.95	-30.34	0.91
31	1.11	-10.71	0.47
32	1.63	-18.26	0.74
33	1.29	24.76	0.42
34	1.45	-6.88	0.74
35	1.97	29.86	0.86
36	1.70	24.54	0.94
37	2.27	-24.69	0.82
38	5.80	-22.11	0.97
39	1.47	54.04	0.75
40	2.59	31.61	0.76
41	1.48	74.90	0.67
42	1.44	26.14	0.87
43	1.35	-79.95	0.77
44	1.49	14.69	0.74
45	1.29	79.28	0.52

Press <RETURN> when ready to continue

T 29 XY
42 DATA POINTS
FLUCTUATION = 103
LOGMEAN Rf =   2.233
ORIGINAL ZERO =   -88.924

TRY AN Rs ESTIMATE.....
Rs Ri = 2.10,1.40

SYMMETRY.....

11   10

10   10
Hard copy now
Press <RETURN> when ready

ORIG ZERO
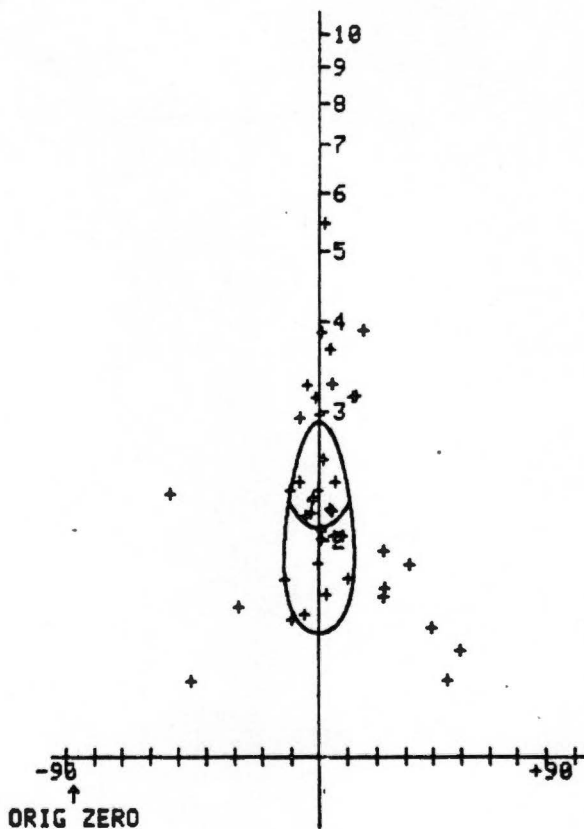
T 29YZ
62 DATA POINTS
FLUCTUATION = 156
LOGMEAN Rf =   2.557
ORIGINAL ZERO =   -0.084

TRY AN Rs ESTIMATE.....
Rs Ri = 2.39,1.40

SYMMETRY.....

15   15

16   15
Hard copy now
Press <RETURN> when ready

ORIG ZERO

104
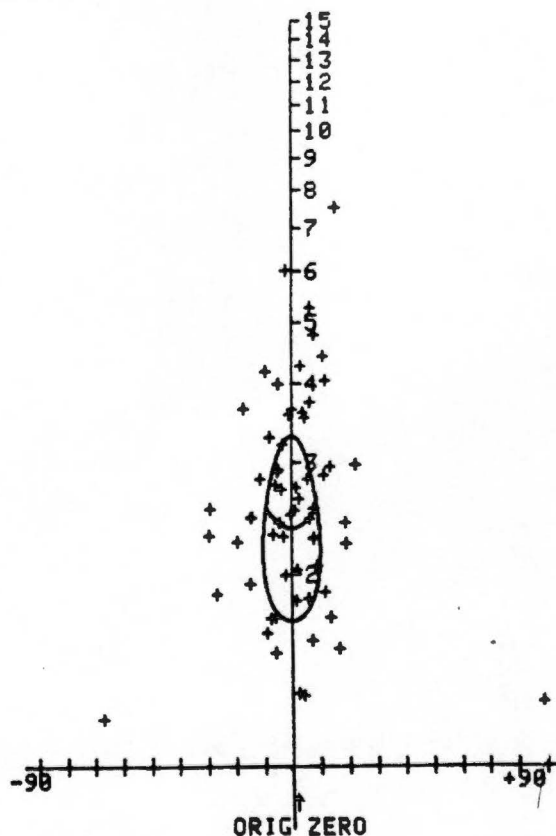
T 29X2
45 DATA POINTS
FLUCTUATION = 172
LOGMEAN Rf =   1.613
ORIGINAL ZERO =   6.573

TRY AN Rs ESTIMATE.....
Rs Ri = 1.23,1.45

SYMMETRY.....

12   10

10   12
Hard copy now
Press <RETURN> when ready

105
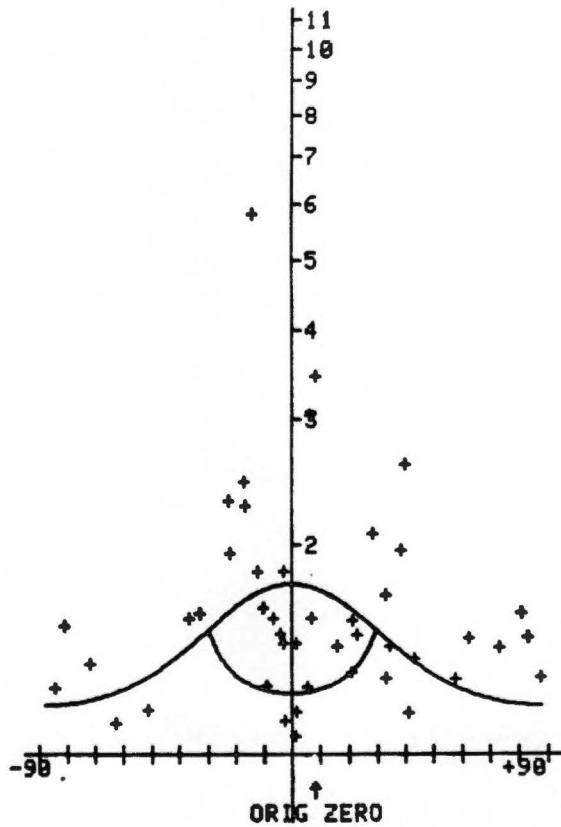
SPECIMEN REFERENCE.....
T 30XY

ELLIPSE NUMBER	AXIAL RATIO	LONG AXIS ORIENT.	CORREL.COEFF.
1	1.36	34.69	0.46
2	1.47	-71.19	0.59
3	2.02	-68.96	0.85
4	2.79	-49.80	0.80
5	3.54	-45.56	0.86
6	1.92	-68.45	0.91
7	4.45	-89.84	0.99
8	3.69	-71.32	1.00
9	1.74	-57.56	0.94
10	3.58	-71.62	0.92
11	1.74	-61.75	0.65
12	1.28	-27.82	0.42
13	3.31	-56.64	0.94
14	1.17	-71.81	0.25
15	2.96	-54.83	0.89
16	1.21	-64.59	0.37
17	2.46	83.01	0.90
18	1.70	-58.90	0.95
19	2.26	-72.75	0.97
20	2.15	-56.26	0.74
21	1.72	-80.99	0.93
22	1.99	-71.63	0.93
23	1.80	89.09	0.02
24	1.19	42.99	0.49
25	2.20	-48.40	0.75
26	2.45	-79.47	0.97
27	2.46	65.33	0.86
28	3.64	-75.67	0.73
29	3.49	-63.35	0.88
30	2.24	-59.02	0.65
31	2.61	-61.62	0.90
32	2.37	-79.29	0.76
33	2.14	-73.24	0.67
34	3.64	-61.26	0.91
35	2.17	-86.03	0.96
36	3.97	-80.69	0.94
37	1.87	77.81	0.91
38	1.98	-89.53	0.95
39	3.67	-80.88	0.95
40	2.47	-64.89	0.97
41	1.65	-60.41	0.74
42	1.69	-74.53	0.82
43	1.74	-58.74	0.87
44	1.94	-12.59	0.83
45	2.44	-79.58	0.96
46	1.85	82.62	0.81
47	4.15	-50.97	0.92
48	2.16	-61.29	0.99
49	1.73	-77.51	0.90
50	2.71	-62.75	0.96
51	2.93	-39.64	0.91
52	2.98	-57.52	0.88
53	17.28	-58.24	0.83

Press <RETURN> when ready to continue

ELLIPSE NUMBER	AXIAL RATIO	LONG AXIS ORIENT.	CORREL.COEFF.
1	3.74	9.78	0.98
2	1.29	8.07	0.63
3	2.03	-19.97	0.69
4	3.03	-17.37	0.89
5	2.12	-13.34	0.78
6	1.35	-16.88	0.77
7	2.15	13.20	0.87
8	1.67	-18.67	0.94
9	2.06	82.95	0.92
10	1.44	-12.10	0.57
11	1.73	-5.75	0.75
12	2.47	-62.39	0.90
13	5.99	-6.00	0.97
14	3.01	5.56	0.95
15	1.48	87.22	0.75
16	1.19	-61.97	0.53
17	1.62	18.97	0.73
18	2.35	-24.27	0.80
19	1.62	40.35	0.76
20	2.71	86.39	0.93
21	1.35	30.65	0.70
22	2.01	16.99	0.93
23	1.88	59.17	0.92
24	1.37	-60.47	0.64
25	1.64	-22.70	0.67
26	1.29	62.72	0.53
27	2.11	52.74	0.80
28	1.65	6.96	0.97
29	3.49	-63.35	0.88
30	2.24	-59.02	0.65
31	2.61	-61.62	0.90
32	2.37	-79.29	0.76
33	2.14	-73.24	0.67
34	3.64	-61.26	0.91
35	2.17	-86.03	0.96
36	3.97	-80.69	0.94
37	1.87	77.81	0.91
38	1.98	-89.53	0.95
39	3.67	-30.88	0.95
40	2.47	-64.89	0.97
41	1.65	-60.41	0.74
42	1.69	-74.53	0.82
43	1.74	-58.74	0.87
44	1.94	-12.59	0.83
45	2.44	-79.58	0.96
46	1.85	92.62	0.81
47	4.15	-50.97	0.92
48	2.16	-61.28	0.99
49	1.73	-77.51	0.90
50	2.71	-62.75	0.96
51	2.93	-38.64	0.91
52	2.98	-57.52	0.88
53	17.28	-58.24	0.83

Press <RETURN> when ready to continue

SPECIMEN REFERENCE.....
T 30X2

ELLIPSE NUMBER	AXIAL RATIO	LONG AXIS ORIENT.	CORREL.COEFF.
1	3.07	-55.70	0.89
2	1.78	-8.21	0.71
3	1.48	-49.87	0.86
4	1.92	60.69	0.85
5	3.11	-11.54	0.78
6	1.71	-6.87	0.95
7	1.63	35.90	0.83
8	1.72	50.88	0.93
9	1.26	43.35	0.72
10	2.84	45.99	0.87
11	1.95	34.33	0.97
12	1.86	22.83	0.94
13	1.38	20.14	0.62
14	2.61	43.53	0.97
15	1.80	-34.17	0.86
16	1.49	-72.67	0.84
17	1.92	9.84	0.94
18	1.23	14.34	0.75
19	1.98	11.46	0.93
20	1.62	-87.50	0.69
21	2.34	6.59	0.88
22	3.18	-70.51	0.99
23	4.18	-39.68	0.99
24	1.93	-30.33	0.98
25	1.18	71.02	-0.48
26	1.44	-74.67	0.69
27	1.74	-15.04	0.94
28	1.46	-4.40	0.69
29	1.47	-53.89	0.75
30	2.25	68.29	0.97
31	1.36	45.03	0.67
32	1.26	-1.56	0.54
33	2.39	-24.04	0.90
34	1.09	47.24	0.39
35	1.46	-33.10	0.93
36	1.35	-53.47	0.73
37	2.11	-37.18	0.99
38	1.30	-73.52	0.83
39	1.80	68.48	0.87
40	8.57	-35.85	0.92
41	1.61	26.33	0.76
42	3.07	-25.21	0.98
43	1.92	-39.44	0.98
44	1.53	-10.69	0.93
45	2.26	28.89	0.84
46	1.99	-5.58	0.99
47	3.51	33.23	0.99
48	1.33	-80.61	0.82
49	1.56	72.91	0.55
50	1.37	64.51	0.78
51	1.49	-22.58	0.87
52	2.03	-78.88	0.97
53	1.39	41.65	0.59

Press <RETURN> when ready to continue

T 30XY
53 DATA POINTS
REBOTUATION = 133
LOGMEAN Rf =   2.354
ORIGINAL ZERO =   68.964

TRY AN Ps ESTIMATE.....
Rs Ri = 1.95,1.45

SYMMETRY.....

12   14

14   12
Hard copy now
Press <RETURN> when ready
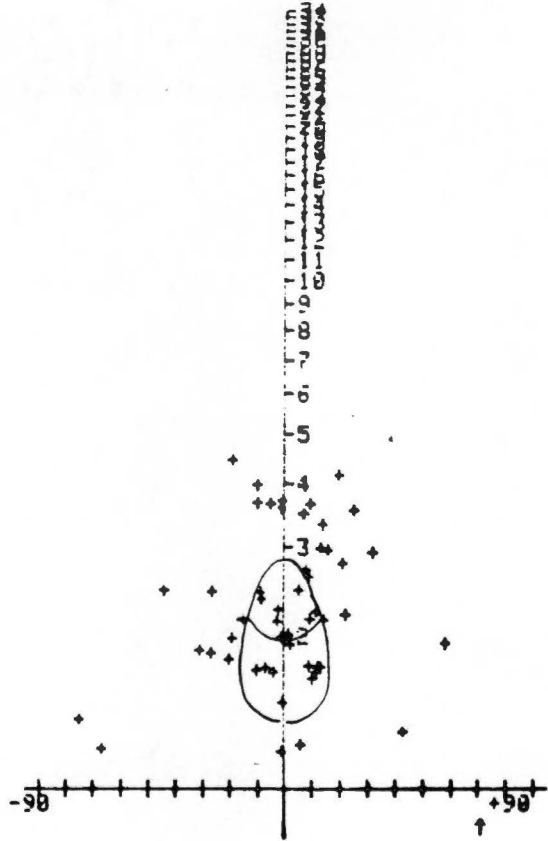
T 30YZ
39 DATA POINTS
FLUCTUATION = 177
LOGMEAN Rf =   1.964
ORIGINAL ZERO =   6.002

TRY AN Rs ESTIMATE.....
Rs Ri = 1.3,1.45

SYMMETRY.....

10   9

9   10
Hard copy now
Press <RETURN> when ready

109

ORIG ZERO
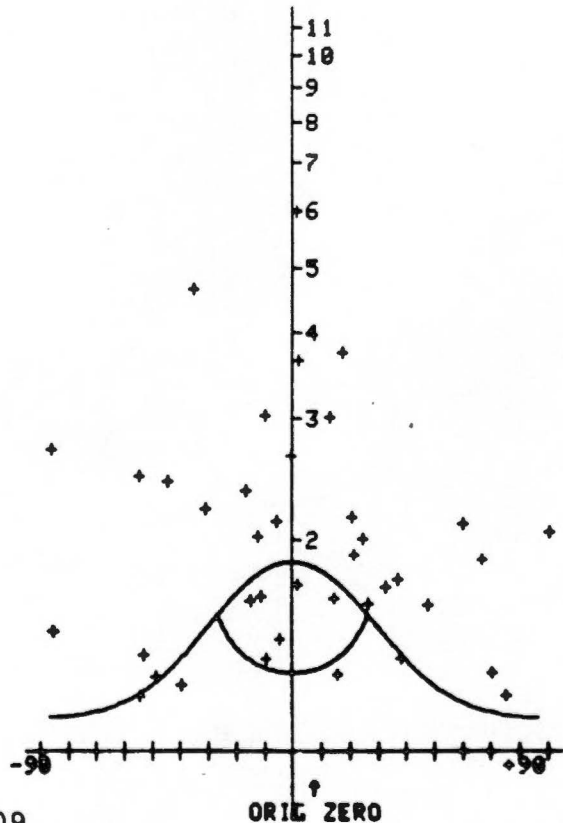
```
T  30XZ
53 DATA POINTS
REBOTUATION = 160
LOGMEAN Rf =    1.860
ORIGINAL ZERO =    5.575


TRY AN Rs ESTIMATE.....
Rs Ri = 1.20,1.45




SYMMETRY.....

16    10

10    16
Hard copy now
Press <RETURN> when ready
```
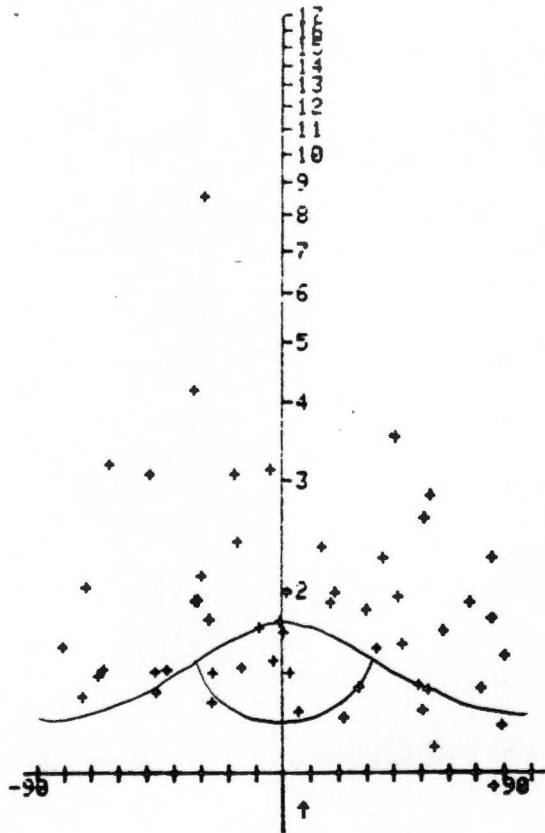
SPECIMEN REFERENCE.....
T32XY

ELLIPSE NUMBER	AXIAL RATIO	LONG AXIS ORIENT.	CORREL.COEFF
1	2.54	-34.09	0.97
2	1.45	-47.81	0.66
3	2.76	60.46	0.84
4	1.44	-46.74	0.88
5	1.50	46.02	0.75
6	1.23	77.02	0.62
7	1.85	-66.98	0.75
8	1.57	10.42	0.73
9	1.67	-45.93	0.84
10	1.88	-31.89	0.66
11	1.77	-14.12	0.77
12	3.50	-22.90	0.92
13	1.06	-32.28	0.13
14	1.31	-23.89	0.74
15	1.67	-15.10	0.86
16	1.35	-54.38	0.66
17	1.92	9.69	0.70
18	1.71	-43.48	0.79
19	1.14	-81.84	0.45
20	1.37	-68.21	0.72
21	1.90	-16.21	0.94
22	2.27	-35.08	0.90
23	1.91	-15.60	0.88
24	2.51	-16.86	0.94
25	3.18	-7.53	0.98
26	1.47	-19.02	0.68
27	1.54	-32.11	0.54
28	3.27	-25.30	0.91
29	1.69	-29.36	0.92
30	2.58	-26.24	0.99
31	1.29	-17.67	0.43
32	1.71	-38.49	0.91
33	3.24	-76.54	0.94
34	1.85	-27.77	0.79
35	2.16	-27.20	0.61
36	2.10	-14.92	0.92
37	3.42	-2.01	0.98
38	3.16	-29.82	0.99
39	2.96	-53.10	0.96
40	1.92	-51.62	0.87
41	6.76	-6.35	0.91
42	1.48	-50.32	0.75
43	1.89	-8.84	0.96
44	3.68	-38.85	0.78
45	2.09	-25.92	0.72
46	1.95	-45.77	0.83
47	2.43	-50.78	0.75
48	1.49	-13.15	0.69
49	1.97	-5.04	0.87
50	3.72	-10.81	0.88
51	2.49	-5.77	0.88
52	2.06	1.71	0.90
53	2.81	-35.60	0.97
54	2.56	-41.94	0.95
55	1.68	-65.08	0.59

Press <RETURN> when ready to continue

111

SPECIMEN REFERENCE. ...
T32YZ

ELLIPSE NUMBER	AXIAL RATIO	LONG AXIS ORIENT.	CORREL.COEFF.
1	2.71	36.64	0.97
2	2.19	6.63	0.72
3	1.50	52.60	0.72
4	1.28	-73.47	0.59
5	3.40	59.44	0.97
6	1.94	69.64	0.74
7	1.74	75.80	0.79
8	2.38	-86.38	0.98
9	2.85	64.19	0.88
10	2.32	67.46	0.84
11	1.61	-71.64	0.82
12	1.84	51.27	0.76
13	1.51	49.03	0.73
14	1.57	59.55	0.87
15	3.05	59.44	0.98
16	1.65	86.36	0.80
17	2.59	35.57	0.94
18	3.51	58.60	0.93
19	2.42	70.83	0.95
20	1.35	87.31	0.90
21	1.88	34.72	0.76
22	2.06	-67.13	0.66
23	2.10	-81.95	0.72
24	1.85	86.17	0.07
25	1.58	56.97	0.94
26	1.75	27.55	0.60
27	1.63	66.81	0.09
28	1.18	65.60	0.90
29	1.69	47.12	0.88
30	2.12	55.51	0.97
31	1.81	67.33	0.93
32	1.17	74.14	0.49
33	1.73	0.89	0.83
34	1.35	77.97	0.73
35	2.47	-3.57	0.96
36	1.61	44.60	0.73
37	1.30	58.89	0.70
38	1.82	52.63	0.78
39	1.18	76.08	0.33
40	1.82	58.16	0.97
41	2.22	88.66	0.75
42	1.82	69.69	0.83
43	2.79	50.47	0.90
44	1.37	-6.59	0.87
45	1.81	59.30	0.72
46	2.35	54.22	0.96
47	2.84	29.23	0.91
48	1.89	1.85	0.91
49	1.15	22.87	0.61
50	1.37	12.04	0.77
51	2.54	70.67	0.76
52	1.45	33.26	0.74
53	1.09	60.07	0.26
54	1.93	-31.75	0.91
55	2.48	58.47	0.91
56	1.44	-88.79	0.63
57	1.69	40.91	0.86
58	1.40	-31.10	0.66
59	1.93	50.43	0.89
60	1.83	73.31	0.01
61	2.24	57.77	0.91
62	1.99	71.14	0.70
63	2.30	40.23	0.96

112

```
64              2.05            -86.74          0.98
65              1.78             26.95          0.88
66              1.52            -89.80          0.73
Press <RETURN> when ready to continue
```

SPECIMEN REFERENCE ...
T32XZ

ELLIPSE NUMBER	AXIAL RATIO	LONG AXIS ORIENT.	CORREL.COEFF.
1	1.75	-20.13	0.59
2	1.48	-32.51	0.97
3	1.59	-54.67	0.30
4	1.16	60.69	0.43
5	2.50	-71.49	0.92
6	1.62	-77.15	0.75
7	2.70	63.03	0.93
8	1.16	-35.70	0.50
9	2.53	-63.84	0.86
10	1.36	-48.23	0.82
11	1.23	-25.17	0.69
12	1.92	-25.42	0.84
13	2.06	-67.93	0.88
14	1.66	-89.77	0.93
15	1.79	-33.27	0.86
16	1.69	-34.28	0.67
17	1.15	20.82	0.33
18	2.06	-50.70	0.01
19	1.52	47.99	0.77
20	2.10	-61.57	0.08
21	1.96	-52.15	0.96
22	2.11	1.80	0.90
23	1.80	-45.33	0.81
24	3.45	72.79	0.91
25	1.90	-49.23	0.76
26	2.59	-64.61	0.06
27	1.51	-50.50	0.93
28	1.48	75.80	0.73
29	1.22	-61.47	0.44
30	2.06	82.19	0.70
31	2.54	-58.77	0.96
32	2.00	81.14	0.99
33	1.34	-26.20	0.69
34	1.10	-10.84	0.36
35	1.41	-82.12	0.81
36	1.63	-59.95	0.67
37	1.75	-11.92	0.94
38	1.85	-62.08	0.89
39	1.65	-41.91	0.89
40	3.35	6.04	0.98
41	3.40	-65.76	0.65
42	1.43	-30.02	0.62
43	2.35	-72.74	0.79
44	2.38	-49.95	0.75
45	1.22	-61.15	0.41
46	1.51	-81.08	0.73
47	1.79	-62.77	0.80
48	3.09	-49.11	0.93
49	1.32	-51.12	0.48
50	1.67	-4.94	0.78
51	1.50	83.67	0.73
52	1.69	36.12	0.72
53	1.46	-30.63	0.96
54	1.93	-43.55	0.94
55	1.99	-53.46	0.86
56	2.07	80.51	0.91
57	1.65	-75.67	0.85
58	1.78	-25.15	0.84
59	1.56	-42.13	0.72
60	3.30	-30.64	0.01
61	1.58	-54.94	0.90
62	1.75	-02.40	0.94
63	1.44	9.10	0.57

114

| 64 | 2.41 | -54.16 | 0.99 |
| 55 | 2.35 | -56.16 | 0.90 |

Press RETURN when ready to continue

T32XY
55 DATA POINTS
FLUCTUATION = 163
LOGMEAN Rf =   2.032
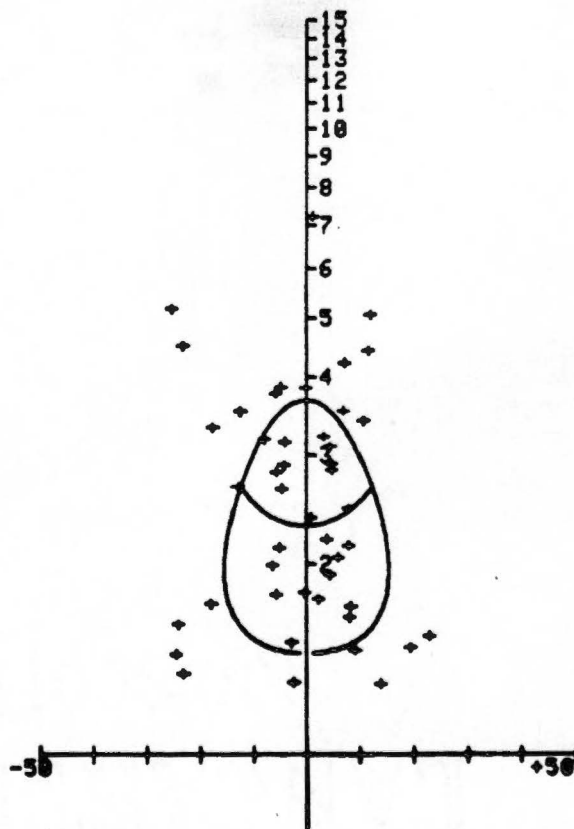ORIGINAL ZERO =   27.774

TRY AN Rs ESTIMATE.....
Rs Ri = 1.66,1.45

SYMMETRY.....

12   15

15   12
Hard copy now
Press <RETURN> when ready
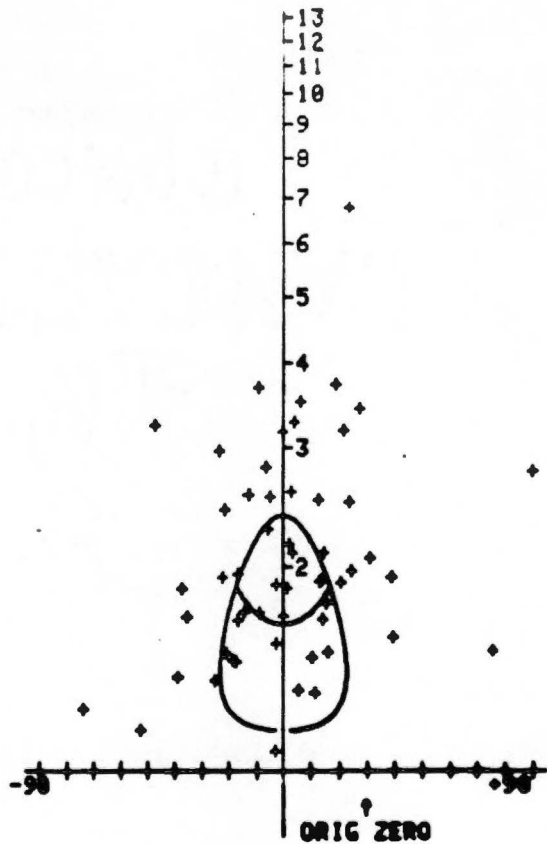
T32YZ
66 DATA POINTS
FLUCTUATION = 155
LOGMEAN Rf =   1.853
ORIGINAL ZERO =   -59.437

TRY AN Rs ESTIMATE.....
Rs Ri = 1.50,1.45

SYMMETRY.....

19   14

14   18
Hard copy now
Press <RETURN> when ready

116
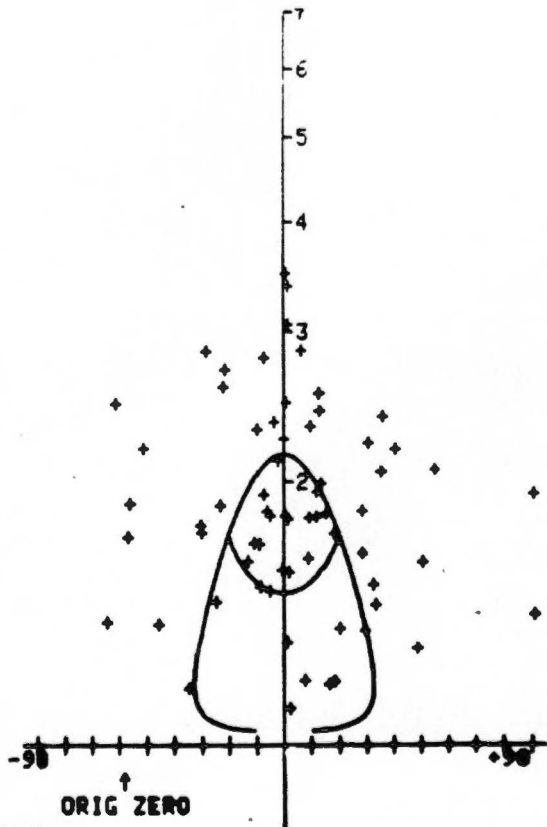
```
T32XZ
65 DATA POINTS
FLUCTUATION = 168
LOGMEAN RF =    1.809
ORIGINAL ZERO =    53.461


TRY AN Rs ESTIMATE.....
Rs Ri = 1.45,1.45




SYMMETRY.....

17    14

15    18
Hard copy now
Press <RETURN> when ready
```


ORIG ZERO

117
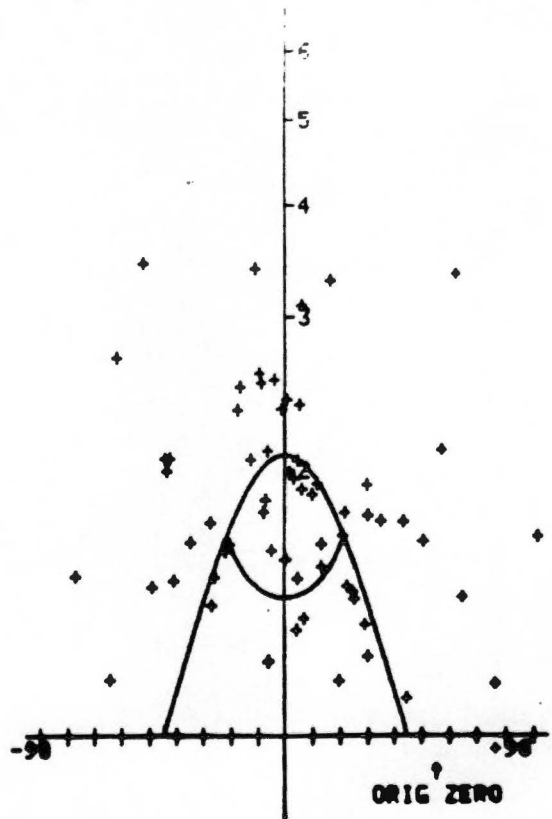
SPECIMEN REFERENCE.....
T5L33XY

ELLIPSE NUMBER	AXIAL RATIO	LONG AXIS ORIENT.	CORREL.COEFF.
1	1.29	59.33	0.49
2	1.26	79.60	0.42
3	1.55	76.60	0.78
4	1.97	47.00	0.83
5	2.14	40.97	0.95
6	1.50	-55.14	0.69
7	1.37	-3.09	0.65
8	2.90	-16.86	0.92
9	2.75	61.50	0.90
10	1.75	-79.80	0.94
11	2.47	-39.23	0.95
12	1.48	-65.64	0.93
13	1.36	-25.92	0.85
14	1.21	-33.30	0.52
15	2.52	-34.80	0.98
16	1.21	-58.38	0.79
17	1.08	-48.42	0.17
18	8.66	-47.64	0.98
19	2.36	-54.27	0.85
20	1.67	-68.52	0.68
21	1.54	-12.61	0.90
22	1.57	-35.12	0.85
23	1.61	23.59	0.97
24	1.27	78.19	0.71
25	1.39	-16.76	0.86
26	1.28	-38.45	0.63
27	1.11	16.87	0.20
28	1.22	79.05	0.38
29	1.29	78.26	0.56
30	1.77	75.98	0.95
31	1.26	24.93	0.55
32	1.50	62.37	0.83
33	1.23	-26.00	0.47
34	1.05	-49.78	0.18
35	1.39	69.52	0.73
36	1.32	-86.25	0.80
37	1.91	-5.01	0.93
38	1.47	84.70	0.82
39	2.61	-75.64	0.79
40	2.29	23.02	0.93
41	1.50	6.33	0.89

Press <RETURN> when ready to continue

SPECIMEN REFERENCE.....
T5L33YZ

ELLIPSE NUMBER	AXIAL RATIO	LONG AXIS ORIENT.	CORREL.COEFF.
1	2.46	14.42	0.76
2	1.19	-2.50	0.36
3	1.82	-38.67	0.94
4	1.23	2.32	0.60
5	3.09	21.74	0.97
6	1.79	7.03	0.70
7	1.81	-4.31	0.95
8	1.37	-11.93	0.87
9	2.97	-26.37	0.82
10	1.05	1.61	0.21
11	2.30	6.54	0.98
12	1.70	-14.85	0.69
13	1.30	-5.08	0.67
14	1.24	33.21	0.67
15	2.08	-13.05	0.91
16	1.35	87.90	0.64
17	1.30	55.98	0.57
18	1.39	-0.05	0.82
19	1.13	22.71	0.39
20	2.11	-12.10	0.86
21	2.46	-26.85	0.94
22	1.62	-58.20	0.70
23	1.21	-33.12	0.36
24	1.50	45.14	0.93
25	1.51	16.56	0.67
26	2.78	-23.46	0.94
27	1.25	-40.15	0.61
28	1.43	1.94	0.61
29	1.21	72.46	0.52
30	1.49	32.23	0.49
31	4.18	-17.43	0.86
32	8.83	57.62	0.94
33	1.06	7.48	0.13
34	1.52	-48.13	0.61
35	2.24	0.13	0.94
36	1.42	39.14	0.95
37	4.46	7.72	0.57
38	1.42	27.21	0.80
39	1.74	-42.15	0.96
40	3.05	9.60	0.79
41	1.43	1.92	0.69
42	2.14	46.64	0.80

Press <RETURN> when ready to continue

119

SPECIMEN REFERENCE.....
T5L33XZ

ELLIPSE NUMBER	AXIAL RATIO	LONG AXIS ORIENT.	CORREL.COEFF.
1	3.17	-60.69	0.99
2	1.25	-39.47	0.72
3	2.03	83.05	0.84
4	2.30	-4.95	0.57
5	2.21	67.11	0.76
6	1.57	-24.05	0.96
7	1.65	-96.70	0.82
8	1.41	36.20	0.64
9	1.54	91.39	0.85
10	5.52	38.51	0.97
11	1.74	41.27	0.92
12	5.64	74.69	0.98
13	2.46	96.61	0.97
14	1.93	71.80	0.78
15	1.59	62.28	0.89
16	2.00	48.88	0.76
17	1.78	75.48	0.91
18	2.07	72.26	0.89
19	1.94	85.51	0.85
20	1.78	74.62	0.95
21	3.30	54.47	0.95
22	1.73	55.34	0.83
23	1.70	-71.80	0.89
24	4.32	89.77	0.86
25	1.33	81.60	0.56
26	1.50	63.08	0.74
27	1.74	38.77	0.68
28	1.60	-63.21	0.90
29	1.64	48.81	0.58
30	1.86	69.94	0.99
31	2.22	81.00	0.94

Press <RETURN> when ready to continue

T 33XY
41 DATA POINTS
REBOTUATION = 164
LOGMEAN Rf =   1.633
ORIGINAL ZEPO =   54.274

TRY AN Rs ESTIMATE.....
Rs Ri = 1.05,1.30

SYMMETRY.....

8   11

12   9
Hard copy now
Press <RETURN> when ready
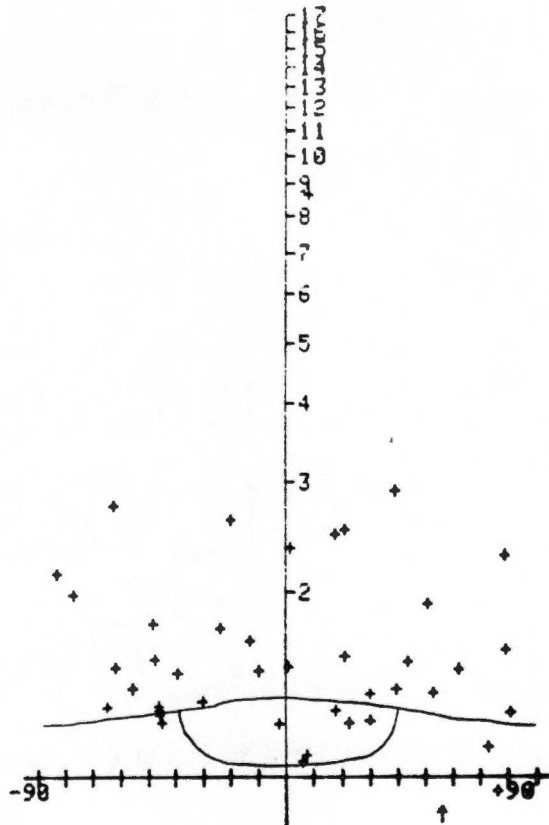
T 33YZ
42 DATA POINTS
REBOTUATION = 146
LOGMEAN Rf =   1.799
ORIGINAL ZEPO =   -1.942

TRY AN Rs ESTIMATE.....
Rs Ri = 1.42,1.30

SYMMETRY.....

12   9

9   11
Hard copy now
Press <RETURN> when ready

121

T 33XZ
31 DATA POINTS
FLUCTUATION = 161
LOGMEAN Rf = 2.036
ORIGINAL ZERO = -74.693

TRY AN Rs ESTIMATE.....
Rs Ri = 1.75,1.40

SYMMETRY.....

7   8

8   7
Hard copy now
Press <RETURN> when ready

-90
↑
ORIG ZERO

122
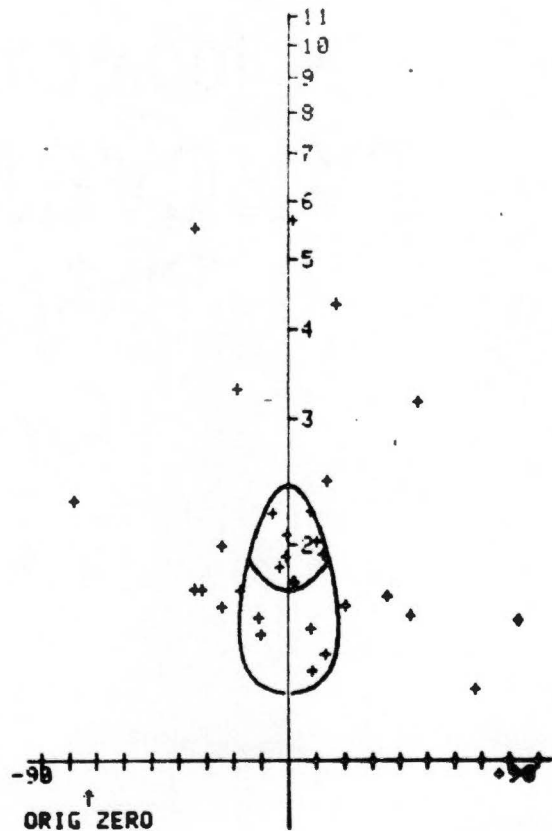
SPECIMEN REFERENCE.....
    T 34XY

ELLIPSE NUMBER	AXIAL RATIO	LONG AXIS ORIENT.	CORREL.COEFF.
1	6.22	77.02	1.00
2	2.47	81.81	0.94
3	1.78	73.30	0.95
4	1.43	76.93	0.70
5	2.13	81.36	0.90
6	3.04	80.78	0.98
7	2.58	74.19	0.97
8	1.79	-40.44	0.85
9	2.29	48.26	0.93
10	1.85	-67.70	0.90
11	1.53	-86.38	0.91
12	4.25	61.25	0.70
13	2.50	73.60	0.94
14	1.36	41.29	0.50
15	1.25	-75.74	0.66
16	1.74	-70.81	0.75
17	3.29	82.55	0.83
18	1.15	28.02	0.37
19	2.49	60.55	0.90
20	1.87	48.10	0.04
21	2.75	-54.43	0.96
22	3.33	64.00	0.89
23	1.67	25.61	0.82
24	1.86	9.11	0.92
25	4.35	58.70	0.90
26	1.17	3.40	0.50
27	2.40	55.52	0.92
28	2.53	-22.50	0.82
29	1.50		0.57
30	1.31		0.90
31	1.90	3.03	0.75
32	1.32	44.52	0.70
33	1.38	71.99	0.89
34	1.22	-71.18	0.72
35	1.68	71.06	0.95
36	1.88	39.09	0.96
37	3.54	-69.99	0.97
38	2.01	71.14	0.84
39	3.66	65.73	0.99
40	1.08	25.33	0.45
41	1.81	30.26	0.95
42	1.67	-52.31	0.86
43	1.50	-28.29	0.75
44	1.22	60.57	0.58
45	1.54	10.61	0.93
46	1.32	-88.60	0.84
47	1.04	-51.63	0.24
48	1.11	-61.08	0.23
49	1.31	50.46	0.04
50	1.58	74.47	0.06
51	2.03	61.62	0.79
52	1.37	66.45	0.74

Press <RETURN> when ready to continue

123

SPECIMEN REFERENCE.....
    T 34XZ

ELLIPSE NUMBER	AXIAL RATIO	LONG AXIS ORIENT.	CORREL.COEFF.
1	2.22	17.17	0.99
2	3.75	12.09	0.90
3	2.05	3.53	0.80
4	2.10	-34.98	0.92
5	2.64	53.19	0.99
6	1.39	73.35	0.69
7	6.02	-6.51	0.99
8	1.53	51.50	0.93
9	2.29	11.22	0.79
10	1.43	-14.91	0.69
11	1.68	-9.15	0.95
12	3.36	4.95	0.99
13	2.48	0.73	0.90
14	2.02	-8.87	0.88
15	2.41	28.79	0.92
16	1.74	8.20	0.82
17	2.55	1.21	0.97
18	1.77	-2.72	0.90
19	3.02	-0.27	1.00
20	1.26	5.67	0.37
21	2.36	-15.51	0.89
22	3.56	-10.13	0.96
23	3.73	-1.32	0.96
24	2.73	-3.25	0.73
25	1.80	-02.21	0.96
26	1.55	-4.53	0.83
27	2.40	12.03	0.90
28	1.99	42.55	0.91
29	2.49	3.57	0.99
30	1.86	3.54	0.96
31	1.85	3.57	0.94
32	3.59	-10.04	0.93
33	5.96	15.04	0.99
34	3.56	-5.11	0.92
35	2.53	2.56	0.94
36	2.75	9.89	0.99
37	1.18	-17.17	0.63
38	4.11	-10.26	0.87
39	3.46	16.03	0.97
40	2.03	10.11	0.86
41	2.04	5.26	0.93
42	2.41	23.63	0.98
43	2.90	-13.31	0.89
44	2.75	-27.88	0.85
45	2.56	4.56	0.98
46	3.20	9.07	0.89
47	1.35	4.83	0.89
48	2.95	-4.09	0.94
49	2.10	10.80	0.93
50	1.16	11.66	0.62
51	3.61	10.43	0.98
52	2.02	-1.74	0.89
53	1.39	-55.23	0.85
54	2.21	3.98	0.96
55	1.22	-37.33	0.72
56	1.26	-5.61	0.85
57	2.60	10.13	0.95

Press <RETURN> when ready to continue

124

```
SPECIMEN REFERENCE.....
   T  34YZ
```

ELLIPSE NUMBER	AXIAL RATIO	LONG AXIS ORIENT.	CORREL.COEFF
1	2.19	60.05	0.77
2	1.34	92.29	0.71
3	1.77	6.99	0.89
4	2.94	71.84	0.95
5	1.64	72.84	0.76
6	1.48	-84.51	0.89
7	1.21	80.72	0.56
8	3.37	-62.57	0.99
9	2.33	-76.70	0.89
10	1.34	29.98	0.92
11	1.81	46.08	0.99
12	4.13	68.26	1.00
13	2.05	-87.41	0.98
14	2.29	89.28	0.88
15	2.97	46.91	0.88
16	2.55	70.63	0.95
17	2.05	73.53	0.95
18	1.74	8.90	0.89
19	1.44	38.98	0.67
20	2.06	67.28	0.92
21	2.37	-48.38	0.99
22	1.51	70.92	0.97
23	1.85	-36.73	0.96
24	1.89	57.96	0.75
25	2.33	69.54	0.80
26	3.35	66.50	0.90
27	2.37	63.64	0.91
28	1.38	52.79	0.60
29	3.20	67.80	1.23
30	2.82	79.94	1.89
31	1.10	29.11	0.21
32	2.45	-71.42	0.71
33	1.36	29.93	0.95
34	1.79	29.92	0.91
35	1.56	58.03	0.91
36	1.60	-42.82	0.92
37	3.21	-75.06	0.93
38	2.05	49.00	0.98
39	3.78	84.51	0.93
40	2.45	73.64	0.95
41	2.75	89.69	0.96
42	3.84	67.93	0.96
43	2.81	59.49	0.97
44	2.05	-99.67	0.97
45	1.89	75.36	1.00
46	2.96	67.55	0.99
47	1.63	75.32	0.87
48	1.45	29.07	0.97
49	3.10	80.49	0.84
50	1.55	53.72	0.79

Press <RETURN> when ready to continue

T 34XY
52 DATA POINTS
FLUCTUATION = 154
LOGMEAN Pf =   1.885
ORIGINAL ZERO = -75.930

TRY AN Rs ESTIMATE.....
Rs Ri = 1.35,1.60

SYMMETRY.....

15   9

11   16
Hard copy now
Press <RETURN> when ready

ORIG ZERO
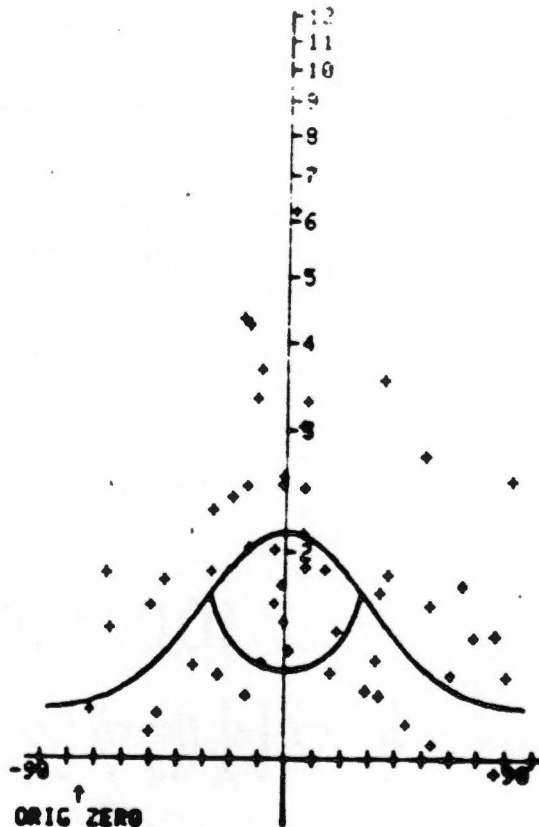
T 34XZ
57 DATA POINTS
REBOTUATION = 156
LOGMEAN Pf =   2.339
ORIGINAL ZERO =   -3.528

TRY AN Rs ESTIMATE.....
Rs Ri = 2.10,1.50

SYMMETRY.....

15   13

13   15
Hard copy now
Press <RETURN> when ready

126
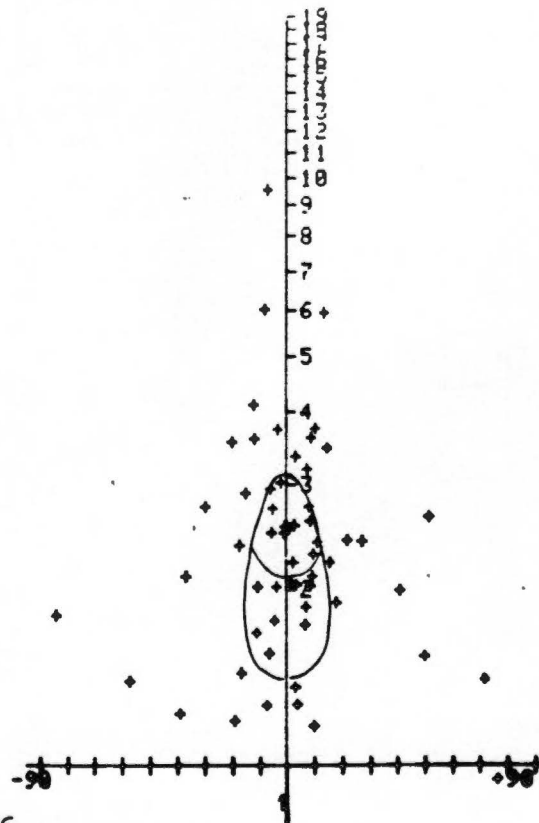
T 34Y2
50 DATA POINTS
FLUCTUATION = 136
LOGMEAN Rf =   2.105
ORIGINAL ZERO = -70.634

TRY AN Rs ESTIMATE.....
Rs Ri = 1.85,1.55

SYMMETRY.....

14   10

11   14
Hard copy now
Press <RETURN> when ready

-90

ORIG ZERO
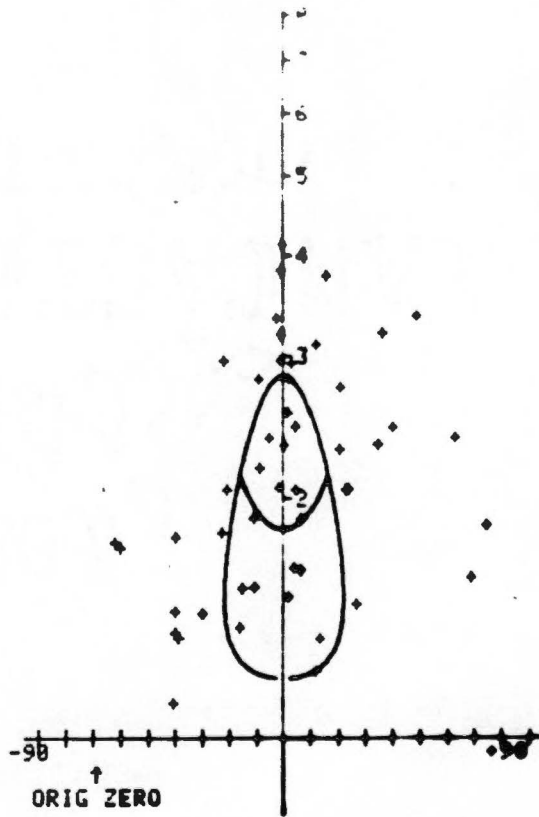
SPECIMEN REFERENCE.....
T45XY

ELLIPSE NUMBER	AXIAL RATIO	LONG AXIS ORIENT.	CORREL.COEFF.
1	4.58	73.92	0.80
2	2.01	-72.31	0.83
3	1.11	-40.22	0.43
4	1.75	-20.14	0.98
5	1.71	79.96	0.81
6	1.42	31.98	0.78
7	2.14	-50.03	0.80
8	2.43	63.40	0.70
9	1.80	-99.81	0.87
10	2.30	80.56	0.88
11	1.25	-71.25	0.59
12	1.54	-45.75	0.56
13	2.64	30.21	0.97
14	1.87	66.42	0.72
15	1.41	-62.61	0.80
16	2.05	-14.70	0.92
17	1.27	46.34	0.52
18	-1.47	-34.75	0.72
19	1.83	84.13	0.97
20	3.08	85.06	0.93
21	1.48	60.79	0.84
22	1.83	-42.13	0.85
23	1.70	60.03	0.93
24	1.92	83.02	0.95
25	1.87	-76.92	0.90
26	1.71	61.10	0.88
27	2.35	-74.49	0.00
28	1.37	-04.53	0.56
29	1.32	-46.57	0 58
30	1.91	-42.05	0 83
31	2.06	72.03	0 86
32	2.11	86.35	0 86
33	1.51	76.37	0. 67
34	1.44	-24.18	0 59
35	1.83	-53.75	0.76
36	1.29	77.53	0.44
37	2.45	36.61	0.99
38	1.34	46.99	0.49
39	1.28	81.03	0.41
40	1.63	-51.79	0.89
41	1.10	4.41	0.22
42	2.23	97.24	0.66
43	3.51	-73.52	0.90
44	1.31	-38.46	0.65
45	2.07	-98.97	0.85
46	1.31	-11.29	0.45
47	1.67	55.94	0.80
48	1.57	50.79	0.72
49	1.23	31.50	0.67
50	1.75	71.63	0.80
51	1.44	81.40	0.51
52	1.67	-53.81	0.93
53	2.59	-12.09	0.98
54	1.58	68.64	0.79
55	1.48	-55.60	0.86
56	3.36	-52.51	0.99
57	3.84	79.45	0.04
58	1.51	75.33	0.73
59	1.59	69.47	0.90
60	1.09	-71.63	0.17

128

61	2.29	-79.78	0.70
62	2.19	64.58	0.71
63	1.58	78.87	0.74
64	1.50	71.74	0.83
65	2.45	89.93	0.96
66	2.30	-89.34	0.50
67	1.95	77.07	0.62
68	1.78	-11.87	0.91
69	3.19	-37.55	0.99
70	1.81	31.48	0.83
71	1.29	-62.49	0.46
72	2.46	-81.97	0.84

Press <RETURN> when ready to continue

SPECIMEN REFERENCE.....
T45YZ

ELLIPSE NUMBER	AXIAL RATIO	LONG AXIS ORIENT.	CORREL.COEFF
1	5.45	-4.18	0.91
2	2.11	-8.42	0.97
3	1.27	-4.41	0.51
4	2.47	9.47	0.95
5	1.95	-2.95	0.90
6	3.48	1.71	0.98
7	4.31	1.34	0.94
8	1.91	-7.43	0.96
9	1.65	-27.98	0.66
10	3.67	-0.16	0.99
11	3.21	12.65	0.82
12	2.48	16.22	0.80
13	2.11	-8.97	0.94
14	1.55	30.80	0.89
15	1.99	42.79	0.89
16	4.30	-5.84	0.97
17	1.66	-5.33	0.65
18	1.61	13.04	0.82
19	1.77	-16.61	0.78
20	2.37	-1.46	0.98
21	3.18	-13.82	0.99
22	1.23	69.23	0.59
23	3.47	1.37	0.94
24	3.89	-4.30	0.89
25	3.02	-2.75	0.90
26	1.66	47.42	0.92
27	1.63	34.90	0.78
28	1.78	5.93	0.92
29	3.04	-10.03	0.97
30	1.43	-22.22	0.83
31	1.95	-18.41	0.69
32	2.78	-3.71	0.86
33	6.38	3.78	0.94
34	3.68	-7.23	0.99
35	3.91	-4.14	1.00
36	2.29	32.39	0.71
37	1.55	13.02	0.55
38	1.97	-9.83	0.99
39	6.08	8.27	0.92
40	3.45	1.23	0.89
41	2.15	-7.85	0.85
42	2.17	-2.14	0.92
43	3.19	-26.47	0.99
44	1.27	14.76	0.46
45	1.87	-8.60	0.70
46	2.75	1.29	0.93
47	1.99	11.21	0.93
48	2.19	4.32	0.93
49	3.34	6.86	0.99
50	1.71	13.42	0.77
51	1.61	2.39	0.71
52	1.92	8.00	0.95
53	1.40	-56.31	0.73
54	2.21	12.61	0.94
55	2.66	20.56	0.79
56	2.27	19.06	0.70
57	2.55	-12.78	0.93
58	2.76	21.98	0.89
59	2.38	-3.47	0.99
60	9.23	-4.99	0.97
61	1.98	29.57	0.90
62	2.46	4.42	0.70
63	3.81	4.76	0.99

64	2.58	20.91	0.97
65	2.94	3.45	0.37
66	3.13	15.06	0.91
67	3.36	-7.88	0.97
68	2.01	24.01	0.95

Press <RETURN> when ready to continue

SPECIMEN REFERENCE.....
T45XZ

ELLIPSE NUMBER	AXIAL RATIO	LONG AXIS ORIENT.	CORREL.COEFF.
1	3.29	-84.80	0.99
2	1.51	81.25	0.63
3	2.01	41.64	0.96
4	2.03	58.26	0.82
5	2.09	-60.25	0.66
6	2.59	75.31	0.99
7	1.65	-81.77	0.70
8	2.11	64.91	0.70
9	2.31	70.48	0.81
10	2.22	-76.27	0.84
11	2.30	55.34	0.92
12	1.33	-84.29	0.59
13	1.65	-53.96	0.72
14	1.25	55.49	0.66
15	1.43	0.23	0.85
16	1.27	74.67	0.58
17	1.48	-62.52	0.85
18	2.11	67.35	0.90
19	2.76	76.77	0.98
20	2.07	87.31	0.93
21	2.50	-21.79	0.77
22	1.63	65.07	0.87
23	2.56	50.89	0.79
24	2.48	61.42	0.93
25	2.55	77.36	0.92
26	2.82	86.97	0.92
27	2.77	-57.49	0.83
28	2.27	-72.79	0.96
29	3.80	68.33	0.98
30	2.32	-84.20	0.80
31	2.43	-84.05	0.97
32	1.48	54.76	0.81
33	2.25	75.77	0.68
34	3.17	80.68	0.97
35	2.05	79.16	0.69
36	2.34	68.45	0.98
37	2.29	47.32	0.57
38	3.07	65.87	0.95
39	1.81	7.31	0.86
40	2.58	57.06	1.00
41	2.46	80.49	0.90
42	2.14	-61.47	0.86
43	1.60	-37.34	0.71
44	1.98	68.17	0.95
45	1.87	13.73	0.83
46	1.57	80.52	0.58
47	2.91	84.84	0.76
48	1.98	-25.17	0.83
49	1.78	-56.97	0.85
50	2.05	72.44	0.97

Press <RETURN> when ready to continue

132

T45XY
72 DATA POINTS
FLUCTUATION = 164
LOGMEAN Rf =   1.809
ORIGINAL ZERO =   89.807

TRY AN Rs ESTIMATE.....
Rs Ri = 1.48,1.40

SYMMETRY.....

21   14

15   21
Hard copy now
Press <RETURN> when ready
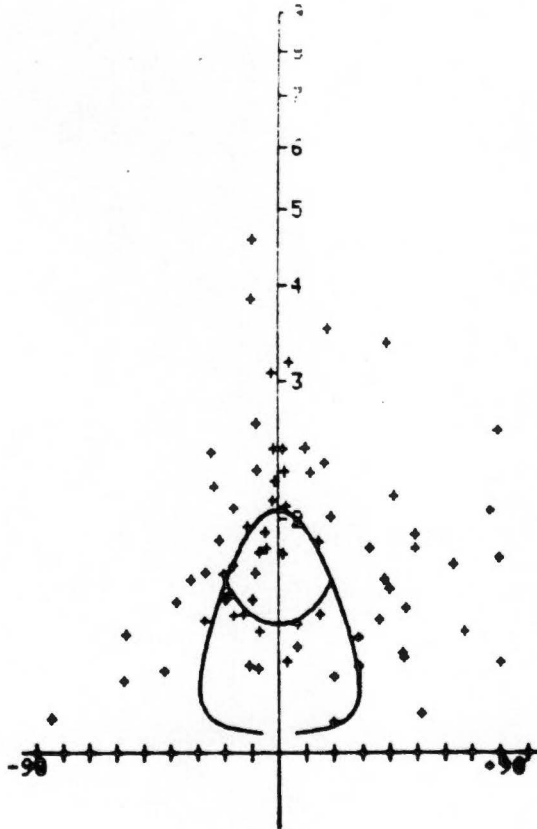
T45YZ
68 DATA POINTS
REROTUATION = 126
LOGMEAN Rf =   2.459
ORIGINAL ZERO =   -1.369

TRY AN Rs ESTIMATE.....
Rs Ri =
2.03,1.40

SYMMETRY.....

20   14

14   19
Hard copy now
Press <RETURN> when ready

133
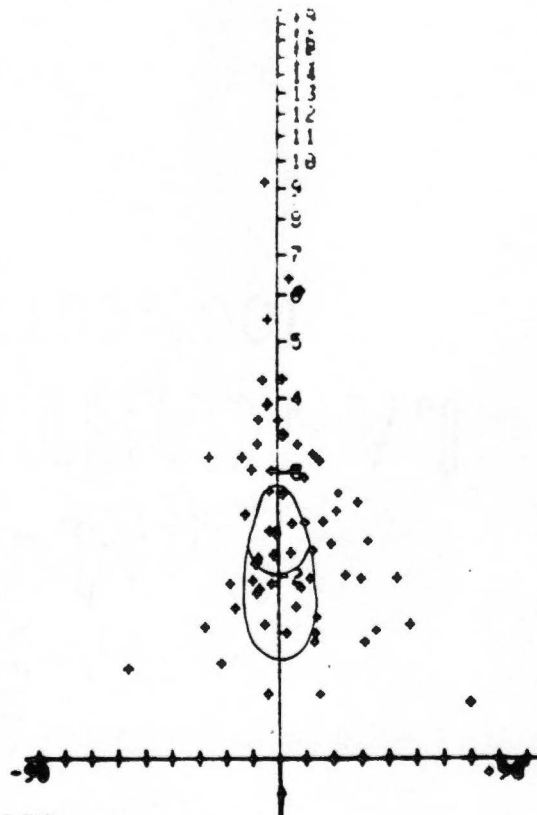
T45XZ
50 DATA POINTS
FLUCTUATION = 158
LOGMEAN Rf =   2.112
ORIGINAL ZERO = -76.772

TRY AN Rs ESTIMATE.....
Rs Ri = 1.89,1.40

SYMMETRY.....

14   10

11   14
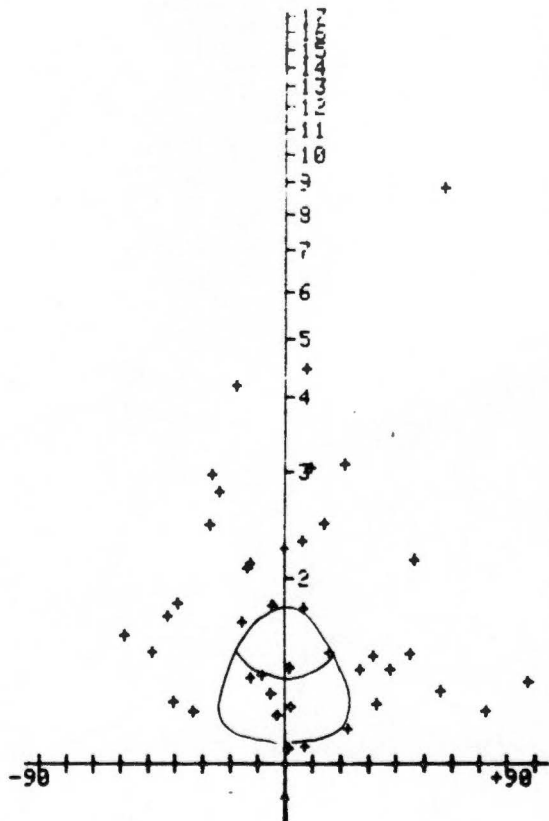Hard copy now
Press <RETURN> when ready

ORIG ZERO
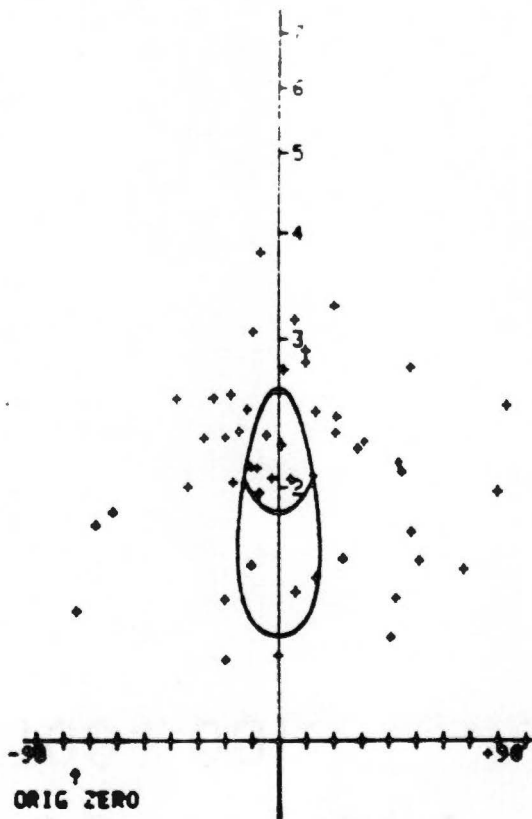
```
SPECIMEN REFERENCE.....
T46XY
```

ELLIPSE NUMBER	AXIAL RATIO	LONG AXIS ORIENT.	CORREL.COEFF.
1	5.60	-39.35	0.95
2	1.42	14.04	0.81
3	2.62	4.02	0.99
4	1.74	-51.20	0.96
5	1.55	-1.14	0.95
6	3.36	9.35	0.92
7	1.50	9.79	0.89
8	1.80	-42.96	0.80
9	1.57	68.05	0.67
10	1.65	53.24	0.71
11	2.55	0.03	0.94
12	1.36	23.81	0.75
13	1.36	37.23	0.74
14	2.14	26.68	0.97
15	1.46	33.88	0.83
16	1.64	-61.15	0.79
17	2.49	-9.26	0.96
18	1.65	-12.73	0.93
19	2.32	73.55	0.97
20	1.26	-23.08	0.77
21	2.11	-0.03	0.88
22	1.86	-3.74	0.89
23	2.12	1.09	0.94
24	2.28	-32.50	0.90
25	1.83	-6.65	0.91
26	1.06	-56.49	0.29
27	1.26	-55.62	0.66
28	3.47	-4.45	0.83
29	1.19	-35.63	0.47
30	1.96	36.23	0.89
31	1.63	-9.14	0.76
32	1.46	63.41	0.48
33	1.66	-37.36	0.84
34	1.34	-31.66	0.61
35	1.32	24.84	0.92
36	1.54	-0.76	0.73
37	2.12	65.26	0.74
38	2.28	-34.60	0.86
39	1.48	-30.64	0.68
40	2.02	-7.37	0.92
41	1.55	40.44	0.81
42	2.09	88.35	0.76
43	1.37	-10.90	0.69
44	1.98	1.37	0.90
45	1.57	-34.86	0.89
46	2.46	-2.62	0.98
47	1.71	-2.43	0.97
48	2.04	-57.54	0.89
49	1.90	-18.94	0.75
50	1.39	24.42	0.85
51	1.62	-38.44	0.59
52	1.92	-21.04	0.94
53	1.62	-5.87	0.65
54	1.82	-3.03	0.92
55	2.07	5.92	0.97
56	3.77	-31.09	0.89
57	1.55	35.83	0.90
58	1.46	-12.65	0.53
59	2.54	12.75	0.95
60	2.97	9.46	0.97
61	1.98	13.90	0.96
62	1.24	20.11	0.84
63	1.20	-23.98	0.60

```
64                    1.23              -69.70           0.44
65                    1.34               81.86           0.74
66                    1.80              -66.26           0.72
67                    1.68                7.08           0.82
Press <RETURN> when ready to continue
```

SPECIMEN REFERENCE.....
T46YZ

ELLIPSE NUMBER	AXIAL RATIO	LONG AXIS ORIENT.	CORREL.COEFF.
1	1.17	-61.15	0.56
2	1.86	83.06	0.86
3	1.80	60.31	0.95
4	1.69	75.92	0.90
5	1.51	84.14	0.68
6	1.52	-32.75	0.79
7	2.90	-64.23	0.76
8	1.11	-76.01	0.35
9	1.32	-46.70	0.73
10	1.68	-82.47	0.82
11	1.87	48.53	0.86
12	1.78	69.59	0.87
13	1.98	66.34	0.92
14	1.42	-40.36	0.97
15	2.41	80.92	0.74
16	1.98	48.45	0.99
17	2.11	61.88	0.82
18	2.43	-80.98	0.77
19	1.58	-8.31	0.71
20	0.49	79.77	0.84
21	2.14	-86.70	0.91
22	2.13	79.08	0.85
23	1.69	53.33	0.80
24	0.83	84.47	0.79
25	2.61	71.36	0.92
26	1.85	88.78	0.98
27	2.99	62.33	0.79
28	2.80	58.40	0.86
29	2.41	62.75	0.93
30	2.36	89.28	0.90
31	1.28	-83.38	0.61
32	1.49	31.56	0.65
33	1.87	71.59	0.79
34	2.16	-72.00	0.78
35	2.01	-27.63	0.74
36	2.31	84.12	0.83
37	1.14	67.08	0.30
38	1.41	-15.39	0.65
39	2.41	72.16	0.95
40	1.85	77.07	0.72
41	1.66	-88.27	0.70
42	1.38	86.28	0.88
43	2.15	71.78	0.98
44	1.44	-85.87	0.79
45	1.25	-75.11	0.56
46	1.25	73.78	0.49
47	2.28	57.53	0.97
48	1.33	70.42	0.52
49	1.61	-80.51	0.79
50	1.26	-23.69	0.38
51	1.45	-27.92	0.83
52	2.35	-71.22	0.91
53	1.45	-78.47	0.58
54	1.03	-18.96	0.07
55	1.69	67.35	0.55
56	1.19	-78.23	0.20
57	1.47	-72.89	0.61
58	2.50	-88.57	0.80
59	1.85	79.03	0.73
60	2.48	-72.11	0.99
61	1.91	59.05	0.71

Press <RETURN> when ready to continue

137

SPECIMEN REFERENCE.....
T46XZ

ELLIPSE NUMBER	AXIAL RATIO	LONG AXIS ORIENT.	CORREL.COEFF.
1	2.31	-80.72	0.95
2	1.67	-76.77	0.98
3	1.80	-51.16	0.91
4	1.44	-36.46	0.89
5	1.86	-56.41	0.89
6	2.06	-55.41	0.92
7	1.48	36.27	0.66
8	2.47	-85.06	0.97
9	1.13	19.05	0.44
10	1.44	-57.72	0.96
11	1.60	77.62	0.63
12	1.53	-87.65	0.66
13	1.42	-52.39	0.81
14	1.91	63.46	0.74
15	2.63	53.52	0.70
16	1.50	-65.81	0.75
17	1.76	78.12	0.94
18	1.51	82.74	0.72
19	1.55	-48.27	0.64
20	1.40	-75.37	0.65
21	1.50	-67.02	0.76
22	2.00	81.59	0.97
23	2.34	-52.64	0.98
24	1.41	-62.40	0.79
25	2.03	-66.56	0.86
26	1.72	20.10	0.78
27	1.57	82.99	0.78
28	1.54	-59.90	0.81
29	1.44	28.65	0.62
30	1.33	-63.15	0.65
31	3.06	-71.90	0.78
32	1.62	2.30	0.83
33	1.71	-20.79	0.58
34	1.99	-76.09	0.91
35	1.83	-32.43	0.90
36	1.11	88.40	0.29
37	1.19	24.31	0.57
38	2.77	-57.55	0.83
39	2.62	-60.23	0.87
40	2.52	-63.55	0.92
41	1.63	-85.64	0.79
42	1.88	-68.43	0.72
43	2.04	-19.08	0.89
44	6.63	-56.85	0.95
45	2.73	-69.82	0.93
46	1.51	-31.01	0.78
47	1.30	-58.19	0.83
48	2.06	42.15	0.64
49	2.09	-8.65	0.84
50	1.40	-53.89	0.83
51	1.37	10.83	0.94
52	2.16	-12.62	0.98
53	1.82	-85.81	0.85
54	2.15	2.50	0.92
55	1.55	-53.24	0.73
56	1.19	56.91	0.35
57	1.76	76.70	0.95

Press <RETURN> when ready to continue

138

```
T46XY
67 DATA POINTS
FLUCTUATION = 174
LOGMEAN Rf =    1.80A
ORIGINAL ZERO =    3.033


TRY AN Rs ESTIMATE.....
Rs Ri = 1.34,1.50




SYMMETRY.....

15    18

18    15
Hard copy now
Press <RETURN> when ready
```
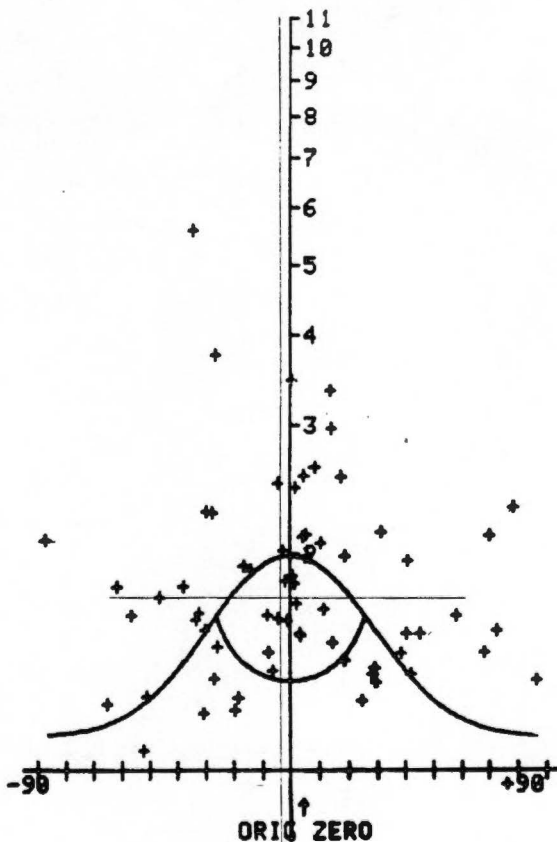


```
T46YZ
61 DATA POINTS
FEBOTUATION = 140
LOGMEAN Rf =    1.863
ORIGINAL ZERO =  -84.466


TRY AN Rs ESTIMATE.....
Rs Ri = 1.52,1.50




SYMMETRY.....

20    10

10    20
Hard copy now
Press <RETURN> when ready
```

139
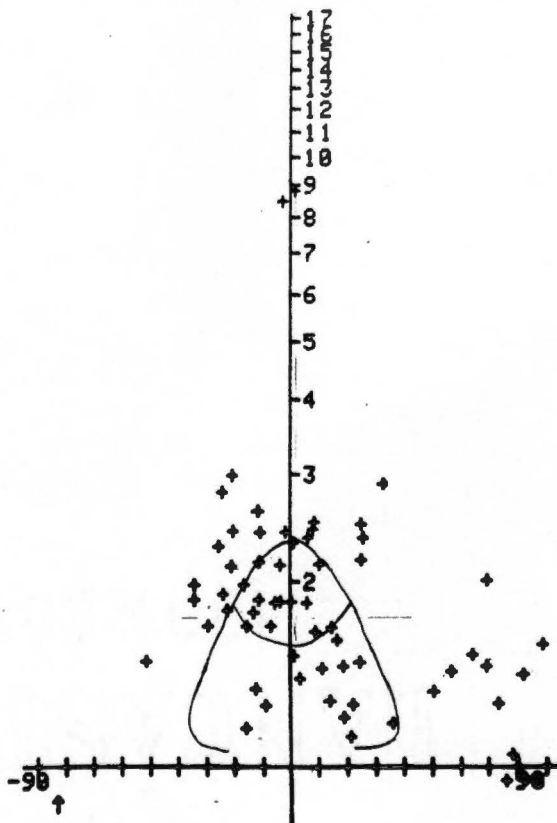
```
T46XZ
57 DATA POINTS
FLUCTUATION = 176
LOGMEAN Rf =    1.784
ORIGINAL ZERO =   63.547


TRY AN Rs ESTIMATE.....
Rs Ri = 1.36,1.50




SYMMETRY.....

12    16

16    12
Hard copy now
Press <RETURN> when ready
```
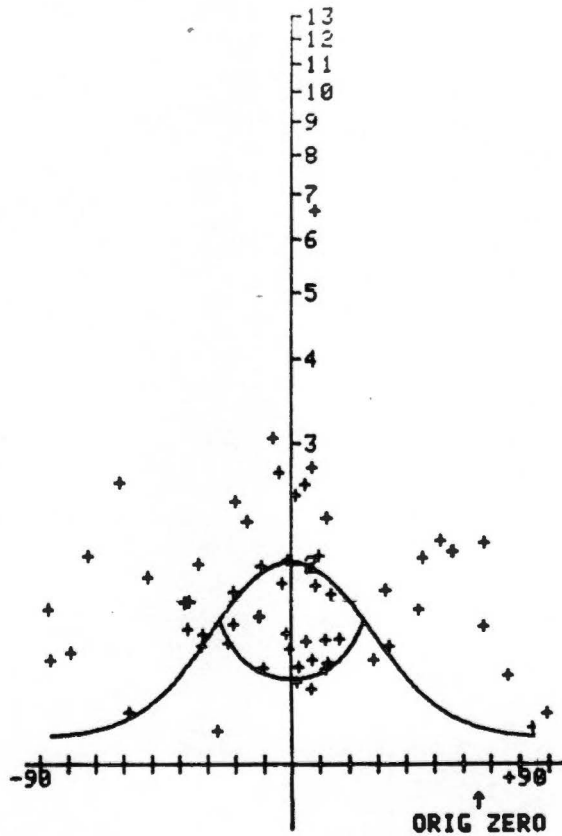
ELLIPSE NUMBER	AXIAL RATIO	LONG AXIS ORIENT.	CORREL.COEFF.
1	1.17	-9.73	0.51
2	2.76	58.22	0.86
3	1.76	77.61	0.88
4	1.45	71.44	0.66
5	2.82	50.77	0.77
6	1.72	81.73	0.98
7	1.91	23.87	0.78
8	3.79	11.88	0.83
9	2.75	48.36	0.94
10	1.37	79.90	0.64
11	1.99	96.83	0.92
12	1.85	-36.26	0.85
13	1.50	48.93	0.68
14	1.92	-44.40	0.70
15	2.20	24.58	0.66
16	1.54	53.76	0.85
17	1.79	54.49	0.94
18	3.63	83.90	0.99
19	1.47	-82.08	0.87
20	1.99	61.85	0.85
21	2.41	42.43	0.92
22	1.26	0.90	0.63
23	2.15	61.36	0.56
24	1.47	30.10	0.76
25	1.08	-28.90	0.26
26	1.36	59.51	0.78
27	2.85	-89.10	0.81
28	4.68	57.92	0.91
29	1.19	85.14	0.55
30	1.53	2.41	0.83
31	1.69	59.92	0.51
32	3.22	72.51	0.99
33	1.69	68.63	0.92
34	1.97	76.76	0.97
35	3.09	-78.37	0.69
36	1.31	77.63	0.59
37	1.94	41.82	0.86
38	1.48	80.19	0.81
39	1.78	74.44	0.85
40	2.00	71.39	0.89
41	1.53	-84.05	0.81
42	1.19	-71.51	0.43
43	1.05	18.83	0.22
44	4.55	68.48	0.88
45	1.36	-33.71	0.52
46	2.06	63.15	0.82
47	3.05	70.60	0.80
48	3.28	49.33	0.90
49	1.21	65.43	0.57
50	1.47	88.36	0.93
51	2.00	41.20	0.74
52	2.09	76.19	0.89
53	2.18	39.04	0.85
54	1.56	49.53	0.72
55	2.27	46.58	0.98
56	3.45	84.95	0.81

Press <RETURN> when ready to continue

SPECIMEN REFEREN E.....
T48YZ

ELLIPSE NUMBER	AXIAL RATIO	LONG AXIS ORIENT.	CORREL.COEFF.
1	4.68	30.85	0.94
2	2.43	44.06	0.91
3	2.33	75.91	0.73
4	1.89	62.30	0.82
5	2.91	66.55	0.99
6	4.20	-86.99	0.97
7	1.25	75.58	0.68
8	2.56	58.93	0.99
9	2.32	-5.04	0.83
10	1.63	14.90	0.61
11	1.72	-7.42	0.87
12	2.53	-72.23	0.82
13	5.19	49.65	0.86
14	1.35	64.58	0.80
15	1.29	-2.10	0.52
16	1.61	79.52	0.53
17	2.35	57.57	0.88
18	1.58	72.61	0.62
19	1.38	-26.53	0.76
20	3.09	79.68	0.76
21	1.39	56.07	0.74
22	1.08	68.28	0.22
23	1.56	37.50	0.77
24	1.49	-89.35	0.62
25	2.22	53.13	0.74
26	1.80	44.89	0.87
27	1.43	-53.45	0.56
28	3.35	-4.72	0.95
29	1.26	23.13	0.54
30	1.65	36.61	0.86
31	1.43	18.47	0.58
32	1.83	29.69	0.82
33	2.32	-30.66	0.81
34	1.60	19.99	0.83
35	2.77	62.43	0.94
36	1.59	86.73	0.60
37	1.44	21.16	0.66
38	2.35	28.63	0.83
39	1.01	71.31	0.05
40	1.64	37.12	0.89
41	1.98	58.21	0.93
42	1.75	50.99	0.87
43	1.05	18.86	0.19
44	2.51	49.11	0.84
45	3.41	71.44	0.98
46	1.29	-79.64	0.69
47	2.34	77.84	0.86
48	1.95	58.55	0.91
49	1.80	58.91	0.84
50	3.08	45.79	0.90
51	2.91	62.34	0.97
52	1.27	3.88	0.61
53	1.48	56.80	0.79
54	1.43	51.62	0.51
55	1.61	48.96	0.92
56	1.24	57.60	0.49
57	3.32	-70.41	0.79
58	1.65	-34.11	0.92
59	2.56	55.26	0.99
60	2.40	89.20	0.86
61	1.69	50.71	0.87

Press <RETURN> when ready to continue

ELLIPSE NUMBER	AXIAL RATIO	LONG AXIS ORIENT.	CORREL.COEFF.
1	1.85	-46.44	0.71
2	1.74	5.54	0.73
3	1.39	-22.30	0.59
4	1.23	34.23	0.68
5	2.35	-37.90	0.90
6	2.21	-29.42	0.97
7	1.71	-35.79	0.85
8	1.75	22.77	0.47
9	1.50	-39.19	0.59
10	4.34	-29.80	0.95
11	2.24	-11.69	0.83
12	1.15	32.28	0.25
13	2.59	-14.41	0.91
14	2.25	-24.01	0.90
15	1.76	-1.63	0.63
16	1.13	-65.25	0.27
17	2.46	-33.79	0.92
18	3.42	-45.91	0.92
19	1.33	37.91	0.62
20	1.92	-18.88	0.88
21	1.96	-13.19	0.77
22	1.66	-3.49	0.93
23	3.10	-3.86	0.94
24	1.61	-22.77	0.79
25	2.10	0.95	0.79
26	1.32	29.72	0.54
27	1.37	18.30	0.53
28	1.50	10.17	0.77
29	1.84	-17.94	0.88
30	2.38	-31.30	0.96
31	2.68	-14.10	0.86
32	1.18	89.19	0.40
33	1.44	-16.88	0.59
34	2.43	-0.26	0.94
35	1.75	-15.19	0.66
36	1.78	-39.50	0.79
37	1.65	-16.53	0.85
38	2.51	14.03	0.89
39	1.66	-64.43	0.79
40	2.97	14.36	0.78
41	1.92	45.88	0.92
42	1.09	48.36	0.12
43	1.63	51.44	0.68
44	1.57	10.80	0.84
45	2.35	3.06	0.77
46	2.53	18.00	0.92
47	2.65	9.63	0.90
48	11.57	-38.97	0.94
49	3.71	-45.49	0.90
50	1.26	-31.45	0.70
51	1.63	45.84	0.91
52	1.52	3.72	0.65
53	1.78	-35.18	0.69
54	2.20	3.41	0.97
55	2.14	-22.31	0.92
56	1.46	-39.78	0.80
57	3.36	-0.93	0.83
58	5.76	-3.01	0.97
59	1.64	13.61	0.73
60	1.62	-22.11	0.78
61	1.31	-20.80	0.47
62	1.68	-18.68	0.76

Press <RETURN> when ready to continue

143

T48XY
56 DATA POINTS
FLUCTUATION = 160
LOGMEAN Rf =   1.926
ORIGINAL ZERO =   -65.429

TRY AN Rs ESTIMATE.....
Rs Ri = 1.66,1.35

SYMMETRY.....

14   14

14   13
Hard copy now
Press <RETURN> when ready
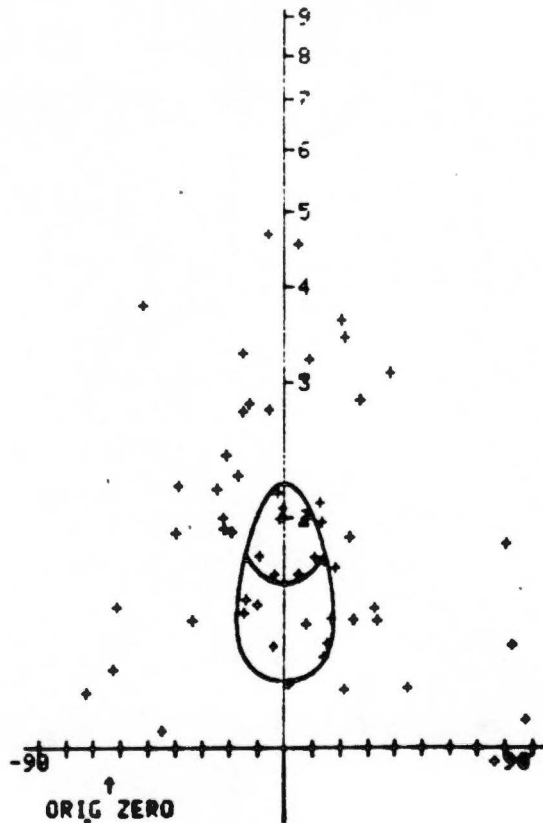
T48XZ
62 DATA POINTS
FLUCTUATION = 142
LOGMEAN Rf =   1.956
ORIGINAL ZERO =   14.098

TRY AN Rs ESTIMATE.....
Rs Ri = 1.51,1.40

SYMMETRY.....

16   15

15   15
Hard copy now
Press <RETURN> when ready

144
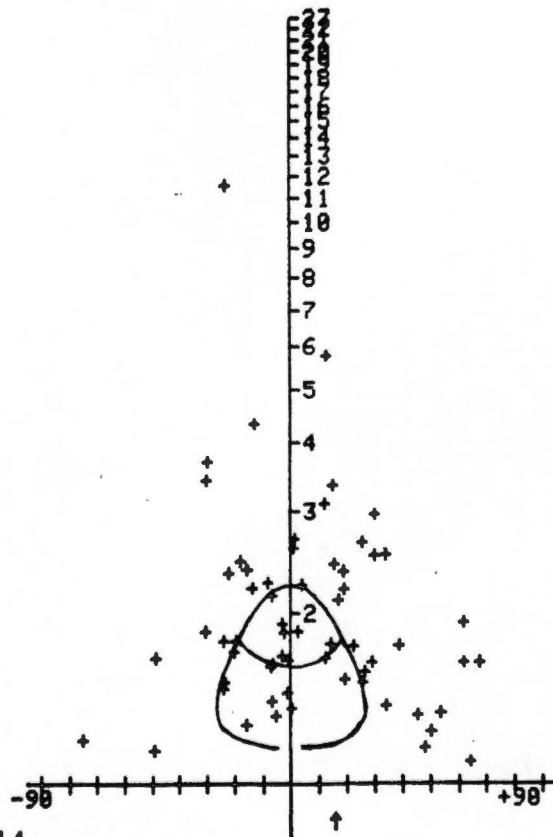
T48YZ
61 DATA POINTS
FLUCTUATION = 177
LOGMEAN Rf =   1.925
ORIGINAL ZERO = -57.567

TRY AN Rs ESTIMATE.....
Rs Ri = 1.47,1.4

SYMMETRY.....

12   18

18   12
Hard copy now
Press <RETURN> when ready
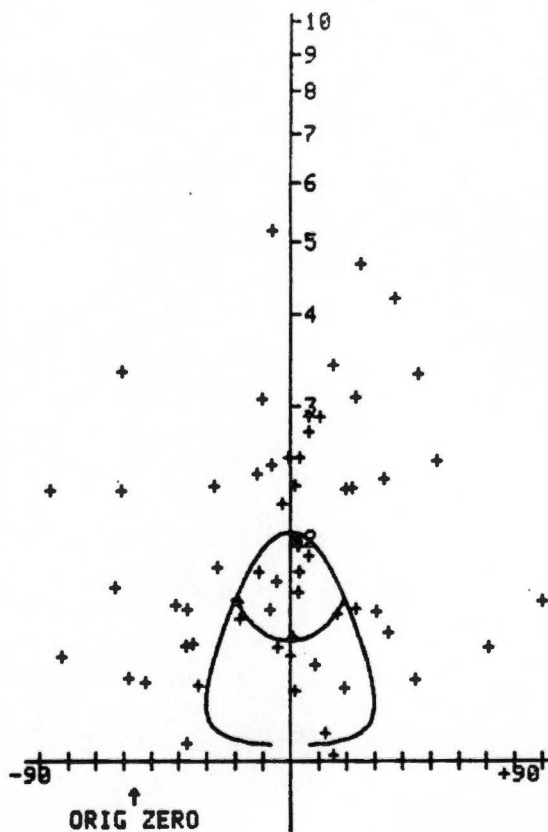
SPECIMEN REFERENCE ....
T49XY

ELLIPSE NUMBER	AXIAL RATIO	LONG AXIS ORIENT.	CORREL.COEFF.
1	12.84	-23.52	0.99
2	1.82	-14.86	0.93
3	1.66	73.11	0.72
4	1.26	-54.01	0.71
5	2.07	-30.91	0.97
6	2.41	-32.44	0.98
7	2.64	-32.04	0.95
8	1.86	-12.94	0.66
9	1.83	-17.47	0.66
10	9.12	12.10	0.98
11	2.29	-34.33	0.94
12	1.71	-6.47	0.94
13	1.57	-35.61	0.79
14	2.66	-8.64	0.99
15	1.43	40.16	0.50
16	2.00	-52.60	0.72
17	2.07	-19.30	0.78
18	1.49	-39.53	0.73
19	1.72	-6.25	0.93
20	1.44	-20.04	0.68
21	2.29	-21.68	0.03
22	1.68	-36.52	0.03
23	2.14	01.74	0.95
24	1.97	7.11	0.94
25	1.74	-10.39	0.94
26	2.56	-22.55	0.99
27	1.61	-40.56	0.06
28	2.10	-5.57	0.94
29	2.41	-29.53	0.88
30	1.95	-31.41	0.93
31	2.16	-10.04	0.81
32	2.16	-9.65	0.88
33	1.62	3.36	0.73
34	1.68	-46.63	0.84
35	2.14	-24.30	0.88
36	2.85	-3.39	0.98
37	1.49	-17.87	0.69
38	2.05	-26.28	0.92
39	2.02	-16.62	0.94
40	1.31	-6.38	0.50
41	1.42	-8.93	0.70
42	1.48	-17.15	0.70
43	1.57	-66.43	0.60
44	2.81	14.37	0.91
45	1.73	-35.88	0.84
46	2.20	-2.88	0.90
47	2.07	-27.61	0.73
48	1.56	-29.24	0.83
49	3.84	-36.89	0.91
50	1.96	0.82	0.97
51	2.26	-53.00	0.73
52	1.99	-10.18	0.92
53	2.03	-10.70	0.92
54	2.05	-5.37	0.89
55	2.40	-35.50	0.91
56	2.22	-20.07	0.86
57	2.41	-4.15	0.94
58	3.30	-9.10	0.79
59	2.58	3.70	0.99
60	2.58	-0.59	0.79
61	1.76	0.03	0.02
62	2.89	-0.06	1.00
63	3.56	30.22	0.99

ELLIPSE NUMBER	AXIAL RATIO	LONG AXIS ORIENT.	CORREL.COEFF.
1	4.08	-68.78	0.93
2	6.24	88.29	0.93
3	2.68	-82.92	0.96
4	1.98	-54.41	0.95
5	4.34	-77.89	0.99
6	1.26	-49.06	0.73
7	2.28	-83.19	0.87
8	1.90	-57.88	0.96
9	1.10	87.37	0.35
10	1.93	-49.12	0.82
11	1.66	78.78	0.75
12	2.28	89.33	0.98
13	3.21	-83.40	0.94
14	2.33	-62.43	0.85
15	2.64	-88.49	0.94
16	1.41	-63.71	0.67
17	1.87	-47.05	0.93
18	2.48	-67.81	0.97
19	2.50	-70.62	0.70
20	2.06	-01.51	0.89
21	1.79	-01.66	0.83
22	1.90	-49.94	0.96
23	2.52	-85.70	0.95
24	2.58	-07.42	0.93
25	1.95	-64.02	0.90
26	2.22	-50.02	0.94
27	2.36	-67.00	0.90
28	2.90	89.20	0.92
29	1.97	-87.71	0.84
30	1.77	-83.40	0.90
31	2.90	-89.65	0.89
32	1.52	-79.49	0.84
33	2.73	-87.32	0.87
34	2.30	-73.35	0.92
35	1.33	98.55	0.73
36	2.25	-82.69	0.69
37	1.14	-12.91	0.33
38	2.64	-85.48	0.88
39	1.46	-72.88	0.98
40	4.25	-65.07	0.99
41	2.04	-84.73	0.74
42	2.37	-88.41	0.82
43	2.17	-86.81	0.77
44	1.83	-51.55	0.97
45	4.86	-71.82	0.97
46	1.42	66.32	0.62
47	1.84	88.67	0.81
48	2.52	-68.79	0.97
49	2.20	-86.83	0.77
50	1.43	-70.37	0.68
51	1.45	-46.57	0.65
52	3.45	-69.08	0.94
53	1.98	-51.51	0.94
54	7.29	-54.97	0.90
55	1.64	00.84	0.55
56	1.80	03.32	0.00
57	2.31	-66.15	0.85
58	1.66	-02.75	0.83
59	2.95	-02.27	0.90
60	2.45	-03.42	0.99
61	1.95	-56.76	0.00
62	2.40	-04.29	0.07

Press ⟨RETURN⟩ when ready to continue

SPECIMEN REFERENCE ...
T49XZ

ELLIPSE NUMBER	AXIAL RATIO	LONG AXIS ORIENT.	CORREL.COEFF.
1	2.27	-60.49	0.32
2	1.93	-30.10	0.94
3	1.92	-43.98	0.95
4	5.91	-39.65	0.86
5	3.79	-48.32	0.86
6	1.79	-37.65	0.92
7	1.36	-61.27	0.64
8	2.57	-48.20	0.90
9	1.84	-29.12	0.79
10	5.00	-57.67	0.95
11	1.79	-38.12	0.97
12	2.74	-50.91	0.97
13	1.21	10.69	0.55
14	2.32	-55.55	0.87
15	1.79	-20.88	0.99
16	1.77	-52.57	0.92
17	1.55	-62.87	0.75
18	1.62	-34.59	0.92
19	1.97	-39.81	0.90
20	1.99	-25.94	0.95
21	1.43	-13.60	0.90
22	2.36	-36.56	0.97
23	3.30	-59.31	1.00
24	2.85	-61.67	0.76
25	4.18	-42.57	0.99
26	1.92	-27.90	0.95
27	3.21	-51.44	0.99
28	2.05	-59.73	0.70
29	4.45	-38.37	0.92
30	1.53	-2.74	0.85
31	1.23	-51.79	0.60
32	1.81	-43.71	0.94
33	2.33	-59.61	0.90
34	1.36	16.77	0.66
35	2.21	-36.69	0.90
36	3.53	-49.55	0.88
37	1.31	-47.14	0.59
38	2.06	-45.29	0.96
39	1.92	-57.15	0.70
40	1.20	78.96	0.45
41	3.71	-45.71	0.97
42	1.80	-37.10	0.97
43	2.15	-49.23	0.91
44	2.12	-55.37	0.92
45	3.93	-49.88	0.88
46	1.21	0.52	0.49
47	1.75	-67.48	0.95
48	1.94	-73.06	0.76
49	1.93	-54.16	0.95
50	1.76	-60.59	0.89

Press <RETURN> when ready to continue

T49XY
64 DATA POINTS
ZEBOTUATION = 171
LOGMEAN Rf =   2.134
ORIGINAL ZERO =   16.624

TRY AN Rs ESTIMATE.....
Rs Ri = 1.87,1.40

SYMMETRY.....

15   16

17   15
Hard copy now
Press <RETURN> when ready
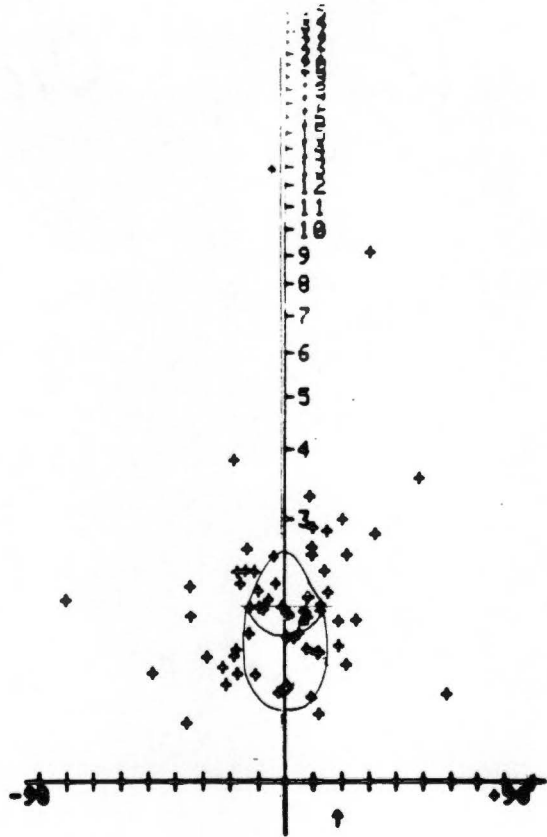
T49YZ
62 DATA POINTS
FLUCTUATION = 101
LOGMEAN Rf =   2.224
ORIGINAL ZERO =   81.507

TRY AN Rs ESTIMATE.....
Rs Ri = 2.0,1.4

SYMMETRY.....

20   10

11   20
Hard copy now
Press <RETURN> when ready

T49XZ
50 DATA POINTS
FLUCTUATION = 118
LOGMEAN PF =   2.136
ORIGINAL ZERO =   47.142

TRY AN Rs ESTIMATE.....
Rs Ri = 1.90,1.40

SYMMETRY.....

14   10

11   14
Hard copy now
Press <RETURN> when ready

ORIG ZERO

150
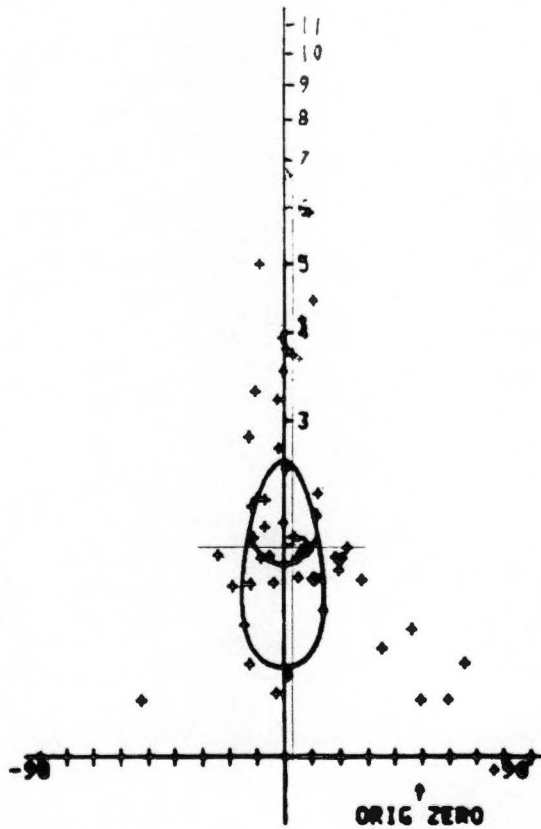
SPECIMEN REFERENCE.....
T52XY

ELLIPSE NUMBER	AXIAL RATIO	LONG AXIS ORIENT.	CORREL.COEFF.
1	1.33	-74.78	0.65
2	1.48	18.42	0.79
3	1.62	-9.90	0.82
4	2.37	0.75	0.90
5	1.78	-8.38	0.92
6	2.07	-19.66	0.90
7	6.85	-42.32	0.94
8	2.12	-3.96	0.97
9	2.41	3.23	0.99
10	2.23	4.30	0.95
11	3.24	-0.11	0.88
12	2.93	34.58	0.78
13	3.22	-10.90	0.98
14	1.60	-20.47	0.93
15	1.29	-66.56	0.49
16	3.34	13.78	0.99
17	1.66	-10.80	0.91
18	1.70	26.02	0.98
19	3.08	11.03	0.95
20	1.76	4.21	0.70
21	1.57	26.91	0.64
22	2.51	17.55	0.97
23	1.55	-6.32	0.95
24	2.06	23.67	0.84
25	1.74	-5.95	0.84
26	1.24	16.79	0.55
27	2.02	19.33	0.93
28	4.03	2.12	0.99
29	2.75	0.73	0.86
30	2.20	-6.13	0.93
31	1.46	-14.05	0.90
32	1.15	69.23	0.58
33	2.50	-17.41	0.98
34	2.42	20.91	0.71
35	2.14	1.76	0.95
36	3.86	7.68	0.99
37	2.41	12.81	0.80
38	2.18	5.70	0.93
39	1.43	-13.00	0.85
40	2.40	-1.14	0.88
41	2.98	-9.31	0.99
42	1.93	82.92	0.88
43	1.53	1.78	0.64
44	3.51	9.97	0.85
45	2.44	9.05	0.98
46	1.43	50.34	0.82
47	2.92	-1.38	0.84
48	1.86	1.18	0.97
49	1.83	-6.85	0.65
50	1.29	-10.24	0.57

Press <RETURN> when ready to continue

SPECIMEN REFERENCE.....
T52YZ

ELLIPSE NUMBER	AXIAL RATIO	LONG AXIS ORIENT.	CORREL.COEFF.
1	2.50	-48.71	0.94
2	1.68	-38.39	0.76
3	1.61	-15.65	0.63
4	1.27	-28.19	0.52
5	2.01	-46.49	0.79
6	1.53	-41.67	0.71
7	1.43	-33.87	0.68
8	2.07	5.25	0.96
9	1.45	-52.66	0.53
10	1.87	-32.40	0.95
11	2.19	-45.22	0.98
12	1.75	-30.37	0.71
13	1.83	44.84	0.80
14	2.03	-52.72	0.79
15	2.16	4.64	0.86
16	1.23	-29.21	0.63
17	2.27	-26.28	0.90
18	2.05	-65.25	0.92
19	2.45	-42.08	0.96
20	2.61	-83.39	0.82
21	2.01	-35.26	0.76
22	1.47	-68.39	0.75
23	2.41	-35.13	0.83
24	1.38	-26.41	0.74
25	2.00	-40.03	0.92
26	2.41	83.68	0.98
27	2.34	-7.79	0.83
28	1.63	-1.55	0.98
29	1.63	-22.06	0.80
30	1.14	79.17	0.31
31	1.38	-78.49	0.96
32	1.35	3.22	0.51
33	1.47	-38.01	0.91
34	1.52	-40.82	0.91
35	1.64	-2.30	0.71
36	2.79	-43.09	0.98
37	3.69	72.67	0.44
38	1.92	-2.45	0.76
39	1.42	-15.13	0.65
40	1.58	-57.48	0.66
41	2.82	-29.36	0.99
42	1.51	-79.05	0.78
43	2.76	9.06	0.88
44	2.28	24.01	0.91
45	1.11	-68.15	0.42
46	2.06	-40.08	0.94
47	2.03	-82.00	0.97

Press <RETURN> when ready to continue

SPECIMEN REFERENCE.....
T52XZ

ELLIPSE NUMBER	AXIAL RATIO	LONG AXIS ORIENT.	CORREL.COEFF.
1	1.63	-71.82	0.69
2	1.65	-46.64	0.83
3	1.87	-51.71	0.92
4	3.55	89.92	0.91
5	2.03	-82.84	0.85
6	2.54	-72.73	0.95
7	2.43	70.85	0.79
8	2.08	-87.04	0.81
9	4.06	-87.80	0.82
10	3.43	-83.45	0.80
11	2.57	83.45	0.98
12	1.39	58.77	0.93
13	3.21	-85.65	0.86
14	1.69	-72.64	0.86
15	4.10	-88.67	0.89
16	1.43	40.66	0.84
17	2.10	89.39	0.84
18	2.48	-81.46	0.70
19	1.32	-85.86	0.79
20	1.84	-74.37	0.86
21	3.59	-71.88	0.96
22	1.75	87.68	0.92
23	1.73	71.23	0.83
24	2.62	-80.88	0.95
25	2.41	81.67	0.87
26	3.17	-71.48	0.95
27	1.22	-78.60	0.59
28	6.12	-62.30	0.99
29	4.20	-26.29	1.00
30	1.46	17.42	0.73
31	2.51	-87.00	0.93
32	2.16	-57.39	0.84
33	4.49	82.09	0.94
34	3.37	89.13	0.97
35	3.23	81.92	0.92
36	2.44	-61.41	0.88
37	2.78	75.03	0.84
38	2.35	71.94	0.91
39	3.59	81.20	0.80
40	1.75	-87.86	0.76
41	2.14	-88.38	0.89
42	1.68	-89.83	0.79
43	2.98	73.36	0.94
44	1.93	88.38	0.91
45	1.82	-23.25	0.86
46	2.72	-62.73	0.97
47	2.76	-83.63	0.76
48	1.89	88.17	0.93
49	1.72	-77.31	0.72
50	1.14	38.79	0.57
51	2.48	57.97	0.98
52	2.09	81.81	0.74
53	1.94	83.50	0.97
54	1.77	77.80	0.85
55	1.98	-88.76	0.89
56	2.12	86.12	0.89
57	2.13	88.49	0.80
58	1.31	85.92	0.95
59	1.77	46.48	0.93
60	1.80	59.53	0.83

Press <RETURN> when ready to continue

T52XY
50 DATA POINTS
FLUCTUATION = 158
LOGMEAN Rf =   2.117
ORIGINAL ZERO =   -1.757

TRY AN Rs ESTIMATE.....
Rs Ri = 1.80,1.50

SYMMETRY.....

12   12

13   12
Hard copy now
Press <RETURN> when ready

T52YZ
47 DATA POINTS
FLUCTUATION = 152
LOGMEAN Rf =   1.843
ORIGINAL ZERO =   38.009

TRY AN Rs ESTIMATE.....
Rs Ri = 1.45,1.50

SYMMETRY.....

14   9

9   14
Hard copy now
Press <RETURN> when ready

154

T52XZ
60 DATA POINTS
FLUCTUATION = 139
LOGMEAN Rf =   2.259
ORIGINAL ZERO =   88.758

TRY AN Rs ESTIMATE.....
Rs Ri = 2.00,1.50

SYMMETRY.....
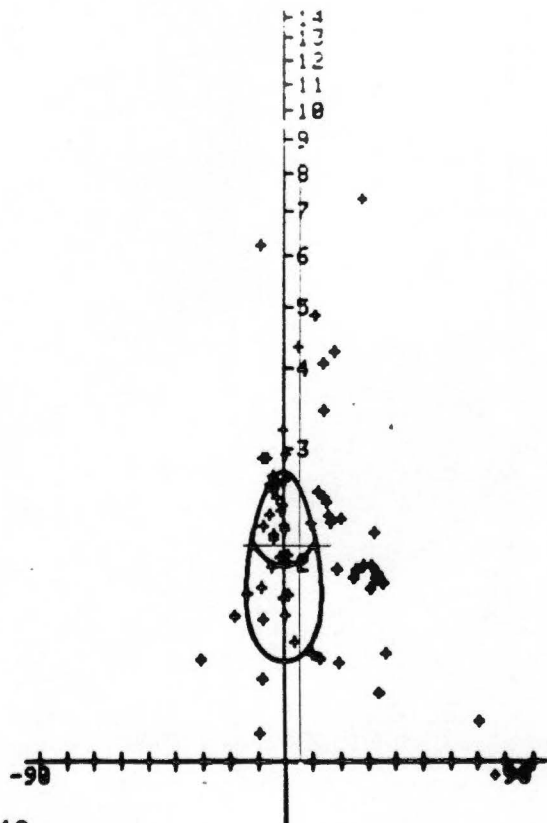
14   15

16   14
Hard copy now
Press <RETURN> when ready

SPECIMEN REFERENCE.....
T53XY

ELLIPSE NUMBER	AXIAL RATIO	LONG AXIS ORIENT.	CORREL.COEFF.
1	2.53	-23.10	0.80
2	1.66	-53.71	0.76
3	1.82	11.83	0.94
4	1.64	-52.26	0.65
5	2.31	-50.10	0.88
6	4.87	-16.19	0.91
7	3.52	-5.84	1.00
8	2.02	18.67	0.99
9	2.23	-6.02	0.83
10	1.64	40.48	0.83
11	2.86	-16.71	0.93
12	1.76	-51.70	0.76
13	2.31	-53.63	0.68
14	1.13	-50.39	0.46
15	2.93	-18.06	0.97
16	1.45	23.55	0.76
17	1.92	-32.67	0.88
18	2.09	-2.03	0.92
19	1.50	-44.38	0.68
20	1.12	-53.76	0.25
21	3.34	-20.66	0.99
22	6.09	-70.43	0.96
23	2.95	-31.81	0.98
24	1.64	-6.42	0.68
25	2.93	-20.12	0.98
26	1.96	-13.86	0.88
27	2.98	-43.56	0.99
28	1.51	-59.16	0.68
29	1.71	42.76	0.80
30	1.77	-6.50	0.96
31	3.18	-36.80	0.98
32	1.90	10.41	0.82
33	1.61	-18.70	0.90
34	2.06	-33.03	0.90
35	2.15	-49.01	0.87
36	3.18	-11.44	0.83
37	1.84	-17.32	0.73
38	2.67	-42.46	0.80
39	1.16	-31.45	0.49
40	1.87	-14.64	0.88
41	3.49	-17.58	1.00
42	2.67	-42.32	0.92
43	1.91	-23.93	0.94
44	1.04	-33.04	0.75
45	1.81	-23.56	0.75
46	2.66	-35.98	0.80
47	1.27	-22.21	0.56
48	4.05	-3.34	1.00
49	2.68	-5.81	0.84
50	1.92	-22.82	0.93
51	1.76	-47.61	0.68
52	1.26	-50.48	0.65
53	1.79	-29.39	0.96
54	1.89	-21.27	0.92
55	2.63	-4.62	1.00
56	1.97	-39.02	0.94
57	1.64	-11.58	0.75
58	1.52	-30.86	0.82
59	2.01	-19.16	0.90
60	1.59	-4.47	0.91

Press <RETURN> when ready to continue

SPECIMEN REFERENCE.....
T53YZ

ELLIPSE NUMBER	AXIAL RATIO	LONG AXIS ORIENT.	CORREL.COEFF.
1	1.84	-21.12	0.71
2	2.23	17.67	0.85
3	2.20	-2.70	0.89
4	3.56	3.57	0.99
5	1.80	27.65	0.85
6	1.77	23.84	0.88
7	2.80	-5.85	0.98
8	2.14	2.38	0.71
9	3.23	-11.75	0.81
10	3.32	-7.71	0.87
11	1.86	-20.45	0.83
12	2.69	-11.81	0.92
13	7.56	0.83	0.90
14	3.32	3.34	1.00
15	3.12	2.41	0.79
16	5.24	-4.66	0.98
17	1.47	-23.52	0.56
18	1.86	-5.31	0.59
19	2.62	-1.76	0.94
20	1.60	-31.37	0.65
21	1.46	-55.92	0.89
22	1.21	22.70	0.78
23	14.43	-10.87	0.97
24	2.02	58.17	0.84
25	1.45	4.22	0.80
26	2.67	-20.79	0.92
27	1.40	49.40	0.49
28	2.74	10.20	0.79
29	5.91	-21.02	0.96
30	1.86	-42.75	0.86
31	2.32	-1.30	0.88
32	2.14	-7.30	0.89
33	1.72	-32.44	0.90
34	2.81	-9.05	0.80
35	2.77	-8.94	0.86
36	1.54	5.74	0.86
37	2.25	4.67	0.96
38	1.95	13.70	0.92
39	2.38	-8.76	0.97
40	2.96	0.88	0.81
41	1.45	-34.35	0.51
42	2.08	19.15	0.93
43	1.47	-11.13	0.65
44	1.91	-20.00	0.96
45	1.59	-22.93	0.91
46	1.87	14.67	0.95
47	2.70	-0.24	0.84
48	1.68	-58.98	0.85
49	2.09	0.29	0.83
50	1.28	60.07	0.71
51	1.37	-51.12	0.87
52	1.81	-6.20	0.78
53	1.28	-14.90	0.70
54	1.42	82.81	0.55
55	2.25	-9.31	0.82

Press <RETURN> when ready to continue

157

```
SPECIMEN REFERENCE.....
T53X2


ELLIPSE NUMBER     AXIAL RATIO     LONG AXIS ORIENT.  CORREL.COEFF.
      1               49.48            -75.27             0.78
      2                3.29            -87.51             0.76
      3                2.38            -86.53             0.96
      4                2.53            -78.54             0.81
      5                2.39            -78.39             0.83
      6                1.88            -89.23             0.77
      7                2.38             -3.00             0.96
      8                5.55            -86.25             0.95
      9                3.05            -85.63             0.96
     10                2.04            -60.32             0.99
     11                2.17            -85.13             0.77
     12                3.71             75.11             0.89
     13                1.68            -81.41             0.87
     14                3.86            -82.02             0.93
     15                2.30             86.82             0.94
     16                1.70            -81.46             0.80
     17                2.21            -74.35             0.79
     18                3.87            -76.61             0.98
     19                2.72             88.74             0.97
     20                2.20            -79.72             0.88
     21                2.21            -74.64             0.97
     22                2.04            -41.38             0.88
     23                3.48            -78.29             0.91
     24                2.79            -84.70             0.85
     25                1.35            -51.52             0.70
     26                3.31            -65.97             0.86
     27                2.44            -76.44             0.91
     28                1.82            -59.61             0.79
     29                1.48            -83.33             0.84
     30                1.46            -86.38             0.72
     31                1.94            -85.75             0.81
     32                2.81            -81.64             0.89
     33                1.83             88.06             0.86
     34                3.46            -75.67             0.91
     35                1.99             86.09             0.69
     36                2.11            -85.11             0.91
     37                3.24             85.83             0.86
     38                2.91            -80.21             0.85
     39                2.79            -84.18             0.91
     40                1.86            -78.09             0.83
     41                4.60            -89.56             0.86
     42                2.49             89.68             0.93
     43                4.00            -76.35             0.88
     44                3.27             73.41             0.98
     45                3.06             88.85             0.92
Press <RETURN> when ready to continue
```
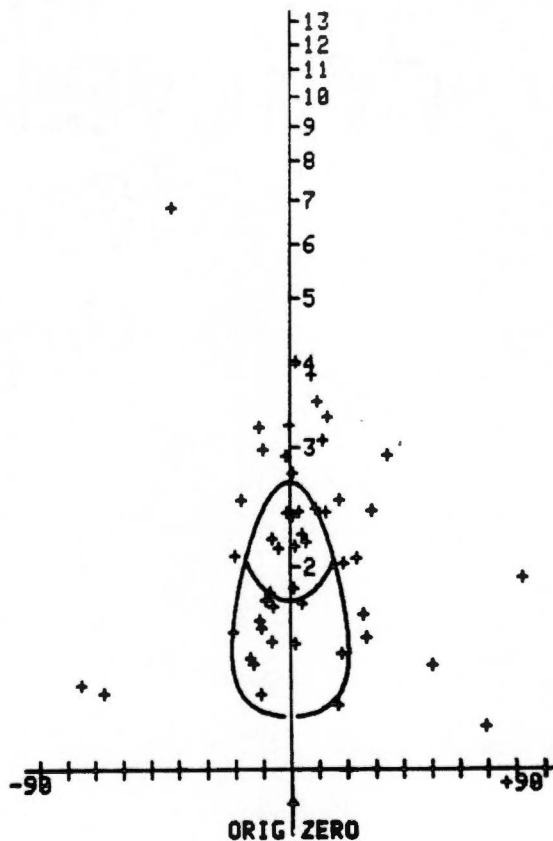
T53XY
60 DATA POINTS
FLUCTUATION = 121
LOGMEAN Rf =   2.097
ORIGINAL ZERO =   22.210

TRY AN Rs ESTIMATE.....
Rs Ri = 1.75,1.50

SYMMETRY.....

12   18

18   11
Hard copy now
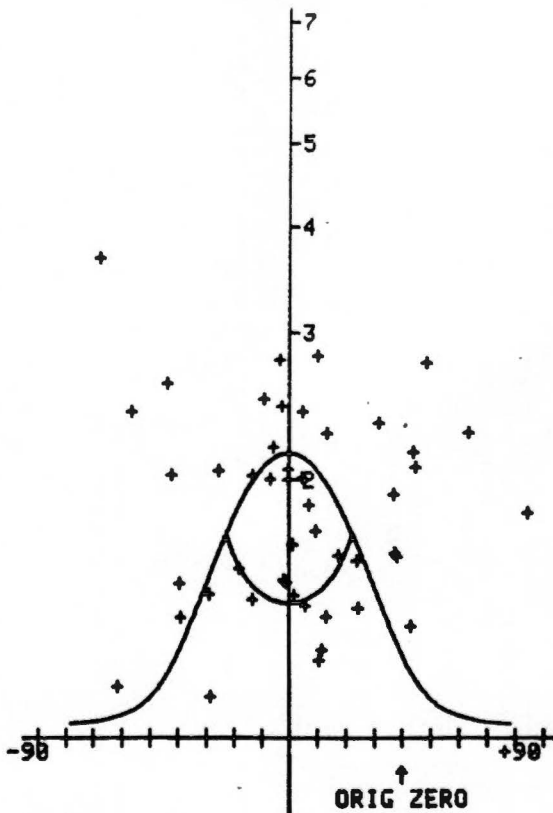Press <RETURN> when ready
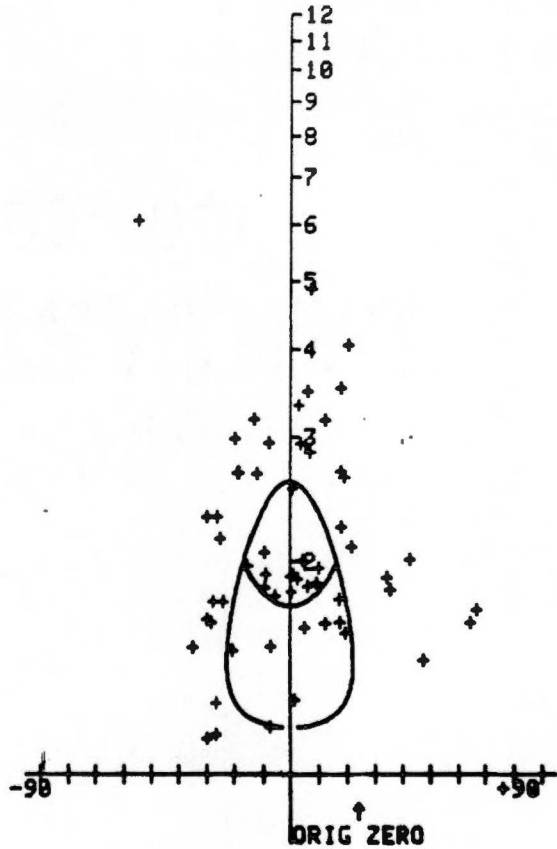
T53YZ
55 DATA POINTS
FLUCTUATION = 142
LOGMEAN Rf =   2.225
ORIGINAL ZERO =   5.312

TRY AN Rs ESTIMATE.....
Rs Ri = 1.77,1.55

SYMMETRY.....

13   14

14   13
Hard copy now
Press <RETURN> when ready

159
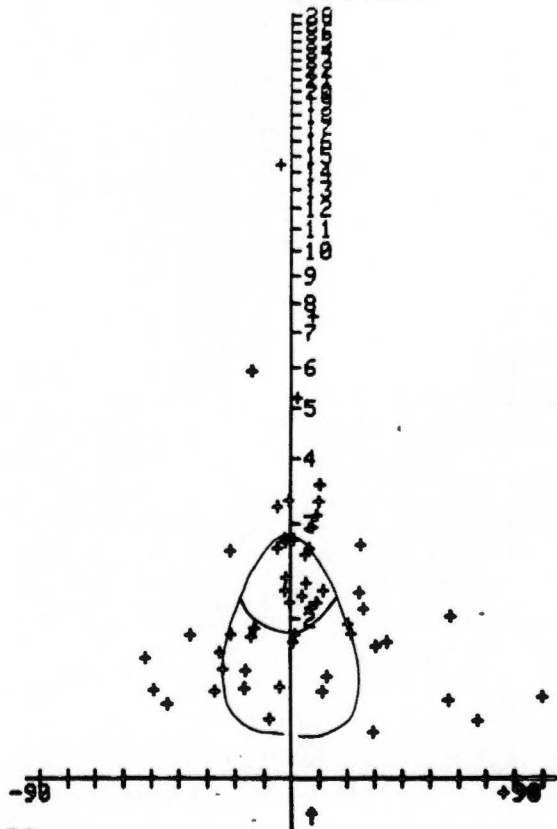
T53XZ
45 DATA POINTS
FLUCTUATION = 104
LOGMEAN Rf =   2.693
ORIGINAL ZERO =   82.024

TRY AN Rs ESTIMATE.....
Rs Ri = 2.35,1.50

SYMMETRY.....
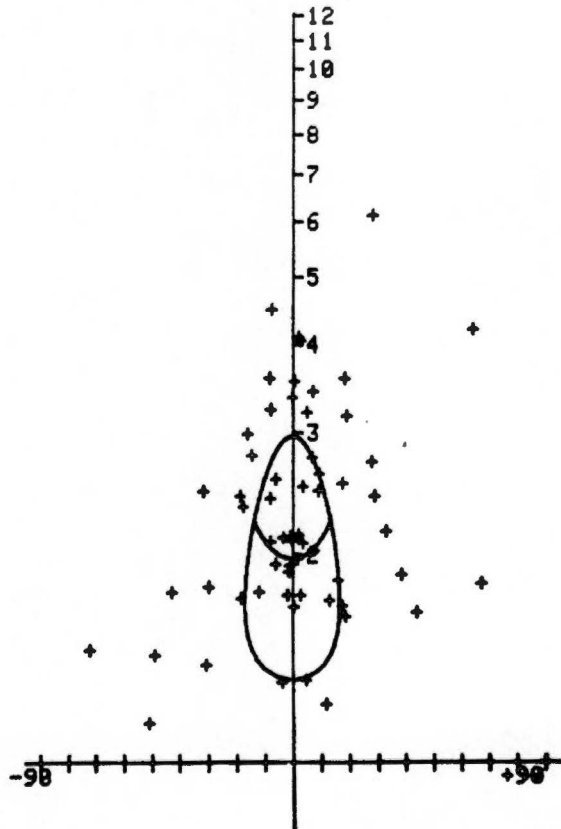
9   12

13   10
Hard copy now
Press <RETURN> when ready
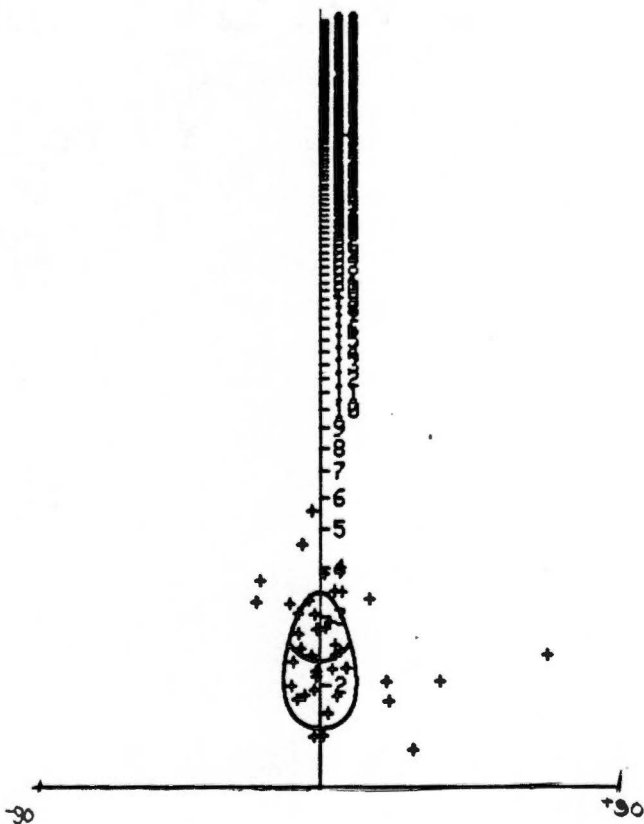
```
SPECIMEN REFERENCE.....
t54xy


ELLIPSE NUMBER     AXIAL RATIO     LONG AXIS ORIENT.  CORREL.COEFF.
      1                4.91              12.47             0.92
      2                1.24             -11.00             0.79
      3                1.49              74.48             0.65
      4                1.29              65.45             0.68
      5                1.24             -88.19             0.69
      6                2.36              46.62             0.97
      7                1.51              36.90             0.90
      8                1.37              59.98             0.83
      9                1.79              47.58             0.79
     10                1.68              38.08             0.73
     11                1.81              25.54             0.92
     12                2.17              42.34             0.95
     13                1.26              62.33             0.70
     14                1.33             -89.02             0.47
     15                1.75              17.15             0.95
     16                1.71              25.76             0.92
     17                1.38              63.50             0.52
     18                2.00              24.88             0.90
     19                1.25             -31.86             0.84
     20                1.43             -51.52             0.69
     21                2.13              44.75             0.99
     22                1.40             -24.11             0.67
     23                1.12              60.75             0.20
     24                1.84              35.37             0.76
     25                1.33              52.32             0.75
     26                1.16              21.54             0.66
     27                1.72              50.52             0.71
     28                2.98              41.33             0.94
     29                1.46              74.13             0.62
     30                2.20              23.78             0.84
     31                1.30              22.61             0.65
     32                1.22              59.28             0.47
     33                2.74              27.83             0.98
     34                1.38              30.96             0.78
     35                1.11             -67.00             0.39
     36                1.21              58.42             0.28
     37                1.90              58.97             0.81
     38                1.26              39.54             0.57
     39                1.48              51.76             0.78
     40                2.00              69.71             0.86
     41                1.27              43.73             0.73
     42                1.99              29.71             0.91
     43                2.36              44.79             0.95
     44                2.50              33.77             0.96
Press <RETURN> when ready to continue
```

SPECIMEN REFERENCE.....
t54yz

ELLIPSE NUMBER	AXIAL RATIO	LONG AXIS ORIENT.	CORREL.COEFF.
1	1.55	75.35	0.71
2	1.28	-48.32	0.57
3	1.85	-69.22	0.95
4	1.21	65.79	0.48
5	1.19	3.38	0.45
6	1.49	5.74	0.67
7	2.53	-16.00	0.96
8	1.96	5.16	0.96
9	1.60	-55.04	0.87
10	1.29	56.23	0.45
11	1.72	-54.36	0.84
12	1.13	-48.33	0.40
13	1.39	-49.18	0.87
14	1.79	74.08	0.93
15	1.64	58.92	0.67
16	3.32	28.38	0.92
17	1.84	36.31	0.73
18	1.23	70.69	0.66
19	1.62	26.36	0.79
20	1.72	14.24	0.94
21	1.56	-36.20	0.66
22	2.42	7.71	0.94
23	1.14	58.11	0.54
24	1.51	-2.68	0.76
25	1.55	77.12	0.61
26	1.25	-62.41	0.53
27	1.27	-55.66	0.54
28	1.49	-6.54	0.88
29	2.42	6.63	0.87
30	1.93	-86.04	0.79
31	1.57	45.76	0.70
32	1.49	7.38	0.81
33	1.81	41.81	0.78
34	1.73	-57.31	0.91
35	3.55	-0.53	0.87
36	1.44	34.63	0.54
37	1.64	-24.64	0.78
38	1.45	23.94	0.94

Press <RETURN> when ready to continue

SPECIMEN REFERENCE.....
t54xz

ELLIPSE NUMBER	AXIAL RATIO	LONG AXIS ORIENT.	CORREL.COEFF.
1	3.46	59.14	0.95
2	1.70	58.93	0.94
3	2.33	30.13	0.84
4	1.19	51.01	0.45
5	2.47	56.37	0.96
6	2.69	62.41	0.73
7	1.30	48.14	0.94
8	1.63	81.45	0.96
9	2.47	74.39	0.98
10	1.54	56.70	0.85
11	1.55	69.14	0.95
12	1.05	8.73	0.13
13	1.61	58.64	0.91
14	2.42	-88.20	0.93
15	1.59	14.26	0.49
16	1.90	63.76	0.81
17	1.79	-45.01	0.88
18	1.48	57.22	0.88
19	1.22	33.40	0.67
20	1.27	56.58	0.82
21	1.16	59.47	0.62
22	3.08	40.96	0.93
23	1.07	18.51	0.18
24	1.77	58.06	0.88
25	1.67	66.81	0.70
26	1.39	-6.45	0.75
27	1.41	-79.99	0.83
28	1.93	42.17	0.86
29	1.41	49.50	0.58
30	3.63	29.77	0.97
31	1.46	-88.68	0.60
32	1.38	40.44	0.65
33	1.20	73.78	0.67

Press <RETURN> when ready to continue

163

t54xy
44 DATA POINTS
FLUCTUATION = 160
LOGMEAN Rf =   1.638
ORIGINAL ZERO = -44.753

TRY AN Rs ESTIMATE.....
Rs Ri = 1.34,1.40

SYMMETRY.....

14   7

8   14
Hard copy now
Press <RETURN> when ready

ORIG ZERO
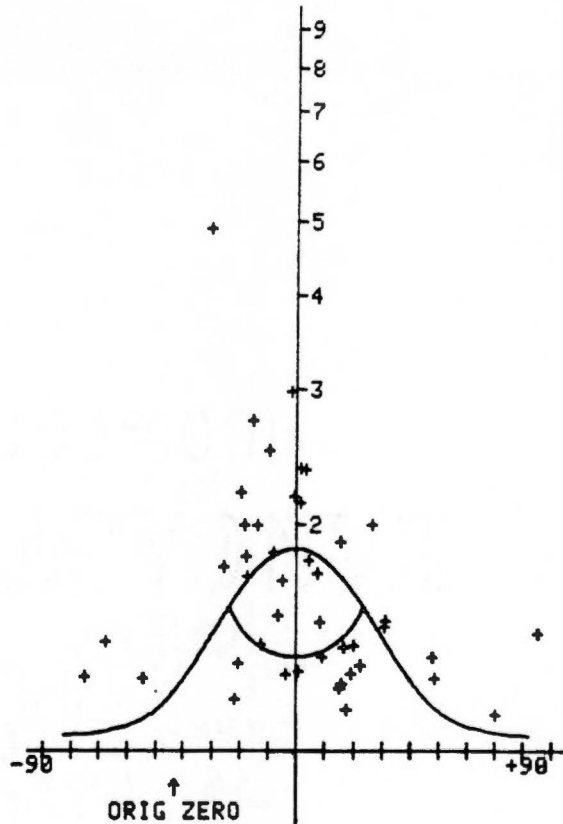
t54yz
38 DATA POINTS
FLUCTUATION = 163
LOGMEAN Rf =   1.633
ORIGINAL ZERO =   -7.380

TRY AN Rs ESTIMATE.....
Rs Ri = 1.15,1.40

SYMMETRY.....

10   8

9   10
Hard copy now
Press <RETURN> when ready

ORIG ZERO

164
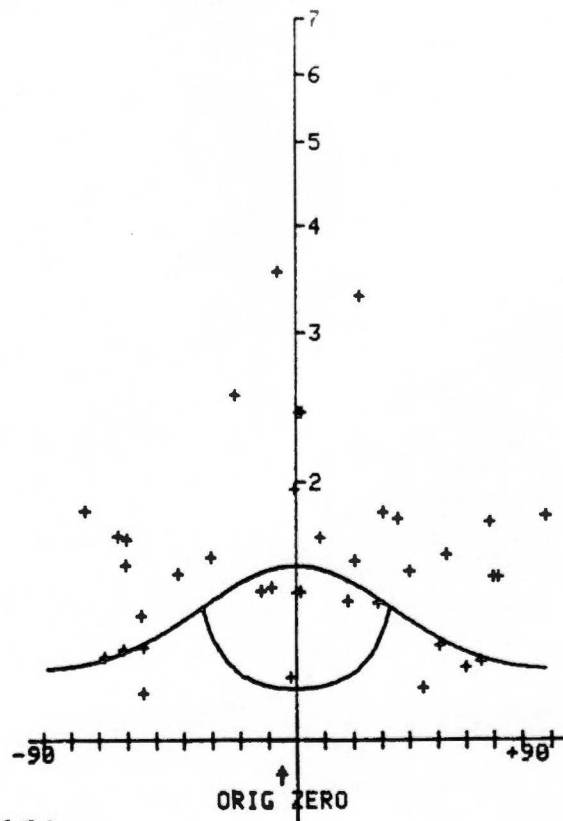
t54xz
33 DATA POINTS
FLUCTUATION = 141
LOGMEAN Rf =   1.695
ORIGINAL ZERO = -57.221

TRY AN Rs ESTIMATE.....
Rs Ri = 1.49,1.40

SYMMETRY.....

7   9

9   7
Hard copy now
Press <RETURN> when ready

165
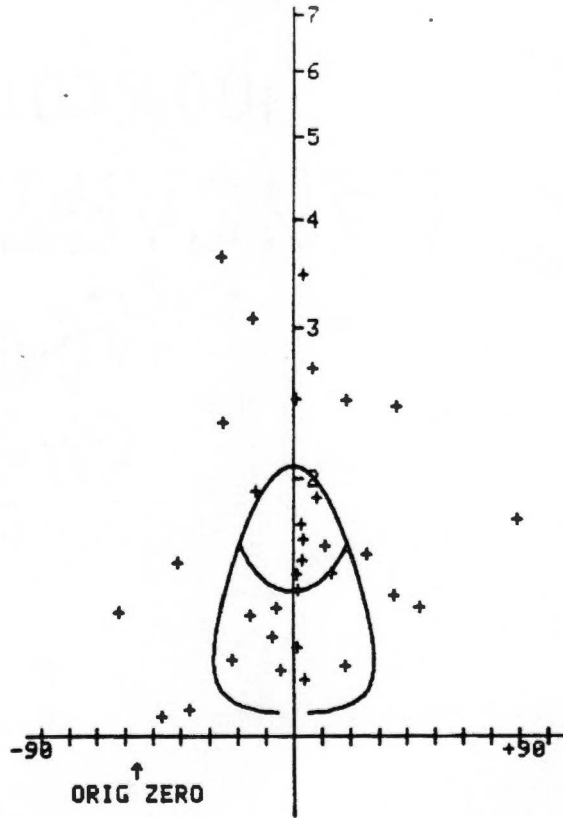
SPECIMEN REFERENCE.....
T56XY

ELLIPSE NUMBER	AXIAL RATIO	LONG AXIS ORIENT.	CORREL.COEFF.
1	3.45	86.87	0.86
2	4.33	85.27	0.93
3	1.82	-89.42	0.84
4	1.88	82.39	0.81
5	1.91	74.06	0.79
6	1.79	-79.47	0.91
7	1.17	-35.69	0.36
8	1.30	-80.92	0.79
9	1.59	-81.25	0.74
10	2.74	74.72	0.98
11	1.85	64.06	0.58
12	2.13	-78.84	0.92
13	4.29	-88.66	0.85
14	5.08	72.88	0.97
15	2.31	-87.76	0.64
16	4.55	81.42	0.82
17	2.17	-84.79	0.99
18	2.28	-62.94	0.74
19	2.14	-73.60	0.91
20	3.25	84.92	0.87
21	9.19	84.45	0.93
22	2.39	-87.53	0.88
23	2.51	86.25	0.79
24	1.57	71.85	0.79
25	2.12	77.00	0.93
26	3.11	84.35	0.94
27	2.56	-84.14	0.71
28	2.75	84.10	0.94
29	1.49	-67.33	0.89
30	3.26	87.27	0.91
31	2.07	60.36	0.91
32	3.34	75.78	0.91
33	1.78	84.56	0.76
34	2.68	-77.18	0.95
35	5.31	73.05	0.95
36	3.36	78.03	0.89
37	1.53	-57.74	0.90
38	9.52	83.06	0.98
39	1.94	-78.78	0.89
40	1.89	66.72	0.52
41	2.49	-64.03	0.90
42	1.48	-54.71	0.86
43	2.01	-82.60	0.88
44	1.32	-31.60	0.92
45	2.95	87.99	0.84
46	4.20	-89.03	0.94
47	2.84	86.01	0.99
48	2.61	73.25	0.76
49	2.08	-86.99	0.78
50	2.29	75.04	0.87
51	1.95	-78.78	0.88
52	1.30	54.95	0.64
53	2.67	-80.77	0.99
54	1.96	64.72	0.86
55	2.76	-81.82	0.91
56	2.51	-78.63	0.89
57	2.29	80.40	0.94
58	2.06	75.20	0.99
59	2.02	-76.34	0.94
60	2.34	79.73	0.99
61	1.46	70.93	0.76

Press <RETURN> when ready to continue

SPECIMEN REFERENCE.....
T56YZ

ELLIPSE NUMBER	AXIAL RATIO	LONG AXIS ORIENT.	CORREL.COEFF.
1	4.14	-6.70	0.98
2	7.11	-6.32	0.94
3	2.42	-11.06	0.99
4	2.67	-28.07	0.94
5	2.53	-1.93	0.94
6	2.04	3.95	0.86
7	9.30	-10.81	0.87
8	2.69	-5.28	0.98
9	3.78	-8.28	0.75
10	3.53	6.78	0.83
11	3.95	-12.29	0.98
12	4.26	-10.58	0.99
13	2.96	-10.95	0.88
14	2.88	12.62	0.95
15	2.82	2.03	0.95
16	1.48	-0.68	0.80
17	3.48	-13.28	0.99
18	1.94	0.14	0.08
19	2.83	-1.66	0.83
20	3.70	3.01	0.95
21	1.91	-27.61	0.74
22	2.02	-42.53	0.95
23	2.01	-4.77	1.00
24	3.09	1.32	0.07
25	2.05	-17.30	0.90
26	3.92	-5.36	0.04
27	4.01	-4.70	0.90
28	1.76	-9.03	0.95
29	1.40	-2.27	0.72
30	3.39	15.74	0.98
31	2.54	-9.29	0.99
32	3.08	0.85	0.88
33	2.30	-6.72	0.97
34	3.70	-3.26	0.96
35	4.53	-5.30	0.99
36	4.57	-1.20	0.98
37	4.17	-1.20	0.91
38	1.03	-40.31	0.13
39	3.54	0.28	0.89
40	3.23	-2.44	0.74
41	11.14	-5.28	0.89
42	4.63	-8.44	0.99
43	3.60	-12.82	0.85
44	13.31	0.54	1.00
45	5.04	-8.62	0.94
46	4.95	-3.34	0.98
47	3.46	0.51	0.89
48	1.67	-6.17	0.88
49	3.84	-9.23	0.98
50	3.80	-3.65	0.92
51	1.62	3.84	0.83
52	2.63	12.30	0.95

Press <RETURN> when ready to continue

SPECIMEN REFERENCE.....
T56XZ

ELLIPSE NUMBER	AXIAL RATIO	LONG AXIS ORIENT.	CORREL.COEFF.
1	2.12	74.73	0.89
2	3.21	62.90	0.95
3	2.88	86.44	0.79
4	2.54	85.84	0.82
5	3.32	70.97	0.93
6	2.15	60.13	0.87
7	3.16	86.94	0.91
8	1.85	62.85	0.83
9	1.97	77.43	0.79
10	1.84	78.04	0.84
11	2.34	-76.45	0.90
12	1.94	-76.19	0.80
13	1.60	70.89	0.67
14	2.07	-61.08	0.87
15	2.93	71.94	0.98
16	3.08	73.54	0.97
17	4.41	67.08	0.90
18	3.07	-85.94	0.86
19	2.24	82.27	0.87
20	1.55	-60.21	0.69
21	1.93	-89.92	0.77
22	1.43	85.49	0.59
23	2.85	66.87	0.84
24	3.14	67.50	0.88
25	2.36	51.67	0.79
26	2.55	-32.44	0.86
27	3.15	83.52	0.94
28	1.96	88.85	0.93
29	2.50	69.27	0.91
30	2.58	-89.75	0.97
31	1.95	-32.96	0.86
32	2.93	89.77	0.86
33	1.54	89.67	0.93
34	1.53	65.31	0.63
35	2.39	78.33	0.93
36	4.77	67.41	0.96
37	1.72	46.76	0.80
38	2.18	-78.73	0.92
39	2.14	82.62	0.78
40	1.94	-52.06	0.73
41	1.89	83.08	0.82
42	2.17	86.71	0.98
43	1.54	78.63	0.76
44	3.64	62.97	0.85
45	1.84	64.63	0.84
46	1.29	-89.91	0.72
47	1.82	-59.82	0.84

Press <RETURN> when ready to continue

T56XY
61 DATA POINTS
FLUCTUATION = 93
LOGMEAN Rf =   2.423
ORIGINAL ZERO =   -86.871

TRY AN Rs ESTIMATE.....
Rs Ri = 2.08,1.48

SYMMETRY.....

17   12

13   18
Hard copy now
Press <RETURN> when ready

T56YZ
52 DATA POINTS
FLUCTUATION = 59
LOGMEAN Rf =   3.219
ORIGINAL ZERO =   4.778

TRY AN Rs ESTIMATE.....
Rs Ri = 2.96,1.48

SYMMETRY.....

15   18

11   15
Hard copy now
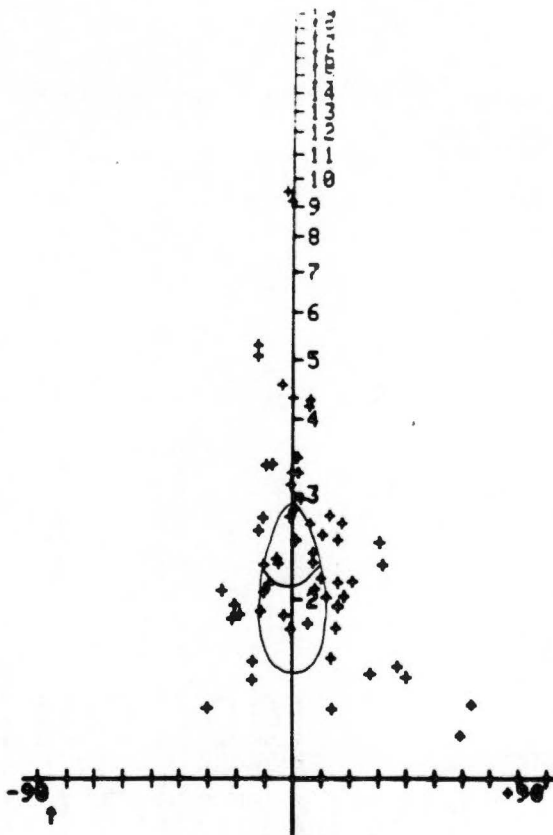Press <RETURN> when ready

ORIG ZERO

169

```
T56XZ
47 DATA POINTS
FLUCTUATION = 101
LOGMEAN Rf =    2.278
ORIGINAL ZERO =  -82.615


TRY AN Rs ESTIMATE.....
Rs Ri = 2.0,1.4



SYMMETRY.....

13   10

10   13
Hard copy now
Press <RETURN> when ready
```
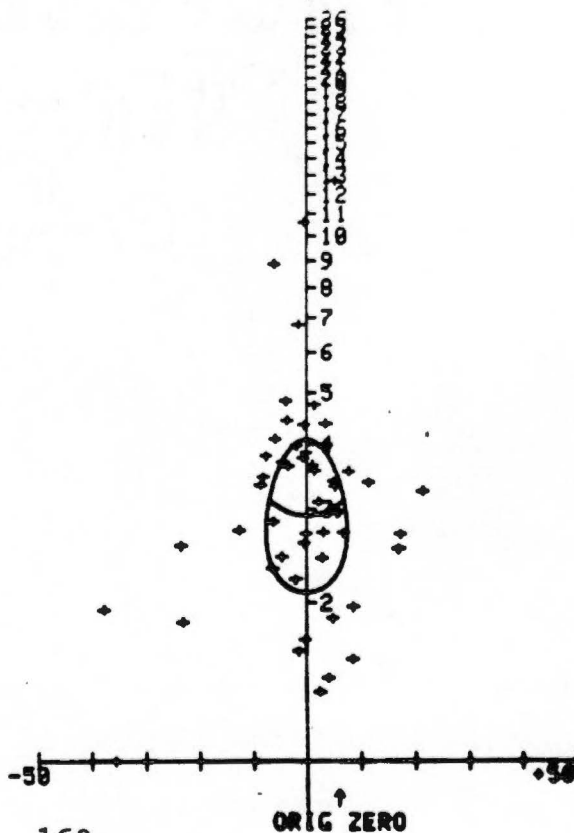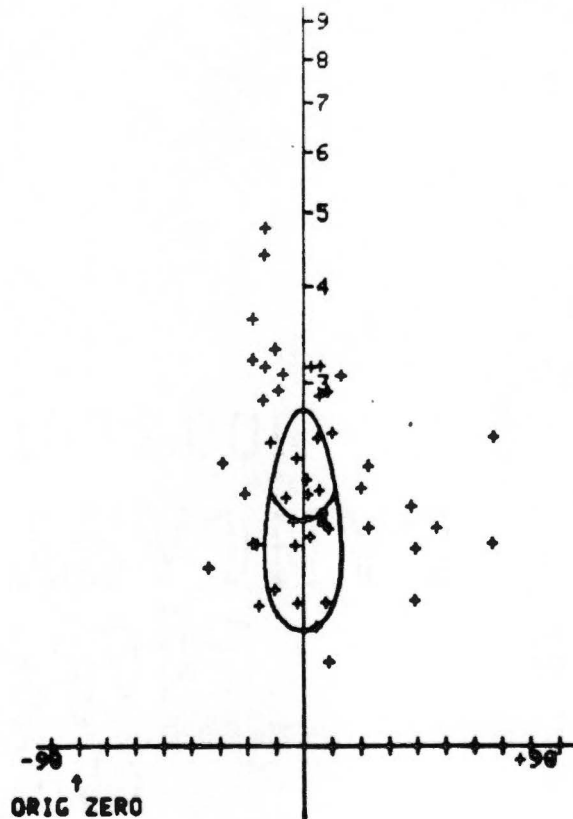
SPECIMEN REFERENCE.....
T58XY

ELLIPSE NUMBER	AXIAL RATIO	LONG AXIS ORIENT.	CORREL.COEFF.
1	2.36	-73.81	0.81
2	1.70	-72.22	0.83
3	1.55	74.72	0.83
4	2.30	-30.31	0.89
5	1.58	-71.25	0.90
6	1.41	-33.07	0.73
7	2.64	-56.11	0.71
8	1.97	-42.83	0.88
9	1.51	-83.20	0.77
10	1.59	-69.88	0.92
11	1.78	-55.10	0.98
12	1.51	-32.34	0.94
13	1.63	-32.57	0.59
14	2.03	-63.01	0.69
15	3.67	-27.75	0.89
16	3.60	-52.72	0.95
17	2.04	-29.85	0.86
18	2.11	-37.98	0.89
19	1.93	-36.49	0.82
20	2.44	-7.98	0.97
21	1.72	-52.26	0.85
22	1.41	-47.37	0.82
23	1.54	-74.07	0.76
24	1.20	-38.69	0.86
25	1.45	-59.06	0.67
26	1.60	-52.06	0.71
27	3.49	-52.37	0.92
28	1.94	-28.09	0.82
29	2.00	-55.84	0.90
30	1.52	-84.92	0.47
31	1.82	-59.37	0.81
32	2.47	-44.10	0.85
33	2.69	-41.34	0.97
34	1.05	-85.15	0.14
35	1.79	-76.10	0.80
36	2.10	-54.06	0.89
37	1.92	-25.21	0.79
38	2.73	-62.70	0.96
39	1.66	-35.48	0.76
40	1.65	-32.86	0.75
41	1.80	-49.88	0.86
42	3.82	-63.22	0.92
43	2.28	-35.49	0.96
44	1.39	-52.87	0.55
45	1.75	-20.18	0.75
46	1.35	-9.35	0.80
47	2.57	-55.93	0.97
48	1.43	-47.21	0.86
49	1.71	-43.89	0.91
50	2.04	-51.83	0.91
51	3.38	-49.46	0.93
52	2.11	-67.56	0.89
53	2.02	-79.29	0.72
54	1.73	-34.63	0.90
55	1.98	-71.35	0.98
56	2.43	-32.92	0.91
57	1.40	-67.61	0.50
58	2.06	-50.51	0.83
59	1.41	-65.77	0.47
60	1.22	-50.67	0.84
61	1.74	26.13	0.88
62	1.58	-67.13	0.64
63	1.47	10.79	0.57

ELLIPSE NUMBER	AXIAL RATIO	LONG AXIS ORIENT.	CORREL.COEFF.
1	1.94	72.83	0.68
2	1.60	17.28	0.72
3	1.49	66.45	0.79
4	2.13	-82.50	0.77
5	4.19	-88.05	0.85
6	1.24	-48.00	0.82
7	1.55	-77.44	0.66
8	1.65	25.81	0.88
9	1.98	-82.50	0.93
10	2.07	-78.02	0.92
11	1.75	88.44	0.99
12	1.35	-66.59	0.61
13	2.09	65.46	0.93
14	1.58	60.98	0.86
15	1.73	67.40	0.60
16	1.60	-20.63	0.83
17	1.69	68.75	0.56
18	1.35	18.93	0.55
19	2.48	22.36	0.83
20	1.87	42.56	0.97
21	1.71	-70.48	0.92
22	2.23	82.31	0.77
23	1.34	63.01	0.73
24	1.61	31.92	0.72
25	2.17	38.23	0.64
26	1.27	60.50	0.56
27	1.49	78.51	0.62
28	2.45	55.75	0.99
29	1.30	74.17	0.71
30	1.05	-83.09	0.19
31	1.41	60.05	0.66
32	1.45	-83.01	0.64
33	1.40	39.64	0.58
34	1.44	-3.59	0.68
35	1.98	36.75	0.82
36	1.92	78.31	0.72
37	1.93	82.36	0.90
38	1.26	-60.39	0.84
39	1.69	-82.94	0.67
40	1.78	73.25	0.89
41	1.23	-49.32	0.65
42	2.62	67.70	0.95
43	1.27	-80.90	0.76
44	1.24	-88.85	0.61
45	1.39	28.95	0.64
46	1.60	71.68	0.63
47	1.33	72.66	0.64

Press <RETURN> when ready to continue

172

SPECIMEN REFERENCE
T58XZ

ELLIPSE NUMBER	AXIAL RATIO	LONG AXIS ORIENT.	CORREL.COEFF.
1	1.75	26.63	0.77
2	1.57	-3.14	0.94
3	2.09	-47.47	0.85
4	2.81	24.80	0.93
5	1.22	23.09	0.47
6	3.17	17.24	0.99
7	3.27	5.36	0.86
8	2.29	35.12	0.97
9	2.04	15.91	0.84
10	2.09	38.51	0.85
11	3.17	33.14	0.85
12	1.34	24.08	0.64
13	1.85	11.42	0.91
14	1.48	43.63	0.65
15	2.64	18.11	0.95
16	2.29	19.81	0.89
17	1.78	8.39	0.84
18	1.85	10.35	0.89
19	2.04	14.91	0.97
20	2.73	-3.82	0.99
21	1.93	-0.68	0.99
22	1.53	1.11	0.94
23	1.09	51.55	0.18
24	1.34	0.48	0.69
25	2.51	8.57	0.99
26	1.87	34.79	0.92
27	2.38	9.27	0.98
28	1.64	16.50	0.68
29	1.76	34.74	0.86
30	1.14	9.19	0.72
31	2.02	-56.15	0.75
32	2.29	-0.96	0.99
33	1.35	2.36	0.75
34	1.88	1.30	0.97
35	1.19	26.38	0.59
36	1.57	-12.92	0.92
37	1.52	-32.23	0.64
38	3.14	15.32	0.98
39	1.85	21.50	0.89
40	1.63	33.92	0.89
41	1.68	32.38	0.87
42	2.44	-3.75	0.89
43	1.69	-2.19	0.87
44	2.62	34.51	0.98
45	1.38	32.70	0.79
46	1.23	6.40	0.68
47	1.78	8.27	0.93
48	1.66	89.53	0.79
49	1.99	5.32	0.77
50	2.28	36.38	0.86

Press <RETURN> when ready to continue

173

T58XY
63 DATA POINTS
FLUCTUATION = 131
LOGMEAN Rf =   1.885
ORIGINAL ZERO =   52.056

TRY AN Rs ESTIMATE.....
Rs Ri = 1.65,1.45

SYMMETRY.....

15   16

16   15
Hard copy now
Press <RETURN> when ready

ORIG ZERO

T58YZ
47 DATA POINTS
FLUCTUATION = 163
LOGMEAN Rf =   1.662
ORIGINAL ZERO = -72.833

TRY AN Rs ESTIMATE.....
Rs Ri = 1.32,1.45

SYMMETRY.....

12   11

11   12
Hard copy now
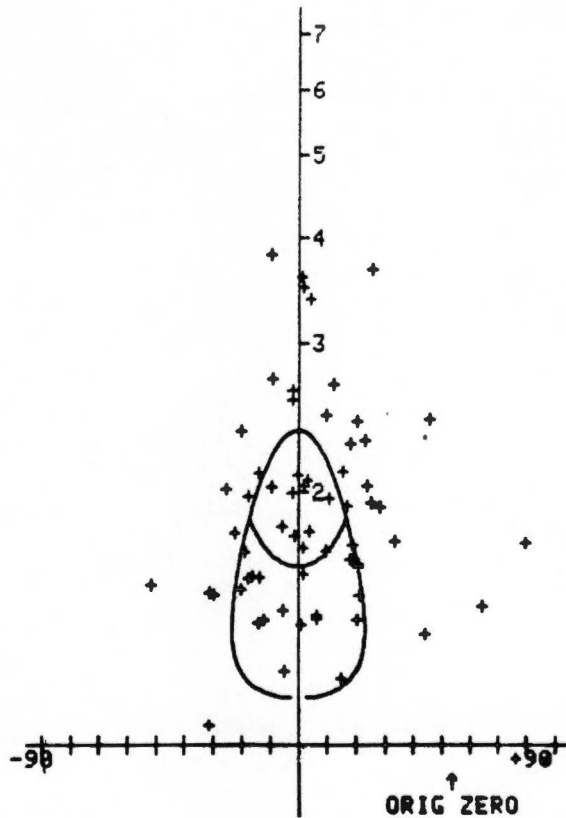Press <RETURN> when ready

ORIG ZERO

174

T58XZ
50 DATA POINTS
FLUCTUATION = 146
LOGMEAN Pf =   1.881
ORIGINAL ZERO = -15.318

TRY AN Rs ESTIMATE.....
Rs Ri = 1.65,1.45

SYMMETRY.....
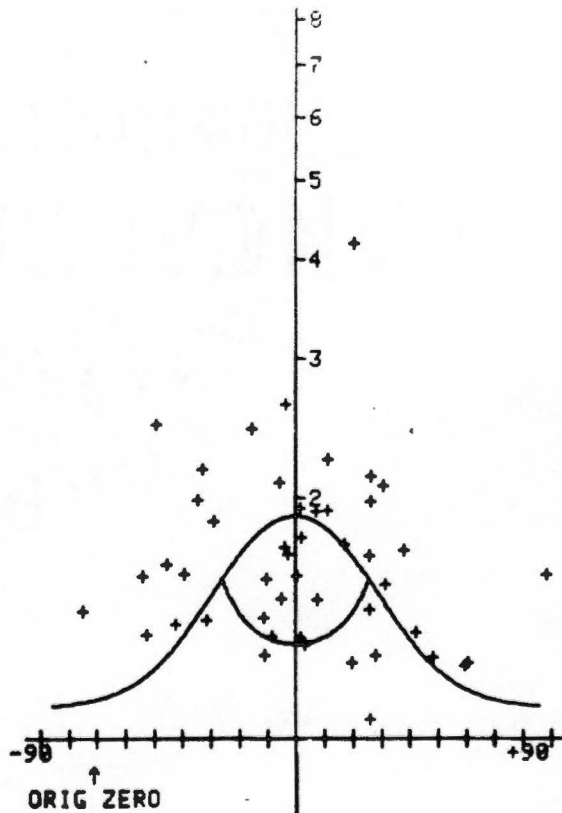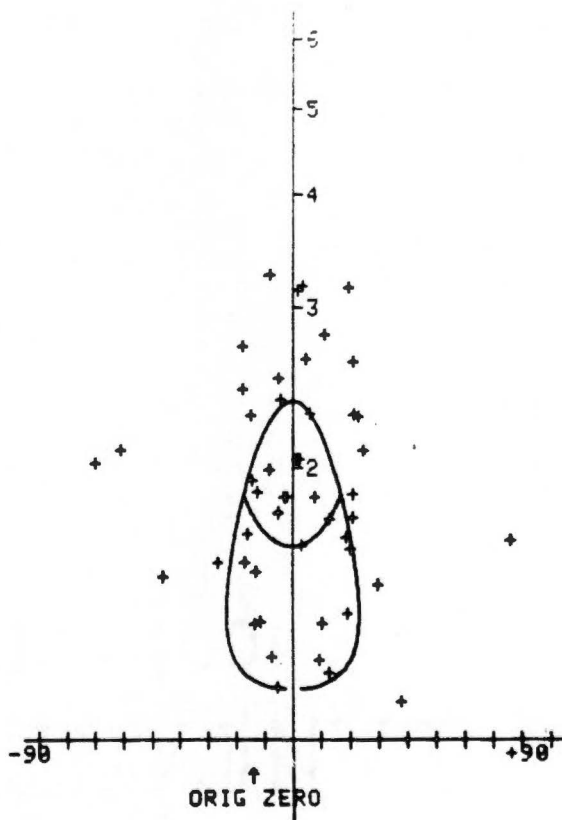
14   11

11   13
Hard copy now
Press <RETURN> when ready

ELLIPSE NUMBER	AXIAL RATIO	LONG AXIS ORIENT.	CORREL.COEFF.
1	1.85	67.38	0.90
2	2.14	59.63	0.84
3	2.68	72.93	0.98
4	2.21	-82.55	0.86
5	1.31	36.80	0.48
6	1.26	-0.85	0.81
7	2.25	-32.23	0.84
8	1.62	34.45	0.63
9	2.38	-84.73	0.80
10	1.21	14.94	0.31
11	1.68	-81.25	0.86
12	1.86	-61.96	0.93
13	1.35	-84.71	0.73
14	2.15	-68.95	0.98
15	2.38	21.83	0.74
16	2.43	47.08	0.95
17	2.27	15.41	0.94
18	2.24	15.18	0.75
19	1.55	43.27	0.87
20	1.52	-32.79	0.76
21	1.51	86.44	0.58
22	2.21	-85.48	0.93
23	1.20	-79.57	0.38
24	1.19	6.11	0.47
25	1.55	89.24	0.95
26	1.65	28.13	0.94
27	1.92	33.33	0.92
28	1.89	15.46	0.97
29	2.84	-3.77	0.94
30	1.41	-60.14	0.53
31	2.53	76.16	0.87
32	1.55	44.83	0.66
33	1.58	15.11	0.78
34	1.46	80.93	0.93
35	1.25	-0.84	0.53
36	2.84	-14.75	0.99
37	2.86	9.66	0.93
38	3.68	24.01	0.82
39	2.03	-13.27	0.84
40	1.51	72.08	0.77
41	1.63	-25.52	0.59
42	2.06	26.24	0.77
43	2.01	-1.54	0.94
44	1.81	22.45	0.91
45	1.41	80.91	0.71
46	1.63	89.48	0.83
47	1.44	30.42	0.59
48	1.87	68.46	0.72
49	2.50	9.50	0.94
50	1.91	-31.21	0.81
51	2.08	21.62	0.73
52	1.51	89.95	0.71
53	1.55	11.72	0.88
54	1.44	46.15	0.76

Press <RETURN> when ready to continue

SPECIMEN REFERENCE.....
T60YZ

ELLIPSE NUMBER	AXIAL RATIO	LONG AXIS ORIENT.	CORREL.COEFF.
1	2.48	-56.44	0.95
2	1.50	-57.74	0.81
3	2.63	-15.63	0.86
4	1.60	-30.29	0.71
5	1.90	0.81	0.96
6	1.87	-33.77	0.77
7	1.47	-18.70	0.68
8	1.21	-46.76	0.50
9	1.66	-44.26	0.93
10	3.96	-22.24	0.95
11	3.45	-29.81	0.92
12	2.15	-34.50	0.85
13	2.12	-68.10	0.96
14	2.12	-23.59	0.96
15	1.22	84.68	0.38
16	3.08	-75.89	0.93
17	1.69	34.91	0.83
18	1.29	-60.36	0.49
19	1.31	55.13	0.67
20	1.72	-31.39	0.93
21	1.38	89.25	0.56
22	1.95	-26.54	0.95
23	1.88	-14.22	0.62
24	2.33	-57.94	0.84
25	2.46	-7.95	0.96
26	1.46	-61.82	0.85
27	1.70	-35.37	0.63
28	1.26	-40.45	0.68
29	1.38	-72.50	0.44
30	1.87	-37.73	0.65
31	1.64	-44.44	0.77
32	1.89	18.95	0.88
33	1.67	-9.79	0.73
34	1.47	-79.14	0.78
35	1.45	-25.93	0.59
36	1.96	4.57	0.69
37	1.30	-63.88	0.74
38	1.91	-27.11	0.81
39	1.83	17.21	0.89
40	1.98	-22.67	0.80
41	5.41	-37.22	0.87
42	1.83	-30.34	0.82
43	1.51	-18.97	0.59
44	6.01	-45.92	0.91
45	1.46	-22.76	0.68
46	1.09	45.69	0.51
47	2.84	5.87	0.82
48	4.44	-68.21	0.74
49	1.86	-27.36	0.75
50	1.85	-22.21	0.83
51	3.62	-58.99	0.90
52	4.27	-34.29	0.86
53	1.41	89.60	0.54
54	2.64	-52.14	0.85
55	2.02	-30.04	0.66

Press <RETURN> when ready to continue

177

SPECIMEN REFERENCE.....
T60XZ

| ELLIPSE NUMBER	AXIAL RATIO	LONG AXIS ORIENT.	CORREL.COEFF.
1	2.16	-64.07	0.88
2	3.73	-49.02	0.87
3	5.18	-52.24	0.85
4	4.85	-45.92	0.99
5	2.08	-49.71	0.79
6	2.73	-62.53	0.96
7	2.46	-75.10	0.93
8	1.86	-46.26	0.99
9	1.81	-61.44	0.93
10	1.70	-54.55	0.98
11	6.65	-60.19	0.99
12	3.16	-58.83	0.73
13	2.47	-52.18	0.95
14	2.38	-71.07	0.95
15	1.96	-59.43	0.78
16	2.38	-51.29	0.90
17	1.34	68.68	0.52
18	1.61	-65.30	0.95
19	1.74	-39.12	0.95
20	1.46	-75.59	0.71
21	2.59	-63.76	0.93
22	1.30	-69.95	0.83
23	1.36	-42.32	0.58
24	1.87	-63.29	0.86
25	2.49	-60.97	0.94
26	2.34	-57.29	0.87
27	2.21	-56.65	0.93
28	2.73	-51.16	0.99
29	2.05	-70.77	0.82
30	3.07	-41.55	0.98
31	2.27	-54.60	0.80
32	1.81	-31.13	0.84
33	2.79	-61.77	0.72
34	2.08	-85.50	0.98
35	2.29	-64.55	0.99
36	3.60	-58.22	0.91
37	2.19	-51.00	0.76
38	2.65	-62.66	0.85
39	2.88	-32.36	0.93
40	1.38	86.57	0.59
41	2.35	-40.81	0.88
42	2.66	-71.32	0.80
43	2.37	77.13	0.99
44	3.90	-60.61	0.98
45	2.80	-42.76	0.87
46	1.31	-59.58	0.63
47	2.10	-57.06	0.97
48	2.58	-59.30	0.81
49	2.22	-77.99	0.79
50	2.28	-76.93	0.88
51	1.65	-24.37	0.85
52	3.08	-60.53	0.91
53	3.49	80.78	0.84
54	2.23	-25.20	0.86
55	1.71	-59.09	0.81
56	1.73	-60.45	0.72
57	2.56	-67.17	0.92
58	2.62	-52.93	0.88
59	2.06	-70.83	0.78
60	1.47	-85.10	0.80

Press <RETURN> when ready to continue

```
T60XY
54 DATA POINTS
FLUCTUATION = 153
LOGMEAN Rf =    1.823
ORIGINAL ZERO =  -34.448


TRY AN Rs ESTIMATE.....
Rs Ri = 1.2,1.45




SYMMETRY.....

17    9

18    17
Hard copy now
Press <RETURN> when ready
```
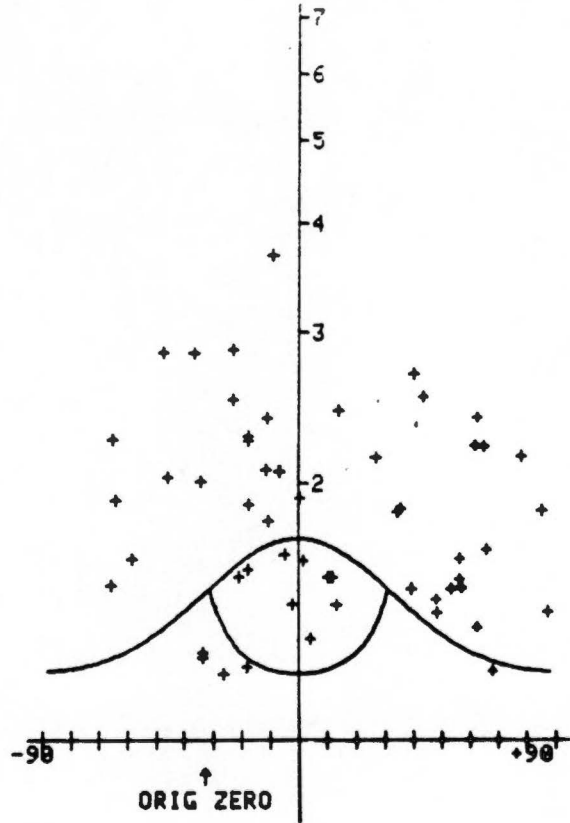


```
T60YZ
55 DATA POINTS
FLUCTUATION = 150
LOGMEAN Rf =    1.959
ORIGINAL ZERO =   31.389


TRY AN Rs ESTIMATE.....
Rs Ri = 1.65,1.70




SYMMETRY.....

13    13

14    14
Hard copy now
Press <RETURN> when ready
```
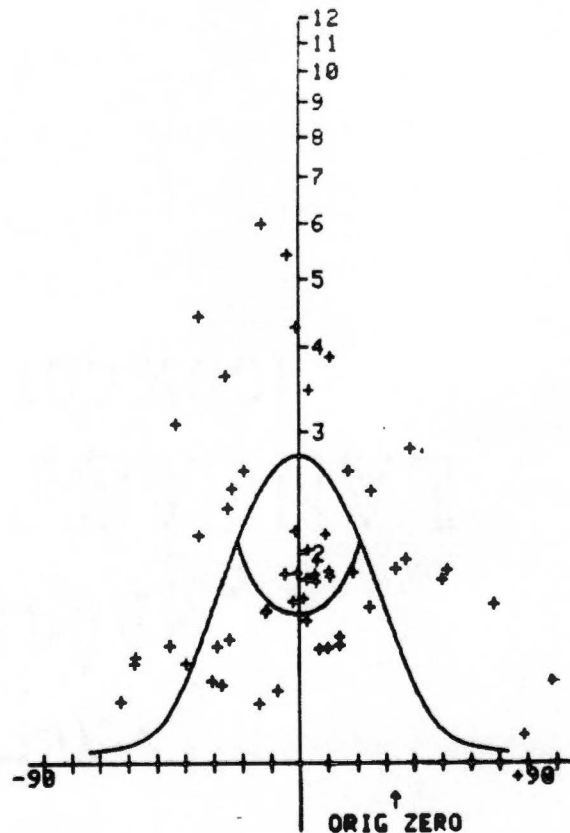
179

T60XZ
60 DATA POINTS
FLUCTUATION = 87
LOGMEAN Rf =   2.306
ORIGINAL ZERO =   59.582
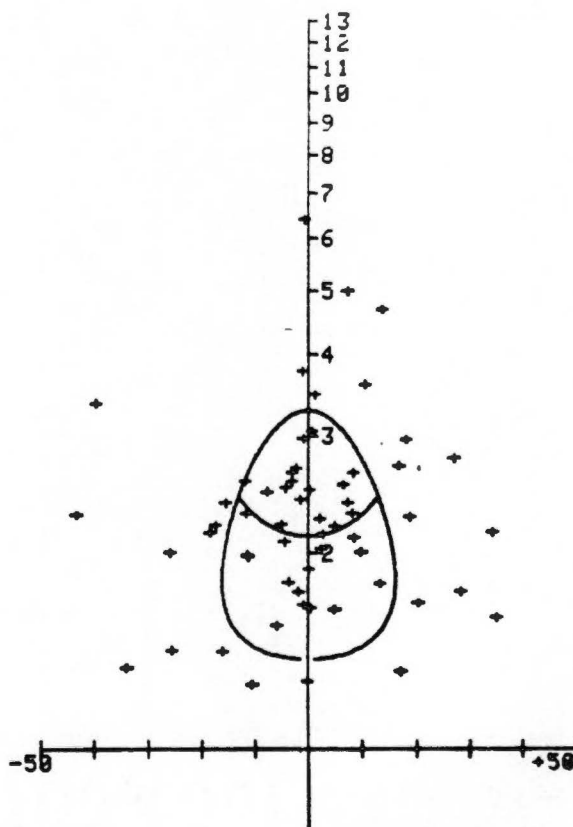

TRY AN Rs ESTIMATE.....
Rs Ri = 2.15,1.55

SYMMETRY.....

14   16

16   13
Hard copy now
Press <RETURN> when ready

SPECIMEN REFERENCE.....
T61XY

ELLIPSE NUMBER	AXIAL RATIO	LONG AXIS ORIENT.	CORREL.COEFF.
1	1.59	-4.22	0.55
2	2.36	-41.00	0.88
3	1.41	-68.95	0.67
4	2.08	-47.18	0.95
5	2.51	-64.98	0.87
6	1.96	-65.67	0.71
7	4.21	-69.56	0.97
8	1.26	-47.47	0.49
9	1.44	-77.74	0.76
10	2.98	-43.58	0.83
11	3.55	-38.84	0.96
12	3.29	23.51	0.81
13	1.04	77.83	0.10
14	2.38	-2.57	0.86
15	1.41	-41.69	0.74
16	1.86	61.40	0.84
17	1.44	-37.72	0.43
18	2.04	-65.69	0.70
19	2.13	-23.92	0.97
20	2.14	44.19	0.75
21	1.78	-51.43	0.82
22	2.54	-62.83	0.90
23	1.62	-21.71	0.78
24	2.43	-12.55	0.80
25	1.17	71.31	0.57
26	1.71	-44.93	0.81
27	2.30	-44.59	0.95
28	1.67	-29.55	0.69
29	2.73	-19.62	0.89
30	1.44	83.47	0.54
31	2.07	-28.15	0.97
32	2.03	-39.48	0.96
33	2.81	-66.45	0.86
34	1.51	-25.17	0.59
35	2.01	-42.42	0.83
36	4.49	-38.95	0.75
37	3.66	-51.27	0.86
38	1.68	-11.83	0.97
39	1.93	-37.95	0.87
40	1.18	14.90	0.84
41	1.62	-28.40	0.77
42	3.49	-44.41	0.97
43	2.92	-54.24	0.94
44	6.39	-20.06	0.97
45	1.35	-15.08	0.62
46	1.84	-45.89	0.92
47	2.15	-82.21	0.71
48	2.35	-57.41	0.97
49	1.64	-34.59	0.77
50	1.56	-66.34	0.70
51	1.36	-13.02	0.73
52	3.21	-49.23	0.95
53	2.11	-12.91	0.91
54	1.45	-8.24	0.88
55	2.89	-10.35	0.95
56	2.68	8.71	0.93
57	2.06	-36.90	0.92
58	1.55	-4.99	0.81
59	2.21	24.50	0.76
60	1.56	-7.98	0.82
61	1.83	1.98	0.87
62	2.23	-29.03	0.63

Press <RETURN> when ready to continue

SPECIMEN REFERENCE.....
T61YZ

ELLIPSE NUMBER	AXIAL RATIO	LONG AXIS ORIENT.	CORREL.COEFF.
1	2.01	-23.60	0.92
2	2.70	-8.80	0.87
3	3.17	-0.77	0.88
4	5.65	-14.82	0.99
5	2.80	3.60	0.95
6	5.37	-17.79	0.96
7	3.88	-12.03	0.90
8	4.17	-5.29	0.98
9	2.40	-11.28	0.97
10	2.12	-9.23	0.79
11	2.18	1.48	0.97
12	2.06	-6.87	0.81
13	2.77	-10.66	0.96
14	3.59	-4.24	0.99
15	2.46	-19.50	0.94
16	1.74	2.53	0.94
17	1.34	-14.20	0.94
18	1.99	-7.26	0.91
19	3.74	6.73	1.00
20	2.23	2.29	0.73
21	2.88	-13.35	0.83
22	2.56	-9.69	0.97
23	2.51	16.39	0.90
24	2.22	-20.62	0.93
25	4.08	-1.74	0.90
26	2.44	-42.34	0.96
27	2.59	-3.34	0.89
28	5.82	-7.04	0.96
29	1.88	-14.49	0.94
30	2.98	-7.88	0.89
31	2.23	-21.10	0.98
32	1.28	-18.89	0.46
33	2.08	-5.00	0.86
34	3.94	-11.14	0.96
35	3.70	-0.58	0.88
36	2.47	-16.23	0.93
37	2.59	-14.56	0.88
38	3.45	-3.84	0.98
39	2.14	-14.07	0.96
40	3.55	-13.54	0.95
41	2.90	12.10	0.94
42	2.05	-14.24	0.85
43	2.11	-19.91	0.89
44	2.92	-4.95	0.87
45	3.19	-17.11	0.99
46	2.78	-8.27	0.97
47	4.00	-5.99	0.99
48	1.66	-4.74	0.90
49	1.28	-44.70	0.61
50	4.26	-11.28	0.99
51	3.24	-32.98	0.92
52	3.22	-7.37	0.99
53	2.18	-8.78	0.99
54	4.83	-10.31	0.99
55	5.47	-12.90	0.97
56	2.24	-13.22	0.97
57	3.61	-21.40	0.96

Press <RETURN> when ready to continue

182

SPECIMEN REFERENCE.....
T61X2

ELLIPSE NUMBER	AXIAL RATIO	LONG AXIS ORIENT.	CORREL.COEFF.
1	6.24	73.94	0.78
2	5.02	81.81	0.96
3	2.09	84.53	0.88
4	1.49	-75.61	0.76
5	1.80	55.67	0.95
6	1.30	40.04	0.55
7	3.00	70.75	1.00
8	3.27	60.47	0.75
9	3.40	64.70	0.93
10	3.74	-87.12	0.97
11	3.20	83.24	0.96
12	1.93	67.76	0.85
13	2.18	-86.56	0.93
14	3.17	75.96	0.95
15	2.69	67.13	0.79
16	2.04	64.40	0.88
17	1.73	-86.23	0.71
18	2.54	-86.06	0.92
19	3.14	69.82	0.96
20	1.58	79.36	0.72
21	2.33	57.86	0.95
22	1.63	-86.95	0.84
23	1.88	80.70	0.97
24	1.63	81.50	0.84
25	1.20	-89.17	0.52
26	1.79	67.14	0.98
27	2.31	81.26	0.92
28	1.74	58.05	0.70
29	3.91	79.27	0.78
30	1.46	-49.95	0.57
31	2.04	73.39	0.91
32	3.12	84.84	0.91
33	2.66	84.37	0.98
34	2.47	53.49	0.87
35	2.94	80.01	0.99
36	2.14	-79.98	0.88
37	2.35	82.61	0.99
38	1.62	-60.42	0.71
39	2.20	82.24	0.79
40	2.13	77.11	0.93
41	5.00	75.55	0.92
42	2.87	70.03	0.91
43	3.56	82.68	0.96
44	2.33	85.09	0.98
45	2.51	84.59	0.97
46	4.22	79.79	0.98
47	2.77	81.78	0.77
48	4.19	81.96	0.82
49	3.64	73.17	0.85
50	2.94	73.04	0.99
51	2.60	83.43	0.76
52	3.47	83.26	0.99
53	1.88	75.68	0.82
54	2.59	57.36	0.91
55	1.61	52.36	0.91
56	1.55	74.62	0.88

Press <RETURN> when ready to continue

T61XY
62 DATA POINTS
FLUCTUATION = 163
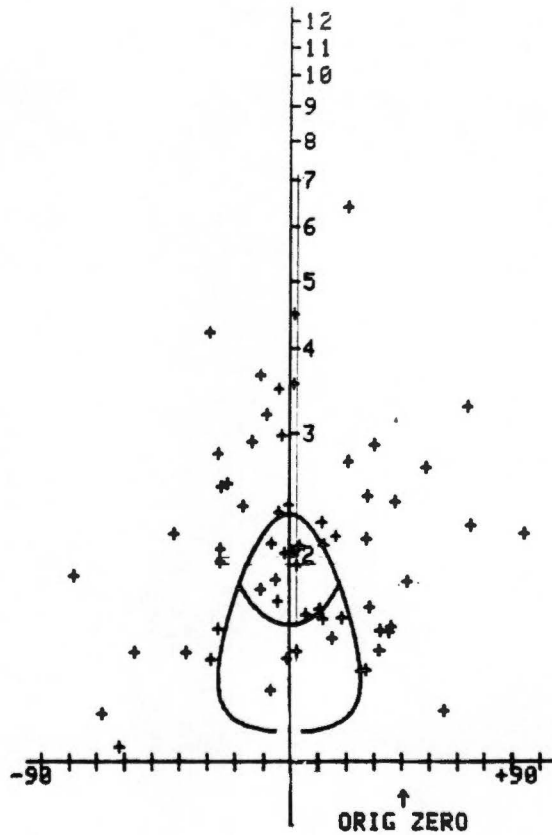LOGMEAN Rf =   2.053
ORIGINAL ZERO =   38.844

TRY AN Rs ESTIMATE.....
Rs Ri = 1.60,1.45

SYMMETRY.....

19   11

12   19
Hard copy now
Press <RETURN> when ready

T61YZ
57 DATA POINTS
FLUCTUATION = 61
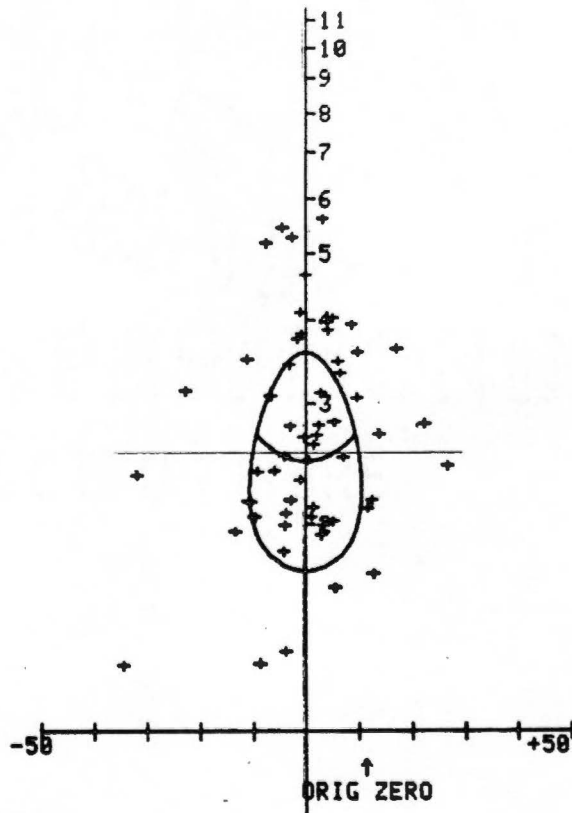LOGMEAN Rf =   2.763
ORIGINAL ZERO =   10.308

TRY AN Rs ESTIMATE.....
Rs Ri = 2.50,1.45

SYMMETRY.....
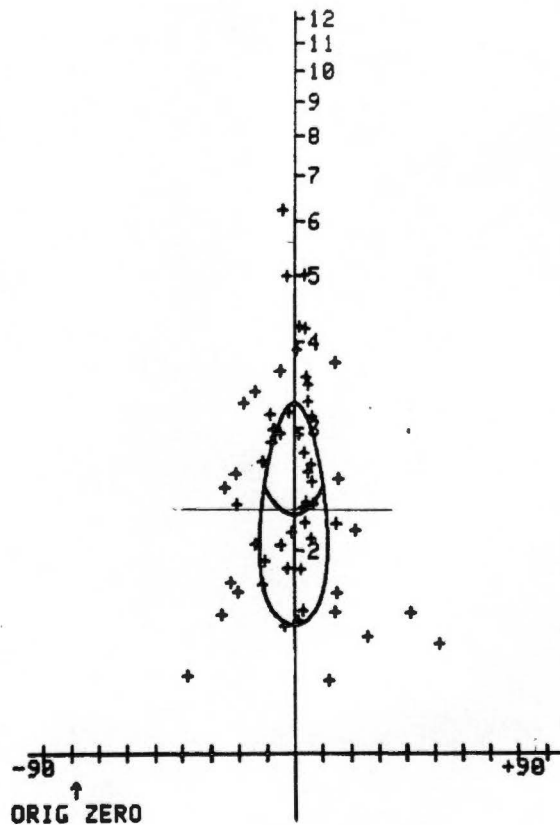
13   14

15   14
Hard copy now
Press <RETURN> when ready

184

```
T61XZ
56 DATA POINTS
FLUCTUATION = 90
LOGMEAN Rf =    2.458
ORIGINAL ZERO =  -80.008


TRY AN Rs ESTIMATE.....
Rs Ri = 2.28,1.45




SYMMETRY.....

12   15

16   12
Hard copy now
Press <RETURN> when ready
```

VITA

Jonathan C. Lewis was born on May 19, 1961 in Washington, DC. He grew up in Bethesda, Maryland, attending Montgomery County Public Schools through high school. He graduated, with no particular honors, from Walter Johnson High School in June 1979. Although the Montgomery County School system boasts of its fine reputation, he felt that he had no particular advantage. After attending Davis and Elkins College in Elkins, West Virginia for one year where he discovered an interest in geology, he attended the University of Vermont at Burlington where he found his educational background to be suspect. Nonetheless, he graduated with a B. S. in Arts and Sciences with a major in geology in May of 1983. The next fall he began his graduate career at the University of Tennessee at Knoxville. After getting married and taking a year to work for the World Champion Boston Celtics he was finally awarded an M. S. in geology in June of 1988.